Affinity peptide mediated site-specific functionalization of native antibodies

September 2019

Kei Yamada

Abstract

Antibody-drug conjugates (ADCs), which consist of three components– antibody, linker, and payload, can function as “magic bullets”. These conjugates offer the ability to target drug delivery to specific cells, based on cell-specific recognition and the binding of an antigen by a monoclonal antibody (mAb). In particular, by delivering a cytotoxic payload to cancer cells, ADCs are expected to provide a breakthrough in oncology treatments by providing a way to increase efficacy and decrease toxicity in comparison with traditional chemotherapeutic treatments. The development of ADC therapeutics has dramatically progressed in the past decade and two ADCs have been approved and used as anticancer drugs in the clinic. However, several critical issues regarding the performance of ADCs are still being discussed and investigated. Indeed, in the past few years, several groups have reported that changing the number and position of the drug payloads in the ADCs affects the pharmacokinetics, drug release rates, and biological activity. Using conventional heterogeneous conjugation methods for ADC preparation results in the drug/antibody ratio and connecting position of the payload having stochastic distributions. Therefore, it is important to investigate how these potential problems can be circumvented through site-specific conjugation.

Here, we report a new method of affinity peptide mediated regiodivergent functionalization that enables the synthesis of ADCs from native IgG antibodies, the technology termed AJICAP™. We succeeded in introducing thiol functional groups onto three lysine residues in IgGs using Fc affinity peptide reagents without antibody engineering. A cytotoxic molecule was then connected to the newly introduced thiol group, and both a surface plasmon resonance binding assay and in vivo xenograft mouse model results showed that the resulting ADC could selectively target and kill HER2-positive cells. This tuneable,

optimized and powerful strategy of regiodivergent functionalization using affinity peptides provides a new approach to construct complex antibody-derived biomolecules.

Table of Contents

1. Introduction

1.1. Antibody-drug conjugates and site-specific conjugation

Preparation of homogeneous biomolecules is one of the important issues in the fields of biopharmaceutical and chemical biology. In particular, in protein conjugates, there are usually several reaction sites derived from the presence of several of the same residues, so that homogeneous protein conjugation technologies have long been of interest to chemists and biologists[1-5]. Antibody-drug conjugates are a rapidly growing class in the field of biopharmaceuticals and the synthesis of these compounds requires the use of site-specific conjugation technologies[6-8]. In general, for ADC production, the chemical modification of antibodies (mAbs) has been performed by random reactions with the activated carboxyl groups of N-hydroxysuccinimide (NHS) esters with lysine residues, or by the reactions of thiol-specific reagents, such as maleimide, with cysteines[9]. Lysine conjugation results in 0–8 conjugated molecules per antibody, and peptide mapping has determined that conjugation occurs on both the heavy and light chains at ~20 different lysine residues (40 lysine residues per mAb). Therefore, greater than one million different ADC species can be generated[10]. For cysteine conjugation, the drug/antibody ratio (DAR) can range from 0–8, generating more than one hundred different ADC species[11]. Examples of representative ADCs prepared by these conventional modifications include Genentech and Immunogen's trastuzumab emtansine (Kadcyla)[12,13] produced by nonspecific conjugation to lysine residues, and Seattle Genetics's brentuximab vedotin (Adcetris)[14,15] constructed by alkylation of cysteine thiols that are exposed by prior reduction of the conserved hinge region disulfide bonds; these ADCs were approved in 2013 and 2011, respectively.

In recent years, various groups have reported site-specific modifications of antibodies designed to produce homogeneous ADCs, and these modifications have had effects on

the antigen binding, stability of the antibodies, and the pharmacokinetics[16-19]. Substantial efforts are currently focused on determining how to direct the sites of conjugation to create more homogenous products with a narrow DAR range (Table 1). THIOMAB™ was the first approved technology that embodied this particular strategy, using strategic cysteine residues developed by Genentech[9]. In THIOMAB™ technology, two engineered cysteines were introduced to antibody. These two cysteines were capped with cysteines or glutathione in the culture media through disulfide bond, and this disulfide bond must be cleaved to obtain the desired intermediate for ADC synthesis. Remarkably, Junutula et al. solved this problem by cleaving the inter-chain disulfide bonds (and those of engineered cysteine caps) with a reducing agent followed by a spontaneous re-oxidation step to re-connect the intermolecular disulfide bond between a heavy chain and a light chain (HC–LC) and/or between two heavy chains (HC–HC). Additionally, the insertion and/or replacement of unnatural amino acids using antibody engineering has also been tested[20,21]. Other groups have added sequence tags, such as FGE (formylglycine generating enzyme) in a method called SMARTag™ developed by Redwood Bioscience.[22,23,24] and Q-tag for using TG (transglu-taminase)[25], using enzymatic drug conjugation. Whilst technically feasible, this approach adds an additional layer of complexity to the production process for ADCs, requiring detailed optimization to determine suitable insertion sites, and introducing potential challenges for the scale-up and reproducibility. Therefore, site-specific conjugation to native antibodies is desirable to overcome the difficulties in the optimization of cell culture conditions, which potentially had a straight forward CMC (Chemistry, Manufacturing and Control) of an ADC development.

Recently, several groups have reported enzyme-directed, site-specific conjugation to native mAbs. All mAbs are glycosylated at Asn297. Variability in the glycan structure of an

antibody exists within a single batch of a mAb, and the exact ratio of isoforms differs per IgG isotype and is moreover highly dependent on the mammalian expression system used. Several groups have reported use of the glycan for the site of site-specific conjugation. Initially, periodate oxidation of terminal galactose residues, followed by oxime ligation of the payload was investigated[26]. Then, Boeggeman et al.[27,28], Zeglis et al.[29], and Li et al.[30] reported the use of chemoenzymatic conjugation technologies using glycans. In 2015, Geel et al. reported practical glycan remodeling using endoglycosidase and glycosyl transferase to incorporate an azido moiety, and this technology achieved the synthesis of a DAR 2 ADC combination using copper-free click conjugation with bicyclononyne (BCN)[31]. This technology was developed by Synaffix and is called GlycoConnect™. Antibodies against a variety of subtly different glycans have been found in humans: for example, N-glycolylneuraminic acid, which differs from sialic acid by the addition of a single hydroxyl group, acts as an antigen in humans[32], and a variety of sialic acid glycoengineering studies have found that other unnatural sialic acids are immunogenic as well[33]. In another methodology, transglutaminase (TG) was applied for modification of non-mutated mAbs. TG recognizes exclusively Gln295 located in the Fc region of deglycosylated IgGs as a site for modification with a suitable substrate[25]. Recently, many groups have reported chemistry-based, site-specific conjugation methodologies for native (non-engineered) antibodies. Chemistry-based methods can be said to be competitive in terms of cost and convenience with the established enzyme-based methods. Precise control over the chemo-, site-, and modification-number selectivity in antibody chemical conjugates, while maintaining structural integrity and homogeneity is highly important, and still represents a major challenge.

Table 1. Site-specific conjugation technologies.

	Engineering required	*Site-specific conjugation to native antibody (non-engineering)*				
	Engineering	**Enzymatic**	**Chemical** [a]			
	A) Cysteine engineering (THIOMAB™) B) Unnatural amino acid incorporation C) Selenocysteine D) FGE method (SMARTag™) E) Q-tag using TG F) Glycoengineering and using TG	G) Glycan remodeling H) TG	Recent residue selective labeling for generating homogeneous ADCs I) Sulfonyl acrylate reagents J) Linchpin directed modification	Disulfide re-bridging	Affinity peptide mediated labeling	
					Peptide traced labeling K) Photo affinity labeling L) Activated ester	Peptide traceless labeling M) Metallopeptide N) Activated ester and cleavable linker
Antibody engineering required	A) Cysteine substitution B) Amber stop codon substitution C) Addition of Sec insertion sequence D) Addition of aldehyde tag E) Addition of glutamine tag F) None for glycoengineering or for pre-existing glutamine tag (Gln295)	None	None	None	None	None
Enzymes required for conjugation	Required for FGE (D) or TG (E,F)	Required	None	None	None	None
Conjugation site location	Any location in A–D and F; limited in E	Glycan (G), Gln297 (H)	1	Hinge disulfide	Depends on peptide	Depends on peptide
Conjugation residues	Cysteine (A), Unnatural amino acid (B, D), Selenocysteine (C), Glutamine (E, F)	Glycan (G) or glutamine (H)	Lysine (I) or histidine (J)	Interchain disulfide	Methionine (K) or lysine (L)	Asparagine (M) or lysine (N)
Drug/antibody ratio	2, 4, or more	2	2 (I) or 4 (J)	4 or 8	Methionine: 2 (K) Lysine: between 1–2 (L)	Asparagine: 1 (M) Lysine: 2 (N)
Antibody variation	Any IgG isotype	Any IgG isotype	Only demonstrated with trastuzumab	Any IgG isotype	Any IgG isotype (Only demonstrated with IgG1)	Any IgG isotype
Risk of immunogenicity	Low (high for adding tag sequence)	Low	Low	Low	High	Low
Institutions exploring methods [b]	Genentech (A); MedImmune; Seattle Genetics (A); Allozyne; Ambrx (B); Sutro (B); National Cancer Institute (C); Glycos (F); Pfizer (E); Catalent (D)	Univ. of Georgia (G); SynAffix (G) (GlycoConnect™); ETH Zürich (H)	Univ. of Cambridge (I); IISER [c] Bhopal (J)	PolyTherics (ThioBridge™); Univ. College London	KST [d] (K); Univ. of Pennsylvania (K); KTH [e] (K); Ajou Univ. (K); Rice Univ. (L); Genentech (K); Kagoshima Univ. (L) (CCAP)	Rice Univ. (M); Ajinomoto (N) (AJICAP™)

a) Recent chemical approaches are focused on in this review. b) Based on publication in peer reviewed journals. c) IISER: Indian Institute of Science Education and Research. d) KST: Korea University of Science and Technology. e) KTH: Kungliga Tekniska Högskolan.

1.2. Recent residue selective labeling for generating homogeneous ADCs

Site- and residue-specific modification of proteins by simple chemical reagents is a challenging area in the fields of chemistry and chemical biology. Recently, two groups have reported site-selective lysine and histidine conjugation using simple commercially available chemical reagents.

Matos et al. have reported sulfonyl acrylate reagents for the modification of a single lysine residue on native protein sequences, using computer-assisted design (Figure 1a)[34]. The site selectivity was predicted computationally, where the lysine with the lowest pKa was the kinetically favored residue at slightly basic pH. Chemoselectivity was also observed as the reagent reacted preferentially at lysine, even in those cases when other nucleophilic residues, such as cysteine, were present. This technology was demonstrated by the quantitative and irreversible modification of five different proteins, including the clinically used therapeutic antibody trastuzumab, without prior sequence engineering. Constant pH molecular simulations (CpHMD) for the antibody trastuzumab showed the lowest pKa value was obtained for lysine at position 207 in the light chain, indicating that this residue is likely the one where the sulfonyl acrylate reagent preferentially reacted.

In 2018, Rai et al. reported an alternative method that could modify native antibodies in a site-specific manner using a simple reagent[35]. Initially, a reversible intermolecular reaction places “chemical linchpins” globally to form imine moieties on all the accessible lysine residues. Then, the epoxide which was in-stalled in the “chemical linchpins” reacts with a proximal histidine moiety. If there is no histidine moiety present, the “chemical linchpins” reverse and re-form an aldehyde for covalent labeling with an oxime moiety. Interestingly, this reaction works in native mAbs, and this group have succeeded in obtaining a DAR 4 ADC using trastuzumab.

These new functionalization/conjugation reactions mark an important step forward in achieving directed and site-selective (rather than stochastic) conjugation of native mAbs using a non-genetic approach. However, these two methods have only been used for site-specific conjugation in trastuzumab, and if alternative antibodies were used, the variable domain sequences of the mAbs may be different and expose other reactive lysine or histidine residues in the antigen recognition region resulting in undesired modifications. A variety of different antibodies need to be tested using these two methods before these methods can be accepted as general site-specific ADC platform technologies.

1.3. Disulfide re-bridging strategies

Generally, there are four interchain disulfide bonds in an antibody. The reduction of these disulfide bonds to obtain eight free sulfhydryl groups in an antibody has been used to obtain high DAR ADCs (approximately DAR 8). Doronina et al. reported the adaption of this DAR 8 system to the chimeric anti-CD30 mAb and conjugated monomethyl auristatin E (MMAE)[36]. However, further investigation revealed that the high drug loading resulted in a poor tolerability, high plasma clearance rate, and decreased efficacy in vivo owing to aggregation, and that a lower drug-to-antibody ratio resulted in a larger therapeutic window[37,38]. Ob-served differences in the physical state were correlated with a dramatic increase in the hydrophobicity and a reduction in the surface tension of the DAR 8 conjugate compared with lower DAR species.

In 2014, Badescu et al. reported the first disulfide re-bridging strategies using bis-alkylating reagents[39]. This technology was developed by the PolyTherics and called Thio-Bridge™. The resulting MMAE conjugates, which had an average DAR of 2.8, retained antigen-binding, were stable in serum, and demonstrated potent and antigen-selective cell killing in in vitro and in vivo cancer models. Around the same time, Schumacher et al. reported an alternative bis-alkylating reagent, which used dithiomalei-mides40. This group showed that this bis-alkylating reagent could be used to control the DAR and to synthesize site-specific ADCs. Chudasama et al. have also developed dibromopyridazinedione reagents that allow for the efficient functional re-bridging of interchain disulfides[41]. Because this type of site-specific conjugation reagent is easy to prepare, many researchers have demonstrated site-specific ADCs with in vivo efficacy, and applied these reagents to other site-specific modified antibody therapeutic formats[42,43]. Disulfide re-bridging strategies can successfully tackle an important shortcoming in current

ADC preparation methods.

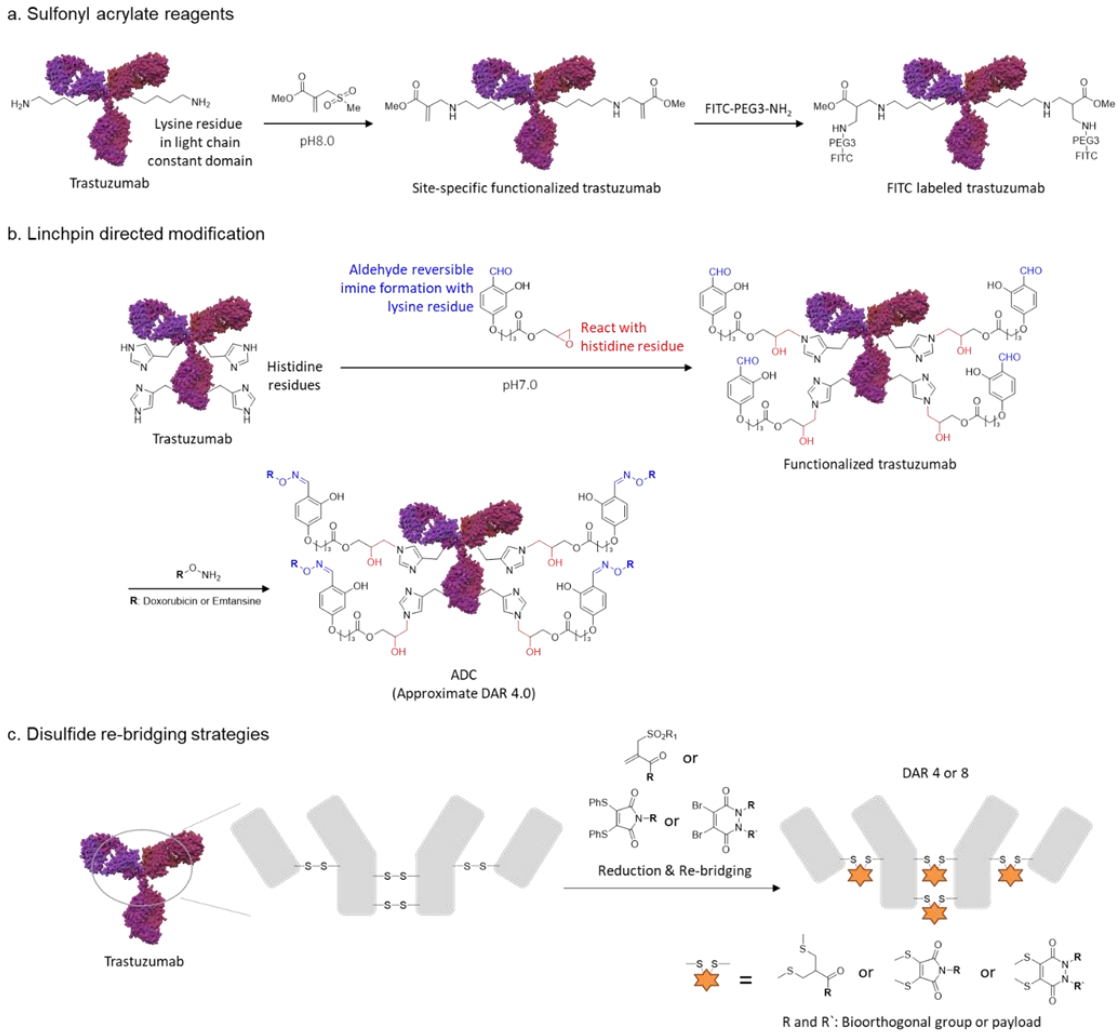

Figure 1. [a,b]Recent residue selective labeling for generating ADCs. [c]Disulfide re-bridging strategies.

1.4. Affinity peptide labeling for site-specific conjugation of native antibodies

1.4.1. Peptide traced labeling

Benzoylphenylalanine (BPA) is a synthetic amino acid that can be incorporated in a peptide during synthesis. Benzophenone (BP), which is part of BPA, is a photoreactive group that forms covalent bonds to other amino acids upon UV-exposure. BPA is considered to be efficient, stable, and also easy to handle[44], and it is primarily used to map protein−ligand interactions. When mapping interactions, the strategy is to produce variants of a protein with BPA incorporated at different positions, and then allow the protein to bind its interaction partner[45]. When the complex is subjected to UV light, BPA forms a diradical, which renders the generation of a covalent bond between the protein and its interaction partner possible.

In the past decade, photo affinity labeling using BPA incorporated in mAb affinity proteins or peptides has been developed by several groups (Figure 2a). Initially, in 2009, Jung et al. developed photoactivatable antibody binding proteins, which enabled irreversible and site-selective (Fc-region specific) antibody conjugation on solid surfaces as well as in solution[46]. Specific residues of the Fc-binding domain of protein G[47,48,49] were mutated to cysteine, and the resulting sulfhydryl groups were modified by maleimide-functionalized benzophenone molecules via a flexible chemical linker. These engineered small proteins could specifically capture intact antibodies and form covalent conjugates upon UV irradiation, therefore, allowing not only covalent antibody immobilization on solid surfaces, but also site-selective tagging of antibodies in solution by genetically adding various tags to photoactivatable proteins. These proteins ensure heavy chain selectivity as determined by SDS-PAGE, but the specific sites which are modified by this reaction have not been determined. Two years after this report, in 2011, Konrad et al. reported a similar

method using the photoactivatable Z domain of protein A[50,51,52,53]. This group showed that a detection-handle, biotin, could be incorporated in a specific position into the mAb by combining the inherent affinity of the Z domain and the Fc fragment with the ability of BPA to create a covalent bond. Specifically labeled antibodies using this method were successfully synthesized, characterized, and tested in different platforms. In 2013, Yu et al. reported using a Z domain photoactivatable protein applied to mouse IgGs[54] and in 2014, Hui et al. reported a similar method using BPA incorporated Z-domain[51,52,53] based, site-specific labeling to immobilize mAbs on nanoparticles[55]. The field of photo affinity labeling of native antibodies is now widespread[56-60] and very recently, Park et al.[61] and Vance et al.[62] have reported BPA incorporation in the Fc-III peptide[63] to modify Met 252 (EU numbering) in a site-specific manner. BPA was incorporated in the same position in the Fc-III peptide. In Vance`s work, BPA was substituted for each amino acid from the N-terminus to the C-terminus. Ac-DCAWHLGEL(BPA)WCT-NH_2 was the only sequence that completed the photo affinity labeling reaction. Furthermore, this group evaluated the equilibrium binding dissociation constants (K_D) to human IgG for each substitution sequence by the surface plasmon resonance (SPR) system. The results indicated that the photoconjugation reaction between the Fc-III BPA variants and the mAb was not driven by the non-covalent affinity of the peptide−antibody complex but rather by the precise positioning of the BPA moiety, suggesting a highly specific reaction with an appropriately positioned residue in the antibody. After site-specific peptide conjugation, MMAE was attached covalently, followed by hydroxylamine driven acetyl deprotection to expose the thiol moiety on the peptide tag and a DAR 1.9 ADC was obtained.

Upon UV irradiation, a photo-cross-linker can cross-link affinity peptides such as protein A (especially the Z domain[51,52,53]), pro-tein G[47,48,49], and Fc-III[63] to an antibody in a

site-specific manner. However, the lack of chemical selectivity of this method can result in nonspecific cross-linking, and a 30−60 min exposure to UV irradiation has been shown to cause protein damage[64]. To avoid the use of UV irradiation, Yu et al.[65] and Kishimoto et al.[66] have reported using a combination of an affinity peptide with the activated ester method to modify a lysine residue in a mAb (Figure 2b). Yu et al. used the Z domain of protein A[51,52,53] for site-specific conjugation. Several amino acid residues in the sequence were substituted with 4-fluorophenyl carbamate lysine (FPheK) and modification of the proximal Lys317 (EU numbering) was attempted. This group also synthesized and incorporated N-acryloyl-lysine (AcrK) and 2-amino-6-(6-bromohexanamido)hexanoic acid (BrC6K) into the appropriate amino acid positions. Substitution with AcrK or BrC6K showed 20−40% conjugation efficiency, which was significantly lower than that of FPheK (95%). Site-specific conjugation with the Alexa Fluor 488 covalently attached peptide reagent was also demonstrated, which had a 95% conjugation efficiency. Kishimoto et al. have also reported a similar lysine modification using a Fc-III -like peptide63, which was independently isolated from a random peptide phage library and optimized, named CCAP (Chemical Conjugation by Affinity Peptide). Conjugation efficiency was very high (close to 100%) and might be similar to that demonstrated by Yu et al., but the conjugation speed was dramatically faster than demonstrated by Yu, the reaction terminated within 15 min. Furthermore, the conjugation site was different from previous work, as the Kishimoto group site-specifically modified Lys248 (EU numbering). Several applications of this method have also been reported: emtansine was covalently attached to a peptide to synthesize a site-specific ADC and VHH was covalently attached to a peptide reagent to create a new bi-specific therapeutic plat-form. For site-specific

ADC synthesis, prepared NHS-Peptide-DM1 reagent was mixed with trastuzumab to obtain the mixture of DAR 0, 1, 2 species (Average DAR is unknown). Both, ADC and VHH conjugate, these newly created therapeutic antibody formats worked efficiently in in vitro assays. The affinity to FcRn was maintained in the monovalent peptide conjugate but was completely lost in the divalent peptides conjugate. It was assumed that this was because the binding site of the Fc-III de-rived peptide overlapped with that of FcRn. In agreement with a previous report63, the Fc-III peptide-binding region is similar to the protein A binding area, and therefore site-specific conjugation through a protein A derivative would give the same results as found by Kishimoto et al. Furthermore, binding to FcγRI was not affected by the Fc-III derived peptide modification, whereas binding to FcγRIIIa was unexpectedly enhanced by the modification by as much as 3.5-fold in the divalent conjugate.

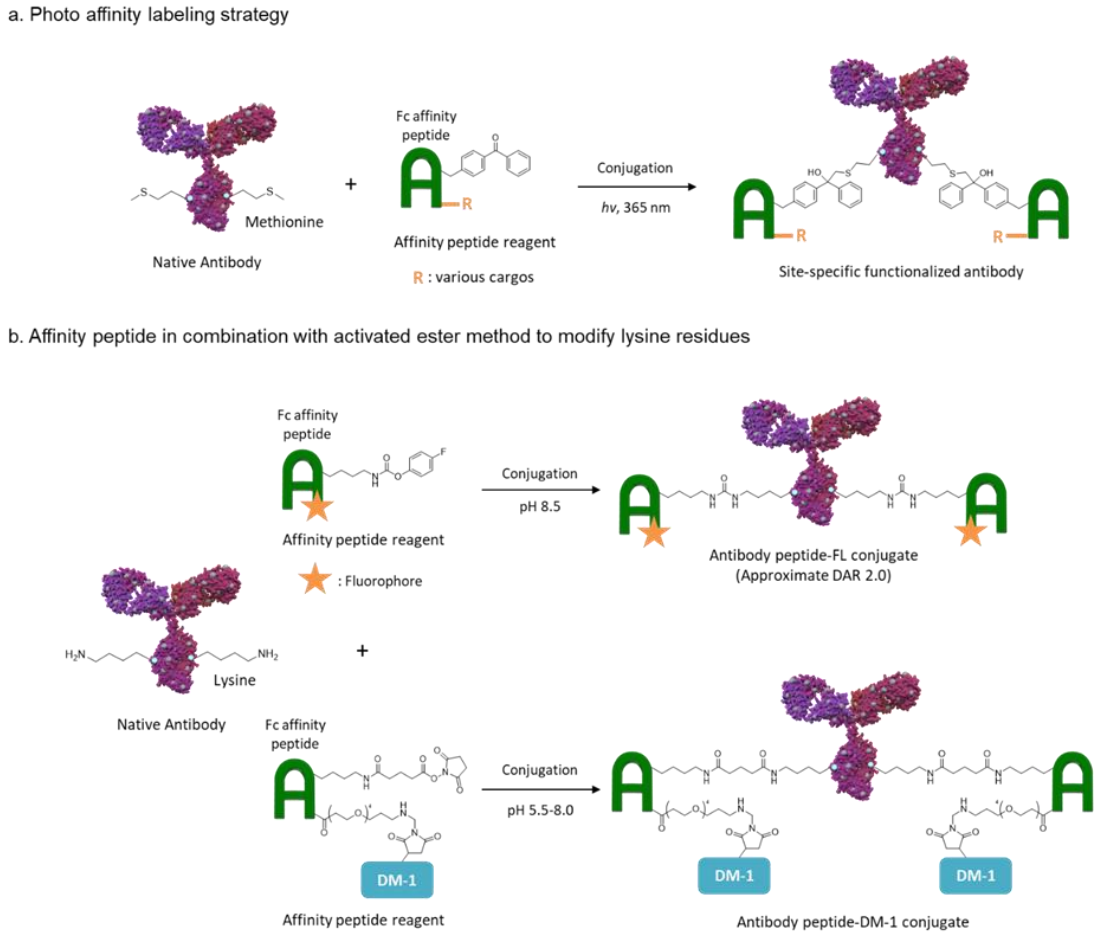

Figure 2. Affinity peptide traced labeling for site-specific conjugation. [a]Photo affinity labeling strategy. [b]Affinity peptide in combination with activated ester method to modify lysine residues.

1.4.2. Peptide traceless labeling

Important factors toward the success of ADCs in clinical use, are that these conjugates involve the use of either chimeric or murine antibodies, which can elicit an immunogenic response, and the use of lower potency drugs. One potential downside to using site-specific peptide traced labeling is that the inserted peptide sequence may be immunogenic in humans. Thus, developing peptide traceless labeling that eliminates the possibility of immunogenicity is highly desirable. Additionally, Kishimoto et al. demonstrated that the preparation of ADCs with DAR 2 by traceless labeling resulted in a loss of FcRn (neonatal Fc receptor) binding affinity, which would result in problematic pharmacokinetics: a lack of a recycling system and a decrease in the half-life of the ADCs.

Further investigation was needed for the affinity peptide mediated labeling system and Ohata et al.[67] have reported a practical method for peptide traceless labeling for ADC development and for immunoconjugate therapies. Ohata et al. used a hexarhodium metallopeptide catalyst to introduce an alkyne moiety to an asparagine residue in the CH2 domain of the mAb Fc region (Figure 3). 33 residues minimized Z domain was used in this reaction and several amino acid residues were substituted with glutamic acid to incorporate hexarhodium moieties. The specific residue modified in these reactions was confirmed by proteomics analysis. Trypsin digestion and tandem MS/MS identified Asn 312 in the Fc fragment as the modified residue. Asparagine has been previously identified as a reactive residue in rhodium-catalyzed modifications of this type[68], and, consistent with a proximity-driven mechanism, Asn312 flanks the binding interface between the protein and the Fc binding domain. Finally, a doxorubicin conjugated ADC was synthesized and the average DAR was calculated to be 1.0. This was the first report that used an affinity peptide for the catalyst to introduce a small functional attachment into a non-

mutated mAb.

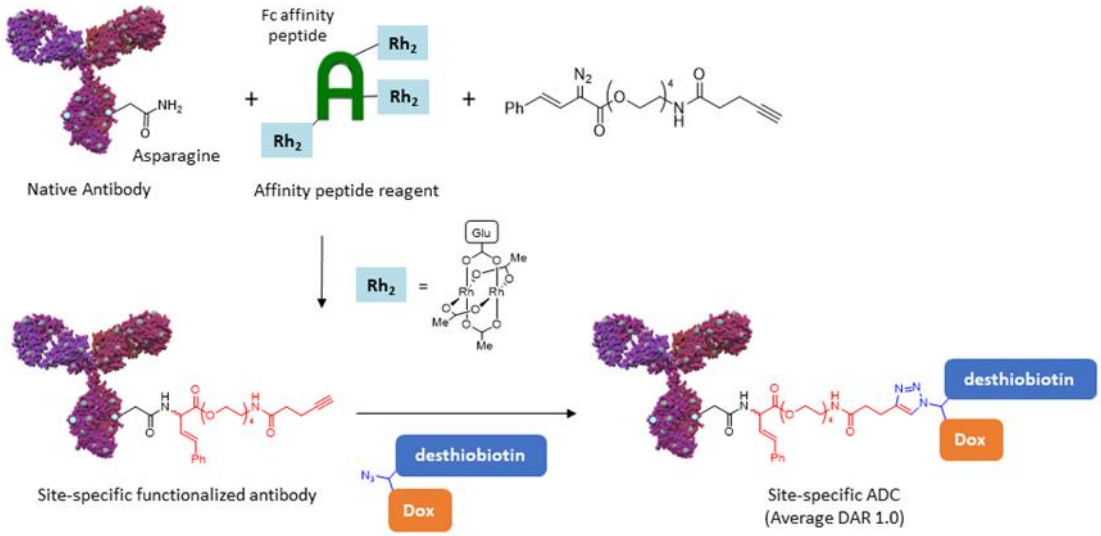

Figure 3. Affinity peptide traceless labeling for site-specific conjugation using the metallo-peptide method.

2. Affinity peptide meditated site-specific conjugation

2.1. Design and synthesis of peptide reagents

An abundance of sequences of mAb-affinity peptides are known[69,70]. Protein A is a versatile protein framework that binds to the Fc region. It is used in the construction of affinity columns, which are essential pieces of equipment for purifying mAbs for the manufacture of mAb-containing pharmaceuticals[70]. Starovasnik et al. selected the core protein framework of protein A and downsized it by Z-domain motif library[71,72], indicating the affinity only in the Fc region of mAbs, at a protein A sequence known as Z34C (FNMQCQRRFYEALHDPNLNEEQRNAKIKSIRDDC). Meanwhile, DeLano et al. [63] selected a tridecapeptide called Fc-III (DCAWHLGELVWCT) by M13 bacterio-phage display, as this phage binds at a common site between the CH2 and CH3 domains of the Fc region, and the binding area is the same as that of Z34C. The *K*d values of Z34C and Fc-III are estimated to be approximately 20 nM at pH 7.4 and 16 nM at pH 6.0. Previously, we identified a peptide consisting of 17 amino acids (RGNCAYHRGQLVWCTYH) through biopanning against human IgG1 from random peptide library constructed on T7 phage display system[66]. This peptide sequence is similar to Fc-III, but it has a high affinity on human IgG Fc compared to Fc-III, which *K*d value of peptide (RGNCAYHRGQLVWCTYH) was 9 nM. Hence, the affinity of these peptides were sufficient to use these sequences to place a reactive electrophilic moiety in the vicinity of a target lysine residue.

To design our peptide reagents, we initially measured the distance between affinity peptides and the antibody lysine residues from the co-crystal structure of each of the two peptides and the Fc region of IgG (Figs. 4–7). According to the co-crystal structure of the Fc-III peptide and IgG1 Fc, the distance between L6 and Fc K248 was approximately 5.9

Å. From the Z34C and Fc crystal structures, the distances of M3, R31, E20 and Fc K248, K288, and K317 were approximately 12.5, 13.7, and 4.0 Å, respectively. This information provided us with reasonable confidence in designing linkers of an appropriate length.

Generally, dithiobis(succinimidyl propionate) (DSP, Lomant's reagent) is a useful tool for labelling proteins with high frequency, and the length of the spacer arm is approximately 12 Å[73]. In terms of chemical properties, the side chains of lysine and arginine are similar among proteinogenic amino acids[74,75]. Therefore, we also carefully designed a peptide sequence to replace the lysine residue with arginine and an appropriate amino acid with lysine so that we could connect the linker only to the lysine residue in the peptides.

The designed peptide sequences were synthesized by the established Fmoc-based solid-phase method, and we conducted disulfide cyclization by treatment with H_2O_2 and methanolic NH_3 for Fc-III and glutathione oxidation for Z34C[76,77]. After the purification of cyclized peptides by reversed-phase chromatography, the DSP linker was attached to obtain the target peptide reagents (see the 2.3. Experimental Section). Owing to partial spontaneous hydrolysis to the corresponding carboxylic acid, the peptide reagent was partially contaminated, but more than 80% nonetheless consisted of the desired N-hydroxysuccinimide (NHS)-activated product.

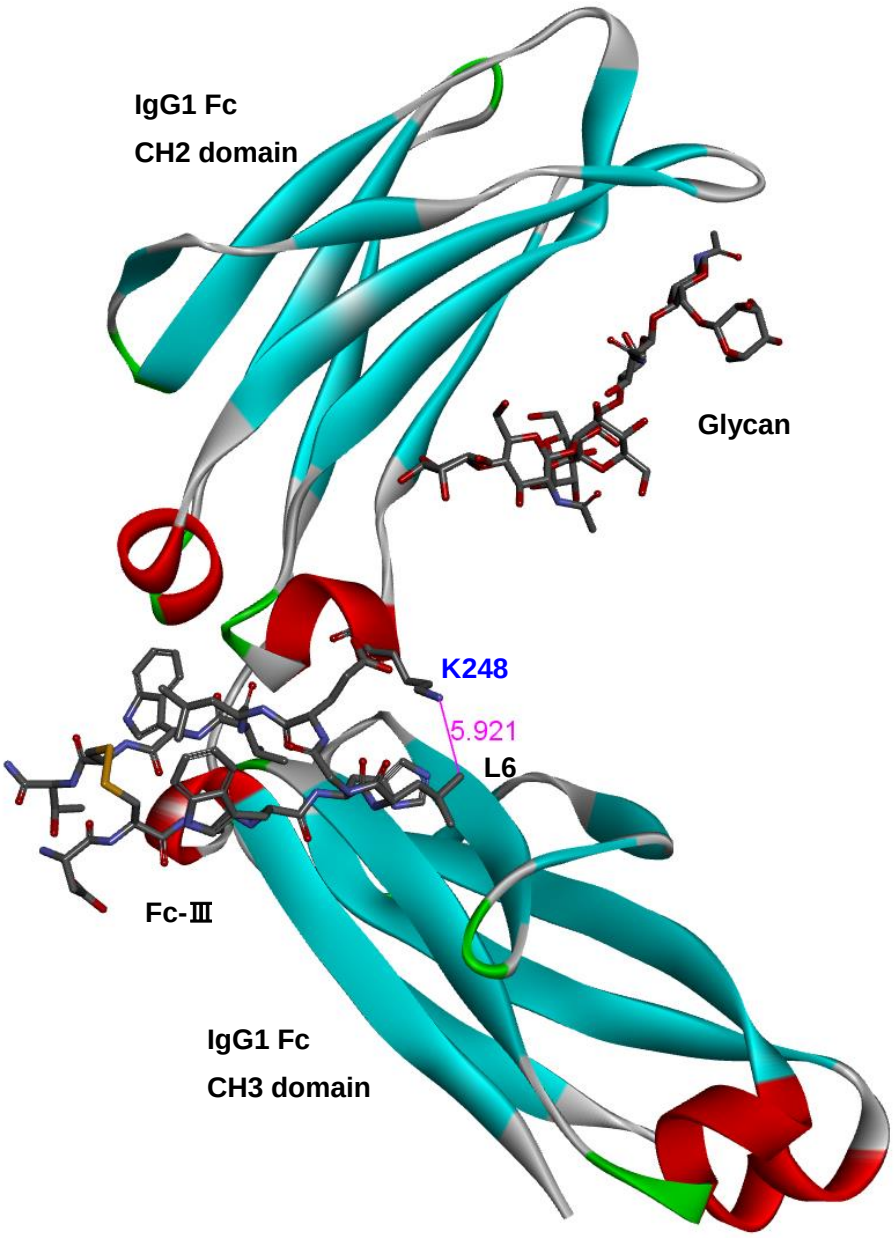

Figure 4. Distance between Fc-III L6 and IgG1 Fc K248 from PDB ID: 1DN2.

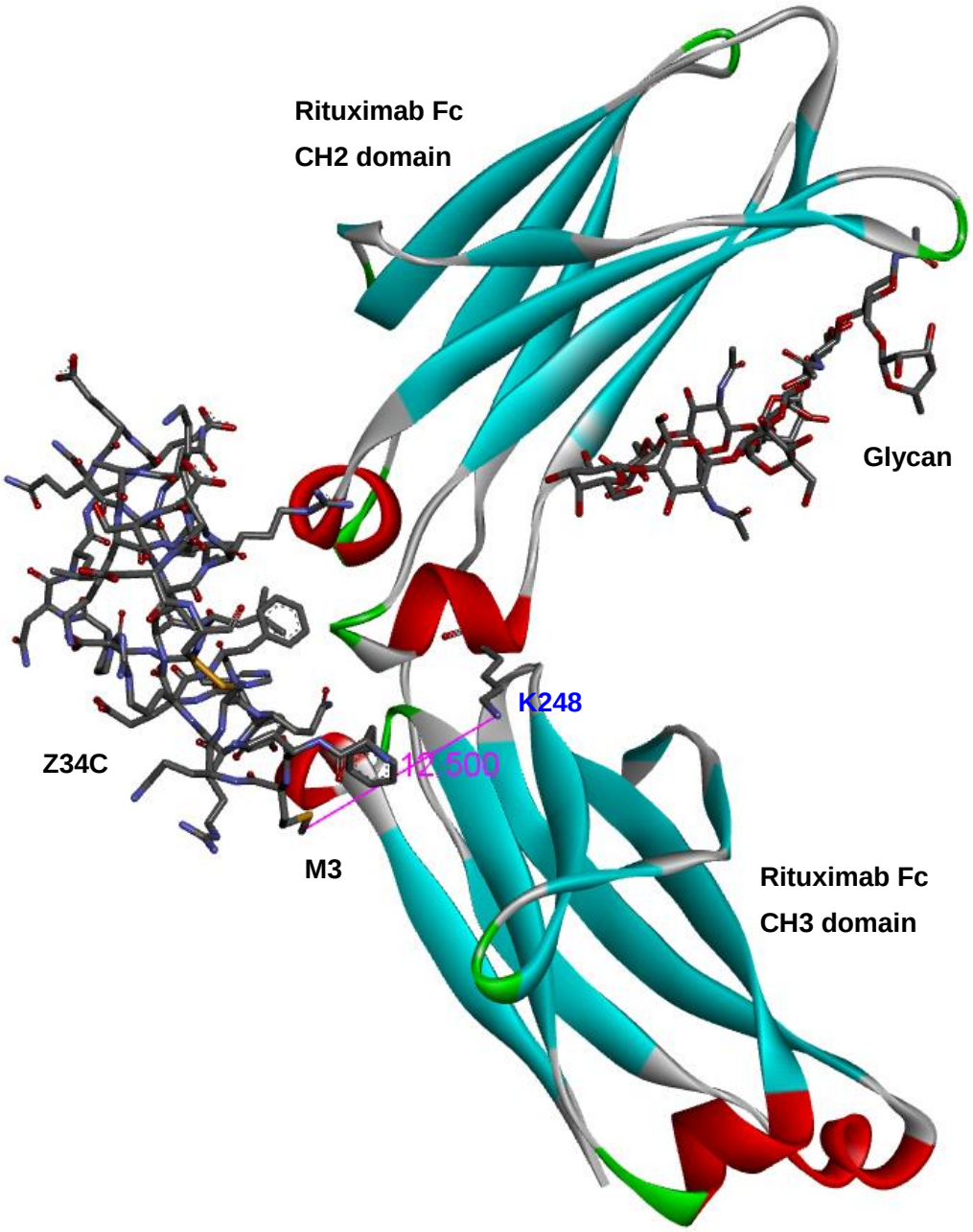

Figure 5. Distance between Z34C M3 and IgG1 Fc K248 from PDB ID: 1L6X.

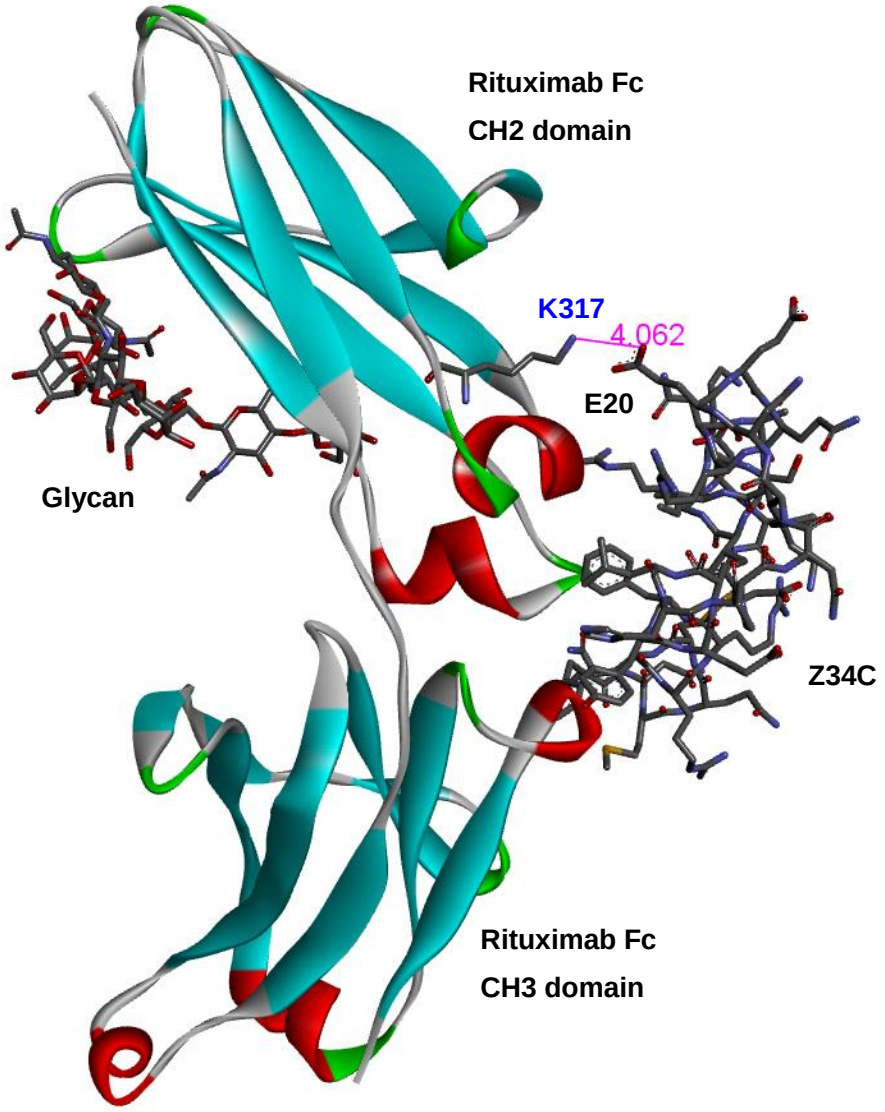

Figure 6. Distance between Z34C E20 and IgG1 Fc K317 from PDB ID: 1L6X.

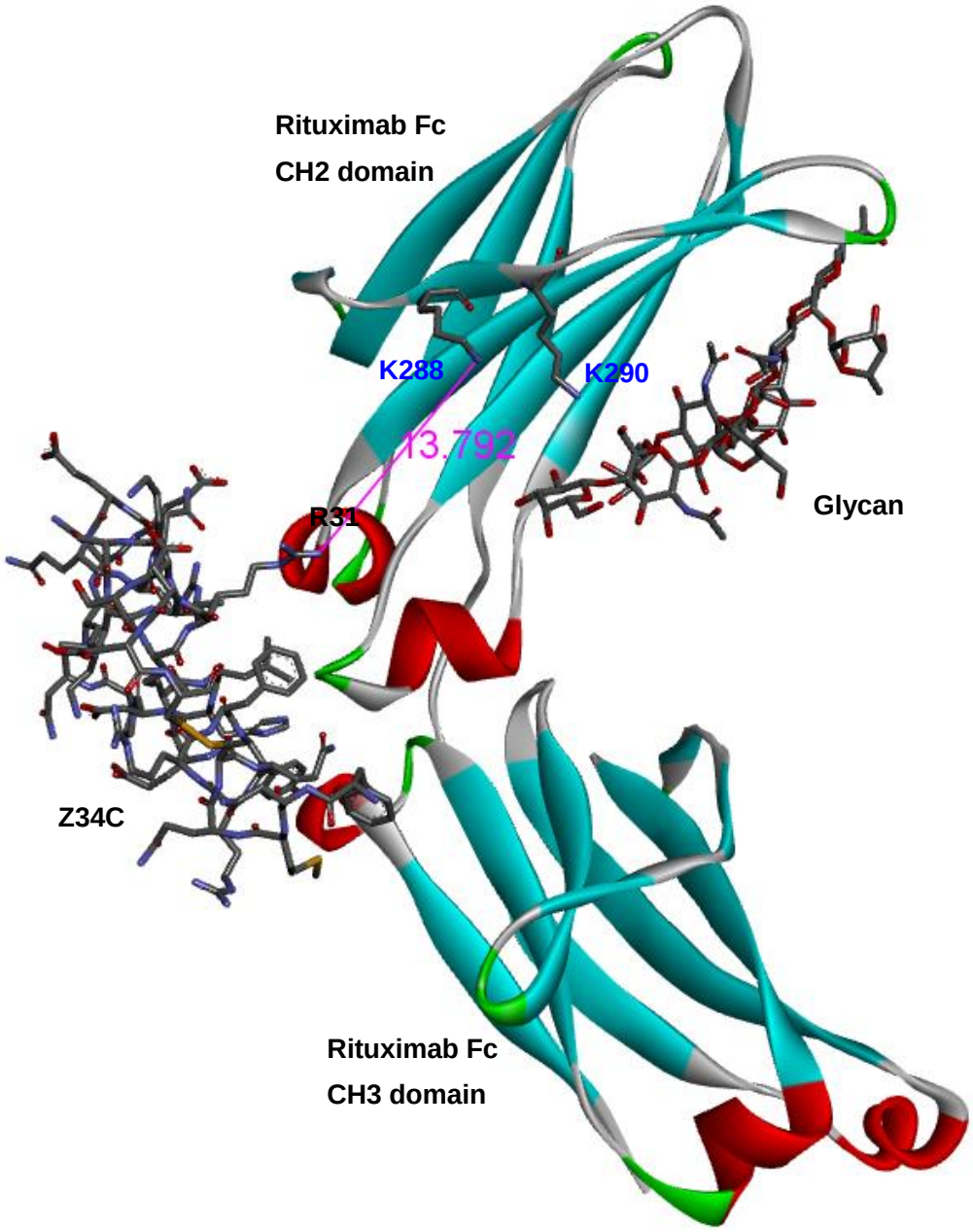

Figure 7. Distance between Z34C R31 and IgG1 Fc K288 from PDB ID: 1L6X.

2.2. Conjugation study to trastuzumab

Notably, the NHS ester group readily reacts with lysine residues in the antibody and/or is hydrolytically decomposed to yield the inactivated peptide reagent at neutral pH[78,79]. From accumulated evidence[80,81], we assumed that a lower pH buffer might decrease the decomposition rate of the NHS ester, and thereby improve the yield of our desired affinity labelling reaction. Determine the applicability of the reaction between the affinity reagent and a mAb, we conducted optimization studies using the commercially avaliable anti-HER2 antibody trastuzumab. The optimal peptide conjugation conditions were determined to be 18 μM trastuzumab in 50 mM sodium acetate buffer (pH 5.5), with the addition of 10 equivalents of peptide reagent (5 mM in DMF) incubated at 20 °C for 1 h (Fig. 8a). In the conjugation of affinity peptide reagent **1a** to trastuzumab, a product with a peptide/antibody ratio (PAR) of 1 was a minor contaminant, but the desired compound with a PAR of 2 was the major product (Fig. 8b,c). To evaluate the initial selectivity of this reaction, we added a 10 mM solution of tris(2-carboxyethyl)phosphine (TCEP) to the reaction tube and analysed the reduced MS spectrum (Fig. 8d). This indicated that only the 3-mercaptopropionate group was introduced at the heavy chain as we expected. Interestingly, even if the amount of peptide reagent was increased to 30 equivalents, the number of PAR was not increased by non-specific conjugation. And also, an acidic pH is important for not only to prevent unspecific conjugation but also for decreasing the decomposition rate of NHS ester during the conjugation reaction. Moreover, the purity of peptide reagent is proportional to the excess peptide reagent required for reaction completion.

The location of the specific residue that was modified by 3-mercaptopropionate in this reaction was confirmed through peptide mapping analysis. Trypsin digestion and tandem

MS/MS analysis identified residues Lys246 and Lys248 (EU numbering) in the Fc fragment as the residues modified (see the 2.3. Experimental Section)[82,83,84]. Although trypsin digestion resulted in a long peptide fragment with 33 amino acid residues, including residues Lys246 and Lys248, due to its vicinal location it was difficult to determine the precise posi-tion with MS data alone – some of the spectra showed the Lys248 modification, but we cannot ignore the possibility that Lys246 was modified. It is also notable that according to the co-crystal structure information, the distance between Fc-III Leu6 and Fc Lys248 (5.9 Å) was shorter than that between Fc-III Leu6 and Lys246 (17.3 Å). From this information, the majority of the modification seems to be located at Lys248 in our affinity labelling of **1a**.

Having achieved conjugation to obtain the antibody affinity peptide conjugate (AAPC) **1** from peptide reagent 1a, we next investigated the conjugation of Z34C peptide reagents **2a**, **3a** and **4a** to trastuzumab (Figs. 9-11). In the case of the synthesis of AAPC **2**, the site selectivity was almost the same as for AAPC **1**, and the results of peptide mapping (see the 2.3. Experimental Section) indicate that selective modification occurred at residues K246 and K248. Presumably, the modification is predominant at K248, as with the conjugation of **1a**. When the peptide reagent **3a** was used in an attempt to obtain AAPC **3**, the starting material trastuzumab and PAR 3 species appeared as minor contaminants, but the major products were PAR 1 and PAR 2 species (Fig. 10). The reaction to produce AAPC **3** did not proceed even when we added **3a** in vast excess. We determined that this result occurred because the spontaneous decomposition of the peptide reagents to their inactivated forms was faster than the desired mAb conjugation reaction, even under acidic conditions. The peptide mapping results indicated that residues K288 and K290 were modified (see the 2.3. Experimental Section). The distances between peptide and antibody

residues were nearly the same as in **1a** and/or **2a** conjugation, and the distances between R31 and Fc Lys288 and Lys290 were approximately 13.7 and 16.4 Å, respectively. We concluded that **3a** labelled both lysine residues. Furthermore, we succeeded in obtaining AAPC **4** from peptide reagent **4a** and, according to our peptide mapping evaluation (Fig. 11 and see the 2.3. Experimental Section), concluded that Lys317 was selectively modified. Collectively, we built to the creation of a panel of peptide reagents to label different and specific mAb lysine residues.

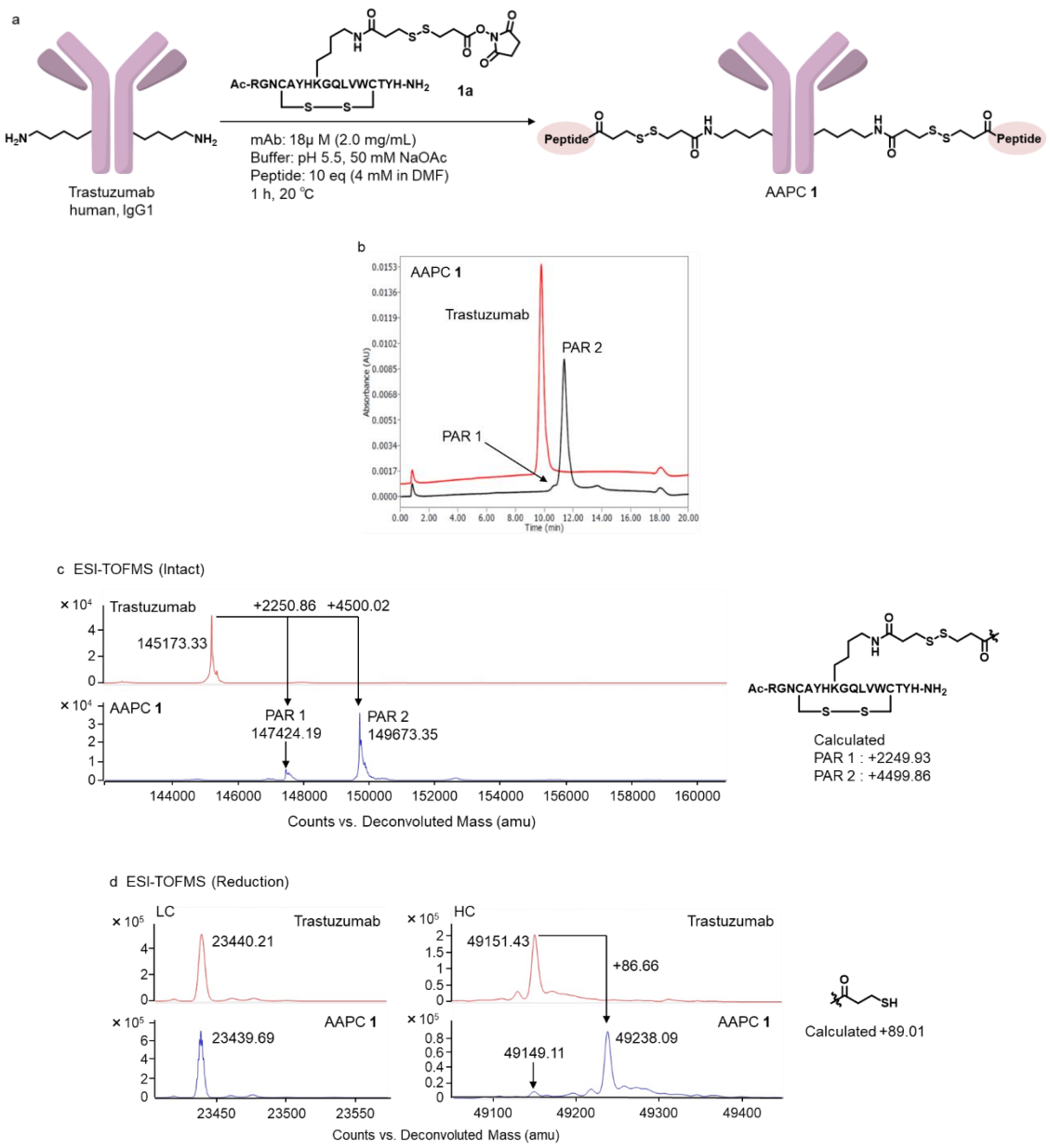

Figure 8. Conjugation of peptide reagent **1a** to trastuzumab. [a]Scheme of conjugation **1a** to trastuzumab. [b]HIC-HPLC. [c]ESI-TOFMS (Intact); observed *m/z* and calculated *m/z* is indicated. [d]ESI-TOFMS (Reduced condition, LC is light chain and HC is heavy chain; observed MS and calculated *m/z* is indicated.)

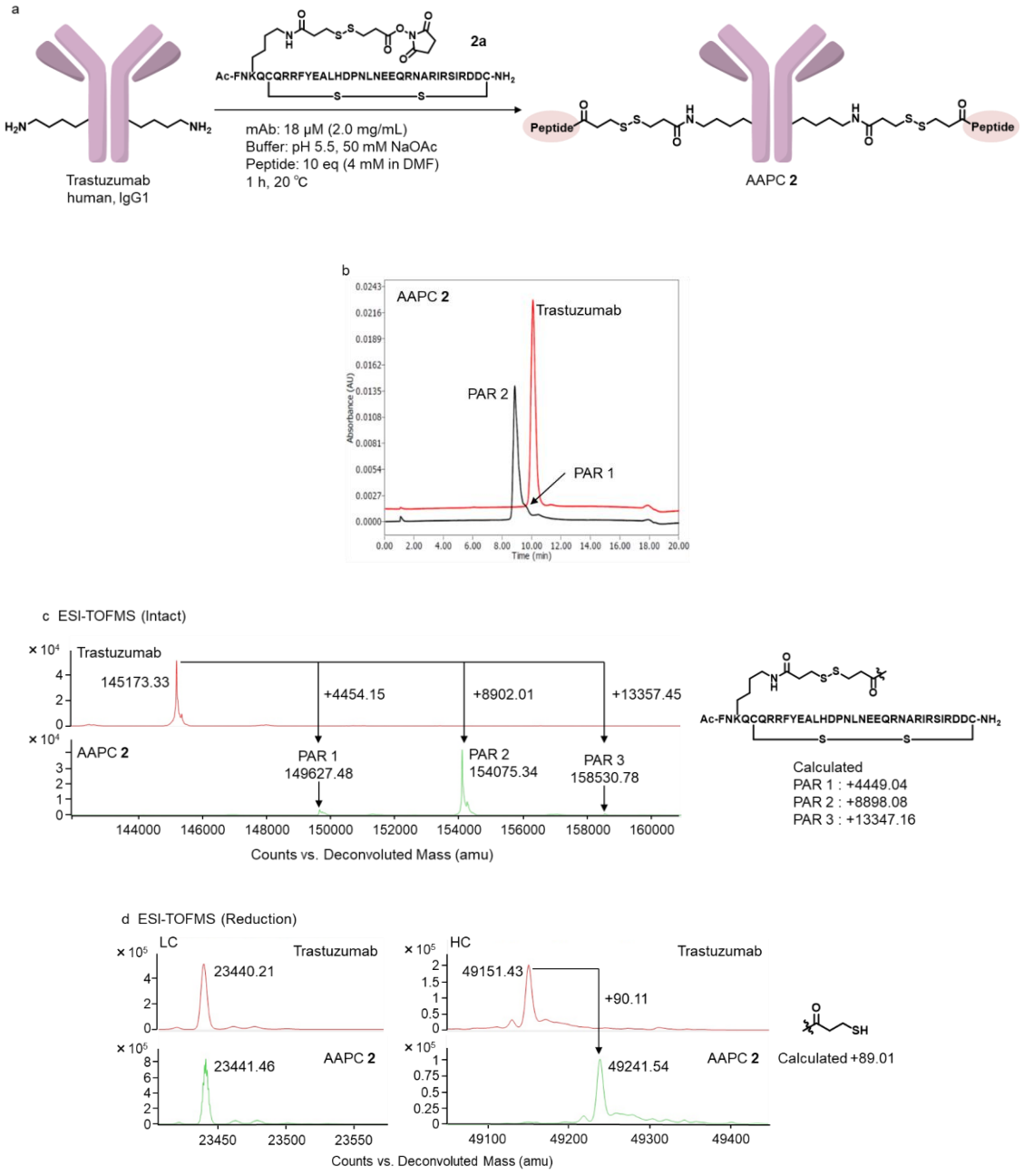

Figure 9. Conjugation of peptide reagent **2a** to trastuzumab. [a]Scheme of conjugation **2a** to trastuzumab. [b]HIC-HPLC. [c]ESI-TOFMS (Intact); observed *m/z* and calculated MS is indicated. [d]ESI-TOFMS (Reduced condition, LC is light chain and HC is heavy chain); observed *m/z* and calculated *m/z* is indicated.)

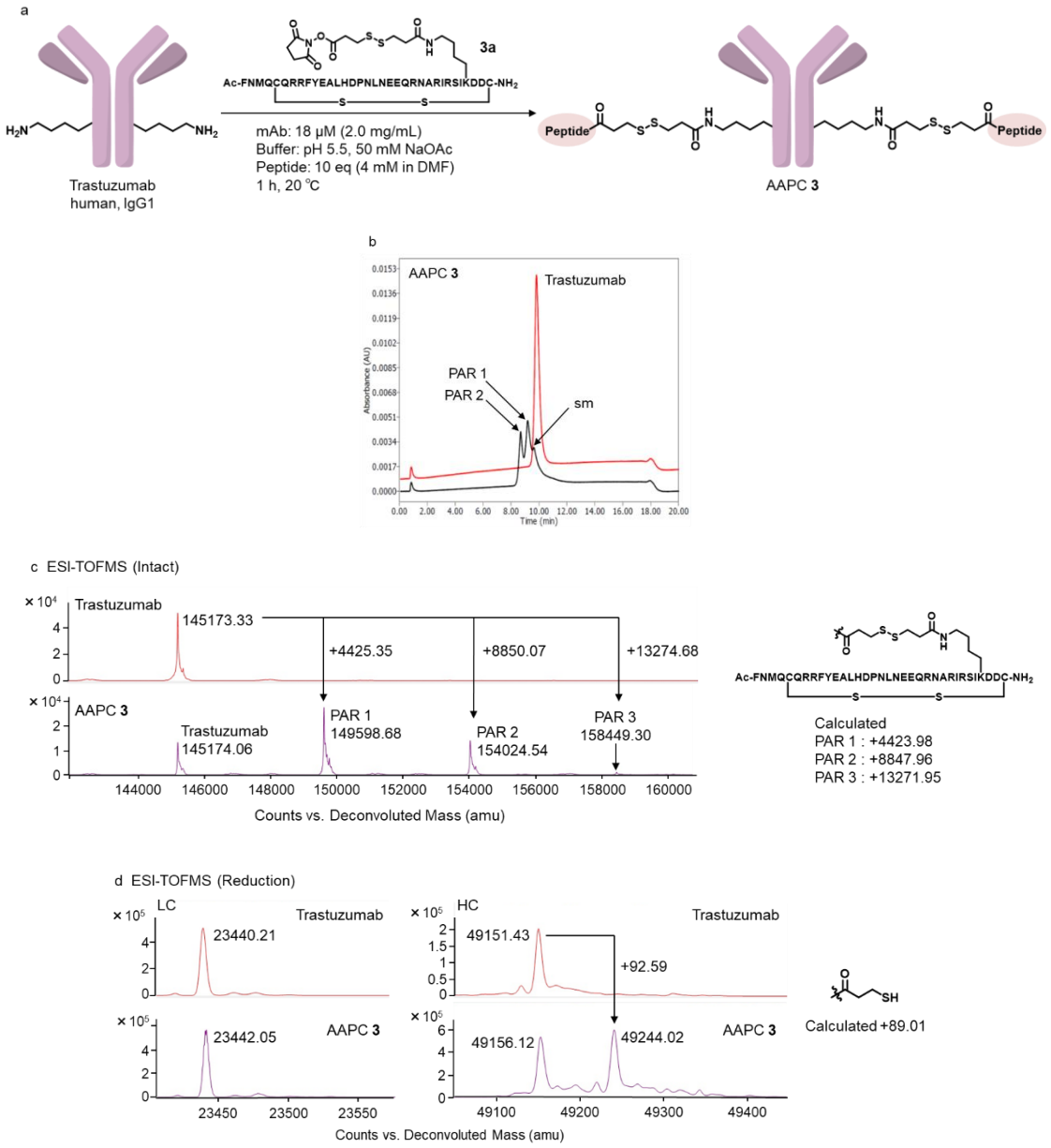

Figure 10. Conjugation of peptide reagent **3a** to trastuzumab. [a]Scheme of conjugation **3a** to trastuzumab. [b]HIC-HPLC. [c]ESI-TOFMS (Intact); observed MS and calculated *m/z* is indicated. [d]ESI-TOFMS (Reduced condition, LC is light chain and HC is heavy chain; observed *m/z* and calculated *m/z* is indicated.)

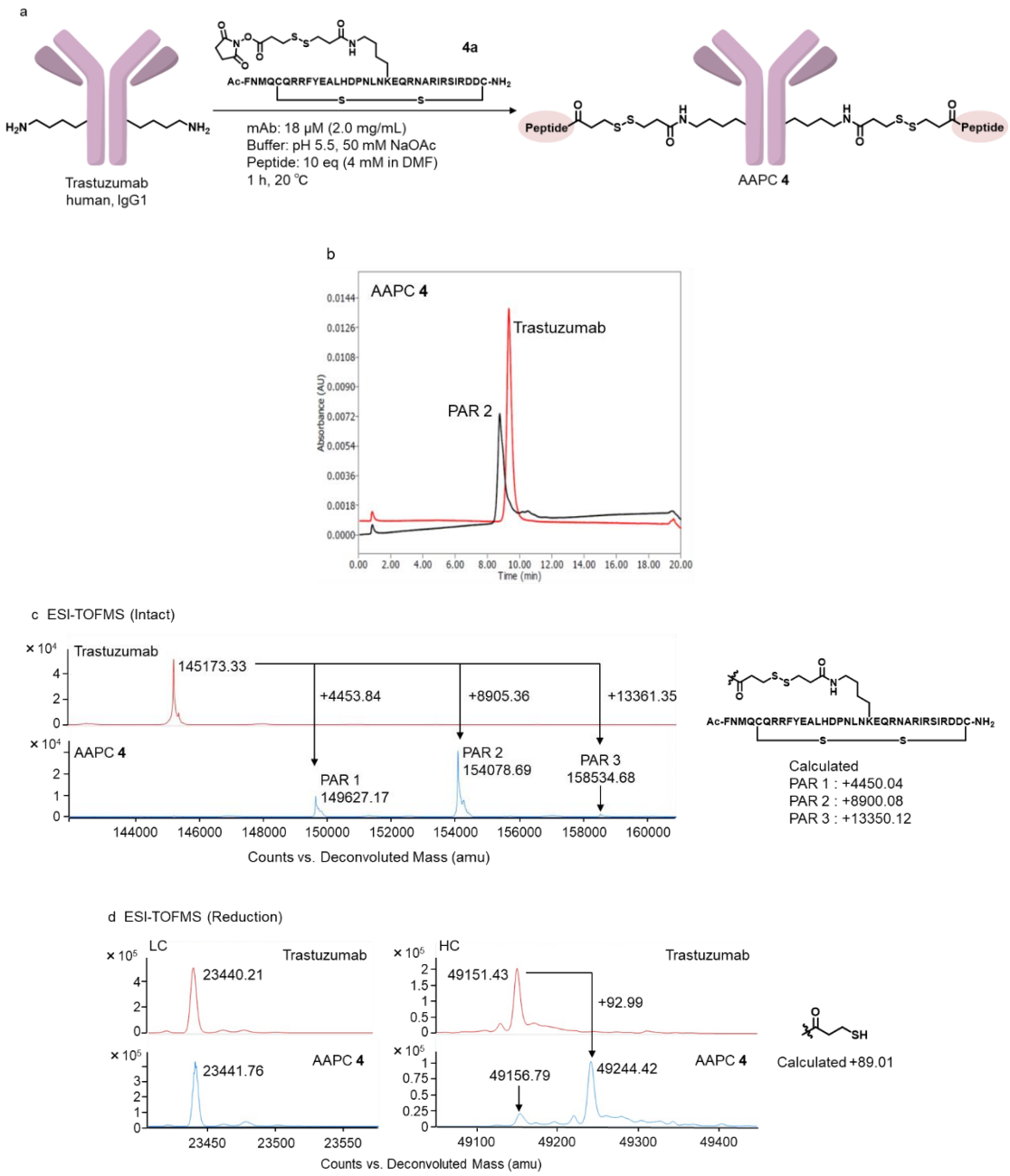

Figure 11. Conjugation of peptide reagent **4a** to trastuzumab. [a]Scheme of conjugation **4a** to trastuzumab. [b]HIC-HPLC. [c]ESI-TOFMS (Intact); observed MS and calculated *m/z* is indicated. [d]ESI-TOFMS (Reduced condition, LC is light chain and HC is heavy chain; observed *m/z* and calculated *m/z* is indicated.)

2. 3. Experimental Section

2.3.1. Chemicals

Unless otherwise noted, the chemicals and solvents used were of analytical grade and were used as received from commercial sources. SMCC-DM-1 was purchased from Abzena (USA). Fmoc-NH-SAL-PEG Resin,HL, 1-Hydroxy-1H-benzotriazole, anhydrous (HOBt), 1-[Bis(dimethylamino)methylene]-1H-1,2,3-triazolo[4,5-b]pyridinium 3-oxid hexafluorophosphate (HATU), Fmoc-Rink amide linker, Fmoc-L-Gly-OH, Fmoc-L-Leu-OH, Fmoc-L-Ile-OH, Fmoc-L-Val-OH, Fmoc-L-Lys(Boc)-OH, Fmoc-L-Ala-OH, Fmoc-L-Cys(Trt)-OH, Fmoc-L-Gln(Trt)-OH, Fmoc-L-Asn(Trt)-OH, Fmoc-L-Glu(OtBu)-OH, Fmoc-L-Asp(OtBu)-OH, Fmoc-L-Arg(Pbf)-OH, Fmoc-L-Phe-OH, Fmoc-L-Trp(Boc)-OH, Fmoc-His(Boc)-OH, Fmoc-L-Ser(tBu)-OH, Fmoc-L-Thr(tBu)-OH, Fmoc-L-Tyr(tBu)-OH, Fmoc-L-Pro-OH and triisopropylsilane (TIPS) were purchased from Watanabe Chemical (Japan). Trifluoroacetic acid (TFA), 1,2-ethanedithiol (EDT), Glutathione oxidized form (GSSG) N-ethyldiisopropylamine (DIPEA) dithiobis(succinimidyl propionate) (DSP), L-Ascorbic Acid (DHAA) and Tris(2- carboxyethyl)phosphine hydrochloride (TCEP HCl) were purchased from Tokyo Chemical Industry (Japan). Chromatography sol¬vents were used without distillation. 2M NH3-MeOH, Peptide synthesis-grade N, N-dimethylformamide (DMF), dichloromethane (DCM), HPLC-grade acetonitrile and diethyl ether were obtained from Fujifilm-Wako (Japan). Hydrogen peroxide ultrapure (30%~32%) was purchased from KANTO Chemical (JAPAN).

2.3.2. Monoclonal antibodies, enzyme and antigen

Human, IgG1 trastuzumab (Herceptin®) 150 mg purchased from Chugai Pharmaceutical Company. Human, IgG1 adalimumab (Humira®) 80 mg purchased from Eisai Pharmaceutical Company. Human, IgG2 denosumab (Pralia®) 60 mg was purchased from Daiichisankyo. Human, IgG4 dupilumab (Dupixent®) 300 mg was purchased from SANOFI, Regeneron. Before use, monoclonal antibodies were dialysis by Spectra/Por® Float-A-Lyzer® G2, MWCO:20kDa, Volume: 10 mL. PNGase F 15,000 units from Flavobacterium meningosepticum, New England Biolabs. HER2-Fc recombinant was purchased from R&D system, which was used for measuring binding affinity of ADC and antibody.

2.3.3. Instruments

Centrifugations were performed with a CT15E (Hitachi, Japan). Peptide were synthesized by the automated microwave peptide synthesizer (CEM, Liberty Blue HT™). HIC analysis was performed by ACQUITY UPLC H-Class PLUS system and Protein-Pak Hi Res HIC, 2.5 µm, 4.6 × 100 mm (waters). Protein purification was conducted by Amicon Ultra Centrifugal Filters-0.5 mL (Merck). For ADC synthesis, we used illustra NAP-10 or NAP-25 for removing excess unreacted payload. Concentration of proteins were determined a NanoDrop™ Lite (Thermo Fischer) instrument or Slope Spectroscopy® method with a Solo VPE system. LC-MS chromatograms and associated mass spectra were acquired using Agilent 6545XT Advance Bio LC/Q-TOF System. X-ray structure analysis were confirmed by Discovery Studio Visualizar. Peptide purity were determined by an L-2200 system (HITACHI) equipped with an Inertsil ODS-3 3 µm, C18, 4.6 × 1250 mm (GL science). Each peptide reagent mass spectrum was detected by an LCMS-2020 system equipped with a ODS-3, 2.1 × 50 mm, 5 µm (GL science).

Peptide map analysis was performed using Easy-nLC (Thermo Fischer Scientific) coupled to Orbitrap Fusion instrument (Thermo Fischer Scientific). SPR study was conducted by Biacore T-200 and CM5 sensor chip (GE Healthcare).

2.3.4. LC-MS for peptide and peptide reagent synthesis

Each samples (1 mg mL–1, 10 μL in 0.5% TFA water) were analyzed using an LCMS-2020 system equipped with a ODS-3, 2.1 × 50 mm, 5 μm (GL science). Elution conditions were as follows: mobile phase A = 0.1% formic acid water; mobile phase B = 0.1% formic acid acetonitrile; gradient 0-5 min, 5%-90% phase B; 5-8 min, 90% phase B; flow rate = 0.2 mL min–1. Detecting absorbance is 190 nm.

2.3.5. Measuring purity for peptide reagents

Each samples (1 mg mL–1, 10 μL in 0.1% TFA water) were analyzed using an L-2200 system (HITACHI) equipped with a Inertsil ODS-3 3 μm, C18, 4.6 × 1250 mm (GL science). Elution conditions were as follows: mobile phase A = 0.1% TFA water; mobile phase B = 0.1% TFA acetonitrile; gradient over 30 min from A:B = 90:10 to 50:50; flow rate = 1.0 mL min–1. Detecting absorbance is 210 nm.

2.3.6. ACQUITY UPLC H-Class PLUS system and Protein-Pak Hi Res HIC

Each sample (1 mg mL–1, 5 μL in PBS) was analyzed using an ACQUITY UPLC H-Class PLUS system equipped with a Protein-Pak Hi Res HIC, 2.5 μm, 4.6 × 100 mm (Waters). Elution conditions were as follows: mobile phase A = 0.1 M sodium phosphate containing ammonium sulfate (2.3 M) (pH 7.0); mobile phase B = 0.1 M sodium

phosphate (pH 7.0); gradient over 30 min from A:B = 60:40 to 0:100; flow rate = 0.6 mL min–1. Detecting absorbance was 280 nm.

2.3.7. 6545XT Advance Bio LC/Q-TOF System

Each samples after conjugation (1 mg mL−1, 0.5 µL in ammonium acetate) was analysed using an Agilent 6545XT AdvanceBio LC/Q-TOF system equipped with a PLRP-S column (2.1 × 50 mm, 1000 Å, 5 µm). The elution conditions were as follows: mobile phase A = 0.1% formic acid water; mobile phase B = 0.1% formic acid in acetonitrile; gradient 0–1 min, 0–20% B; 1–3 min, 20–50% B; 3–4 min, 50–70% B; flow rate = 0.5 mL min−1. The absorbance was measured at 280 nm. Automatic data processing was performed with MassHunter BioConfirm software (Agilent) to analyse the intact and reduced MS spectra. For intact deconvolution, we used a mass range of 100,000–180,000 and a limited m/z range of 1000–4000. For reduction deconvolution, we used a mass range of 20,000–60,000 and a limited m/z range of 1000–3000. Moreover, we used DAR Calculator software (Agilent) to determine the PAR and DAR.

2.3.8. Synthesis of peptide reagents

2.3.8.1. Synthesis of peptide reagent **1a** (Fig. 12)

Synthesis of **S1**

Peptide synthesis was conducted by CEM Liberty Blue HT™ standard method. To remove a Fmoc-protecting group after each coupling, resin (100 µmol) was treated with piperidine (5 mL of 20% in DMF) and washed with DMF. For the coupling Fmoc protected amino acid (4 eq) was mixed with 1-[bis(dimethylamino)methylene]-1H-1,2,3-triazolo[4,5-b]pyridinium 3-oxid hexafluorophosphate (HATU, 4 eq), 1-Hydroxy-1H-

benzotriazole, Anhydrous (HOBt, 4 eq) and *N*,*N*-diisopropylethylamine (DIPEA, 6 eq) in DMF.

Synthesis of **S2**

After completion of peptide elongation, the resin was treated with 30% acetic anhydride in DMF for 30 min and then washed with DMF (2×5 mL) and DCM (3×5 mL). The acetyl-capped resin containing protected peptides was treated with 3 mL of TFA/EDT/TIPS/H_2O=95:2:2:1 solution at room temperature for 3 h. The solution was concentrated by evaporator and the crude peptides were precipitated with cold diethyl ether (5–6 mL) followed by collecting white crystals by filtration. The peptide pellet was dissolved in 0.05% TFA containing water to purify by reverse phase chromatography. After purification the acetonitrile was removed under reduced pressure and water was removed by sublimation to obtain **S1** (50.8 mg, 24.4 μmol) in 24.5% yield as an amorphous colorless solid. To the crude **S1** was added DMSO 5 mL, followed by 20 eq of 30% H_2O_2 aq (49.8 μL, 488 μmol), and 2 eq of 2 M NH_3-MeOH (24.4 μL, 48.8 μmol) and the reaction mixture was stirred for 12 h at room temperature. To this solution was added 2 mL of 0.05% TFA in water and the product was purified by preparatory reverse phase chromatography. Elution conditions were as follows: mobile phase A = 0.1% TFA water; mobile phase B = 0.1% TFA acetonitrile; gradient over 50 min from A:B = 100:0 to 50:50; flow rate = 1.0 mL min^{-1}, detected by 210 nm absorbance. The fractions containing the desired **S2** product were collected and combined. Acetonitrile and volatile organics were removed under reduced pressure and water was removed by sublimation to obtain target molecule **S2** (44.9 mg, 20.7 μmol) in 84.8% yield as an amorphous colorless solid.

Synthesis of **1a**

To **S2** (44.9 mg, 20.7 μmol) was added DMF 2 mL and DSP (dithiobis(succinimidyl propionate)) (167 mg, 414 μmol, 20 eq) and the reaction mixture was stirred for 12 h. To this solution was added 5 mL of 0.05% TFA in water and the product was purified by preparatory reverse phase chromatography. Elution conditions were as follows: mobile phase A = 0.1% TFA water; mobile phase B = 0.1% TFA acetonitrile; gradient over 50 min from A:B = 100:0 to 50:50; flow rate = 1.0 mL min^{-1}, detected by 210 nm absorbance. The fractions containing the desired **1a** product were collected and combined. Acetonitrile and volatile organics were removed under reduced pressure and water was removed by sublimation to obtain target molecule **1a** (41.0 mg, 17.3 μmol) in 83.5% yield as an amorphous colorless white solid.

MS (ESI) *m/z*: z=2 1183.20 $[M+2H]^{2+}$, z=3 789.10 $[M+3H]^{3+}$ (calculated: z=1 2364.68, z=2 1182.34, z=3 788.23) (Fig. 13)

Purity: 84.4% (15.6% was identified as the hydrolysis decomposition byproduct) (Fig. 14)

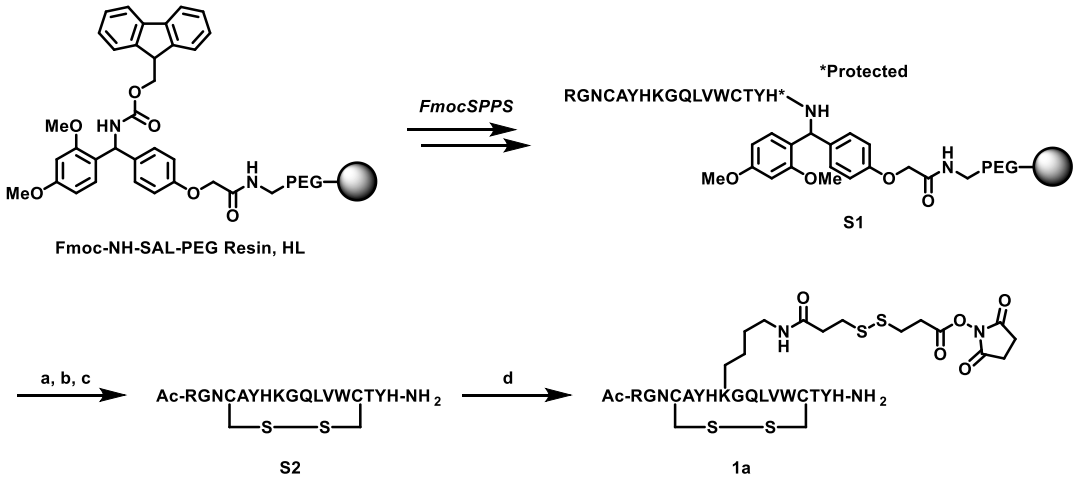

Figure 12. Synthesis of peptide reagent **1a**. Conditions of FmocSPPS Coupling: Fmoc-amino acid (4 eq), HATU (4 eq), HOBt (4 eq), DIPEA (6 eq). Fmoc deprotection: 20% piperidine in DMF. Reagents and conditions: (a) 30% Ac_2O/CH_2Cl_2, room temperature, 30 min. (b) TFA/EDT/TIPS/H_2O=95:2:2:1 solution, room temperature, 3 h. (c) H_2O_2 (2 eq), 2 M NH_3-MeOH (20 eq), DMSO, room temperature, 12 h. (d) DSP (dithiobis(succinimidyl propionate)) (20 eq), DMF, room temperature, 12 h.

a.

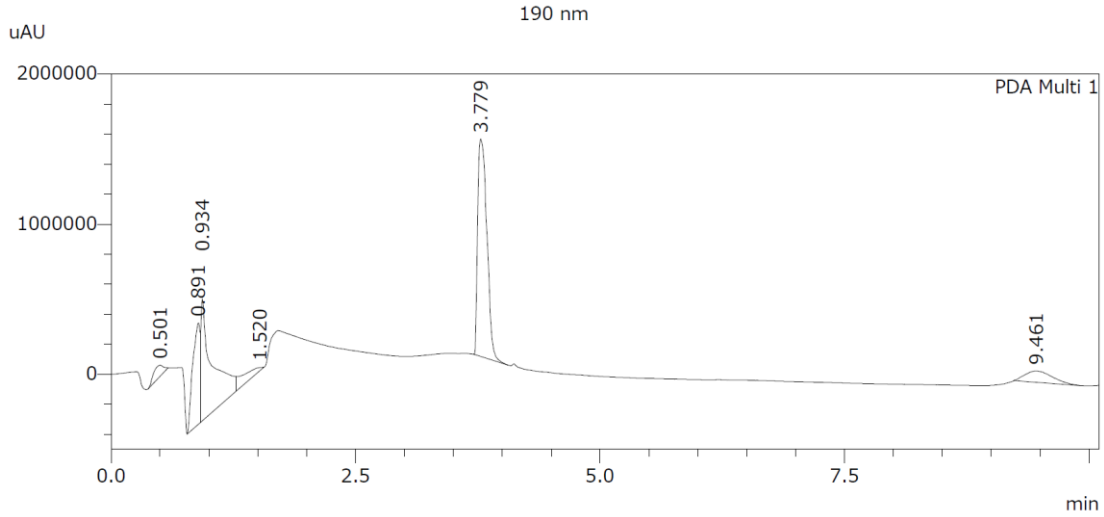

b. ESI-MS at 3.779 min.

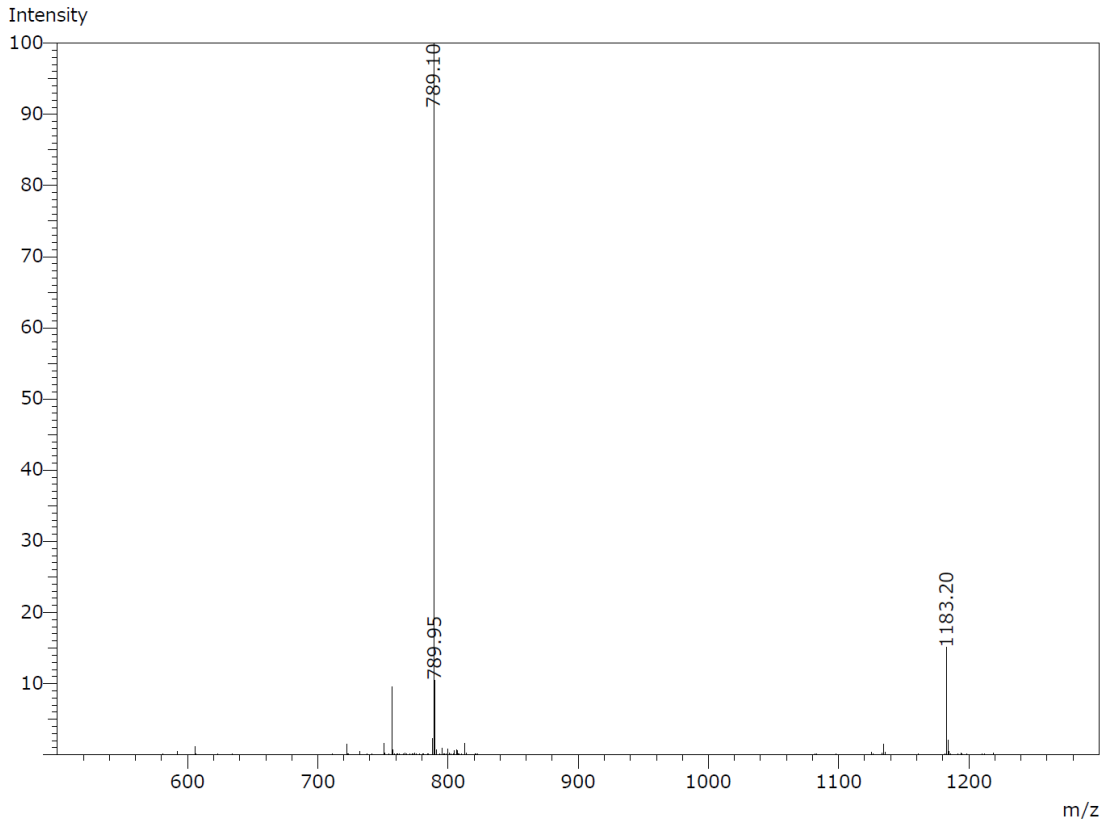

Figure 13. LC-MS results of **1a**. [a]HPLC trace (absorbance 190 nm) and [b]low-resolution ESI-MS spectrum.

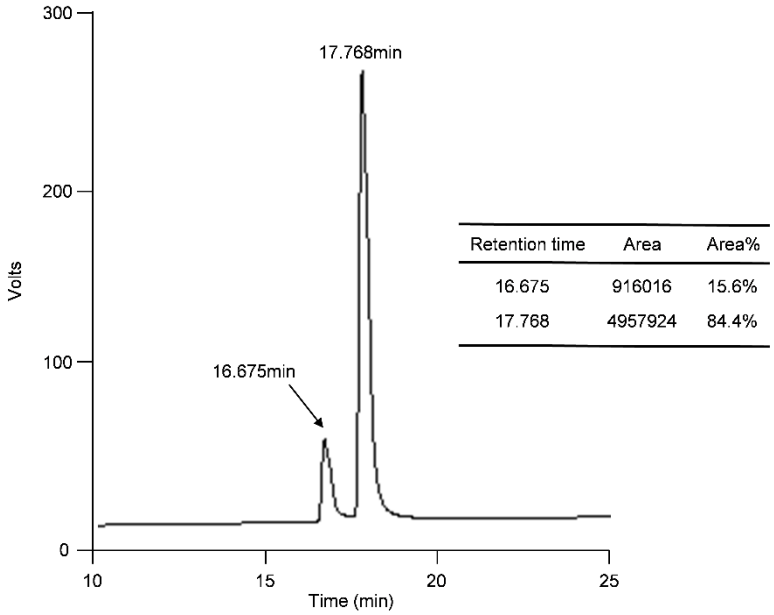

Figure 14. HPLC results of pure product **1a**.

2.3.8.2. Synthesis of peptide reagent **2a** (Fig. 15)

Synthesis of **S3**

Peptide synthesis was conducted by CEM Liberty Blue HT™ standard method. To remove a Fmoc-protecting group after each coupling, resin (100 µmol) was treated with piperidine (5 mL of 20% in DMF) and washed with DMF. For the coupling Fmoc protected amino acid (4 eq) was mixed with 1-[bis(dimethylamino)methylene]-1H-1,2,3-triazolo[4,5-b]pyridinium 3-oxid hexafluorophosphate (HATU, 4 eq), 1-Hydroxy-1H-benzotriazole, anhydrous (HOBt, 4 eq) and *N*,*N*-diisopropylethylamine (DIPEA, 6 eq) in DMF.

Synthesis of **S4**

After completion of peptide elongation, the resin was treated with 30% acetic anhydride in CH_2Cl_2 for 30 min and then washed with DMF (2×5 mL) and DCM (3×5 mL). The acetyl-capped resin containing protected peptides was treated with 3 mL of TFA/EDT/TIPS/H_2O=95:2:2:1 solution at room temperature for 3 h. The solution was concentrated by evaporator and the crude peptides were precipitated with cold diethyl ether (5–6 mL) followed by collecting white crystals by filtration. The peptide pellet was dissolved in 0.05% TFA containing water to purify by reverse phase chromatography. After purification the acetonitrile was removed under reduced pressure and water was removed by sublimation to obtain **S3** (48.3 mg, 10.6 μmol) in 10.6% yield as an amorphous colorless solid. To the crude **S3** was added 0.1 M Tris-HCl (pH 8.0) 5 mL followed by 10 eq of GSSG (64.8 mg, 105.8 μmol) and the reaction mixture was stirred for 12 h at room temperature. To this solution was added 2 mL of 0.05% TFA and the product was purified by preparatory reverse phase chromatography. Elution conditions were as follows: mobile phase A = 0.1% TFA water; mobile phase B = 0.1% TFA acetonitrile; gradient over 50 min from A:B = 100:0 to 50:50; flow rate = 1.0 mL min^{-1}, detected by 210 nm absorbance. Acetonitrile and volatile organics were removed under reduced pressure and water was removed by sublimation to obtain target molecule **S4** (36.4 mg, 8.5 μmol) in 75.4% yield as an amorphous colorless solid.

Synthesis of **2a**

To **S4** (36.4 mg, 8.5 μmol) was added DMF 2 mL and DSP (dithiobis(succinimidyl propionate)) (68.7 mg, 170 mol , 20 eq) and the reaction mixture was stirred for 12 h. To this solution was added 5 mL of 0.05% TFA in water and the product was purified by preparatory reverse phase chromatography. Elution conditions were as follows: mobile

phase A = 0.1% TFA water; mobile phase B = 0.1% TFA acetonitrile; gradient over 50 min from A:B = 100:0 to 50:50; flow rate = 1.0 mL min^{-1}, detected by 210 nm absorbance. The fractions containing the desired **2a** product were collected and combined. Acetonitrile and volatile organics were under reduced pressure and water was removed by sublimation to obtain **2a** (20.9 mg, 4.6 μmol) in 54.1% yield as an amorphous colorless white solid.

MS (ESI) *m/z*: z=5 913.80 $[M+2H]^{2+}$, z=6 761.70 $[M+3H]^{3+}$ (calculated: z=1 4565.04, z=5 913.01, z=6 760.84) (Fig. 16)

Purity: 88.4% (11.6% was identified as the hydrolysis decomposition byproduct) (Fig. 17)

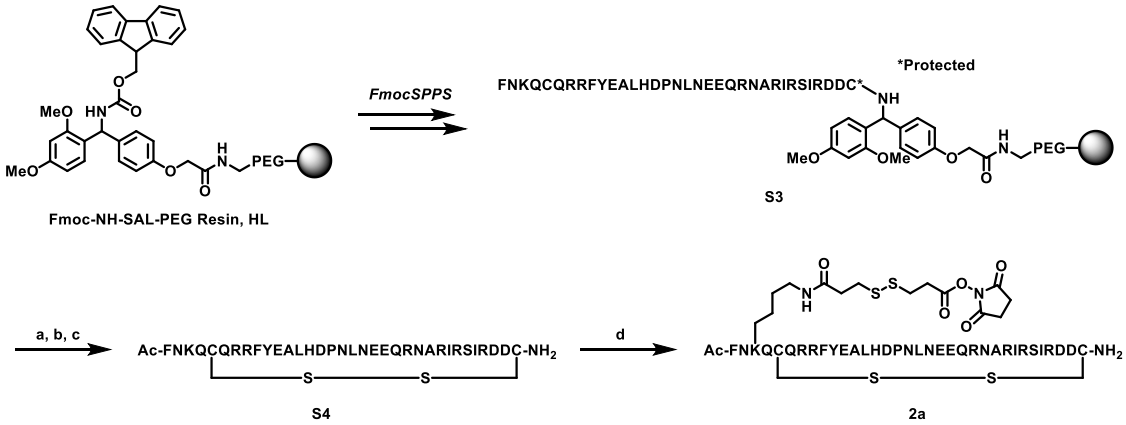

Figure 15. Synthesis of peptide reagent **2a**. Conditions of FmocSPPS Coupling: Fmoc-amino acid (4 eq), HATU (4 eq), HOBt (4 eq), DIPEA (6 eq). Fmoc deprotection: 20% piperidine in DMF. Reagents and conditions: (a) 30% Ac_2O/CH_2Cl_2, room temperature, 30 min. (b) TFA/EDT/TIPS/H_2O=95:2:2:1 solution, room temperature, 3 h. (c) GSSG (10 eq), DMSO, room temperature, 12 h. (d) DSP (dithiobis(succinimidyl propionate)) (20 eq), DMF, room temperature, 12 h.

a.

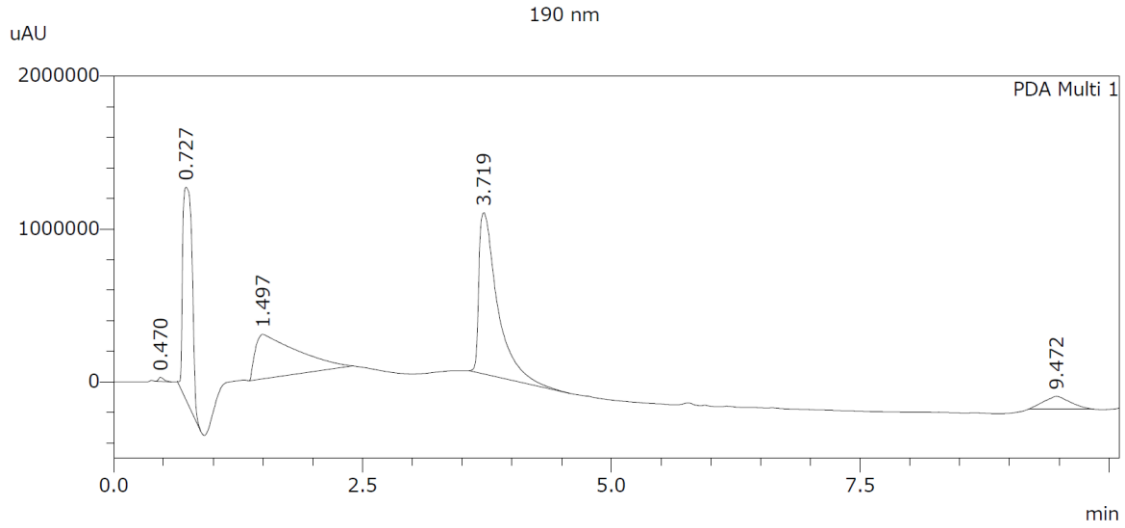

b. ESI-MS at 3.719 min.

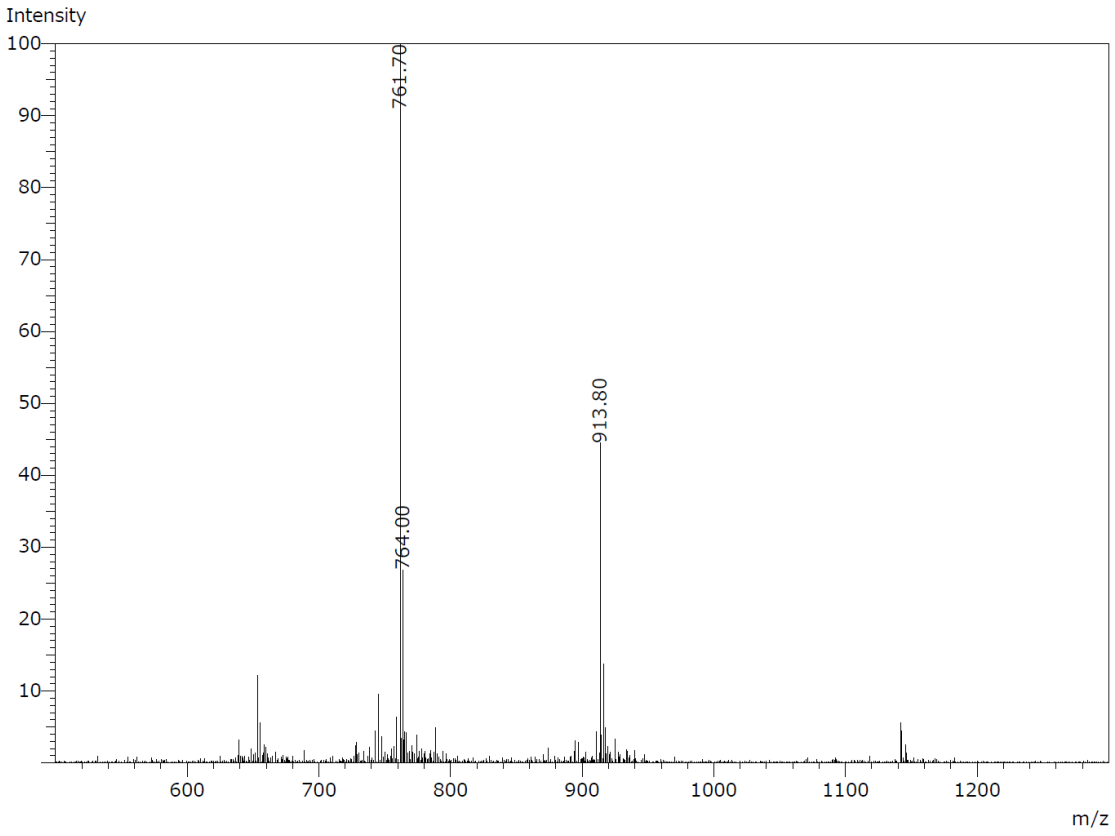

Figure 16. LC-MS results of **2a**. [a]HPLC trace (absorbance 190 nm) and [b]low-resolution ESI-MS spectrum.

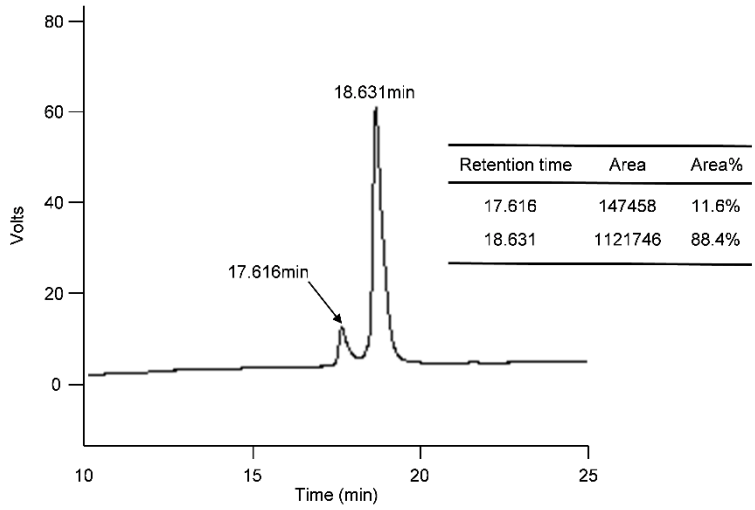

Figure 17. HPLC results of pure product **2a**.

2.3.8.3. Synthesis of peptide reagent **3a** (Fig. 18)

Synthesis of **S5**

Peptide synthesis was conducted by CEM Liberty Blue HT™ standard method. To remove a Fmoc-protecting group after each coupling, resin (100 µmol) was treated with piperidine (5 mL of 20% in DMF) and washed with DMF. For the coupling Fmoc protected amino acid (4 eq) was mixed with 1-[bis(dimethylamino)methylene]-1H-1,2,3-triazolo[4,5-b]pyridinium 3-oxid hexafluorophosphate (HATU, 4 eq), 1-Hydroxy-1H-benzotriazole, Anhydrous (HOBt, 4 eq) and *N*,*N*-diisopropylethylamine (DIPEA, 6 eq) in DMF.

Synthesis of **S6**

After completion of peptide elongation, the resin was treated with 30% acetic anhydride in CH_2Cl_2 for 30 min and then washed with DMF (2×5 mL) and DCM (3×5 mL). The acetyl-capped resin containing protected peptides was treated with 3 mL of

TFA/EDT/TIPS/H_2O=95:2:2:1 solution at room temperature for 3 h. The solution was concentrated by evaporator and the crude peptides were precipitated with cold diethyl ether (5–6 mL) followed by collecting white crystals by filtration. The peptide pellet was dissolved in 0.05% TFA containing water to purify by reverse phase chromatography. After purification the acetonitrile was removed under reduced pressure and water was removed by sublimation to obtain **S5** (48.3 mg, 10.6 μmol) in 10.6% yield as an amorphous colorless solid. To the crude **S5** was added 0.1 M Tris-HCl (pH 8.0) 5 mL, followed by 10 eq of GSSG (64.8 mg, 105.8 μmol) was added and the reaction mixture was stirred for 12 h at room temperature. To this solution was added 2 mL of 0.05%TFA in water and the product was purified by preparatory reverse phase chromatography. Elution conditions were as follows: mobile phase A = 0.1% TFA water; mobile phase B = 0.1% TFA acetonitrile; gradient over 50 min from A:B = 100:0 to 50:50; flow rate = 1.0 mL min^{-1}, detected by 210 nm absorbance. Acetonitrile and volatile organics were removed under reduced pressure and water was removed by sublimation to obtain target molecule **S6** (40.2 mg, 9.5 μmol) in 89.6% yield as an amorphous colorless solid.

Synthesis of **3a**

To **S6** (40.2 mg, 9.5 μmol) was added DMF 2 mL and DSP (dithiobis(succinimidyl propionate)) (76.8 mg, 190 μmol, 20 eq) and the reaction mixture was stirred for 12 h. To this solution was added 5 mL of 0.05% TFA in water and the product was purified by preparatory reverse phase chromatography. Elution conditions were as follows: mobile phase A = 0.1% TFA water; mobile phase B = 0.1% TFA acetonitrile; gradient over 50 min from A:B = 100:0 to 50:50; flow rate = 1.0 mL min^{-1}, detected by 210 nm absorbance. The fractions containing the desired **3a** product were collected and combined.

Acetonitrile and volatile organics were removed under reduced pressure and water was removed by sublimation to obtain target molecule **3a** (29.8 mg, 6.6 μmol) in 69.5% yield as an amorphous colorless white solid.

MS (ESI) *m/z*: z=4 1136.10 $[M+2H]^{2+}$, z=5 909.05 $[M+2H]^{2+}$, z=6 757.70 $[M+3H]^{3+}$ (calculated: z=1 4540.05, z=4 1135.01, z=5 908.01, z=6 756.68) (Fig. 19)

Purity: 83.3% (16.7% was identified as the hydrolysis decomposition byproduct) (Fig. 20)

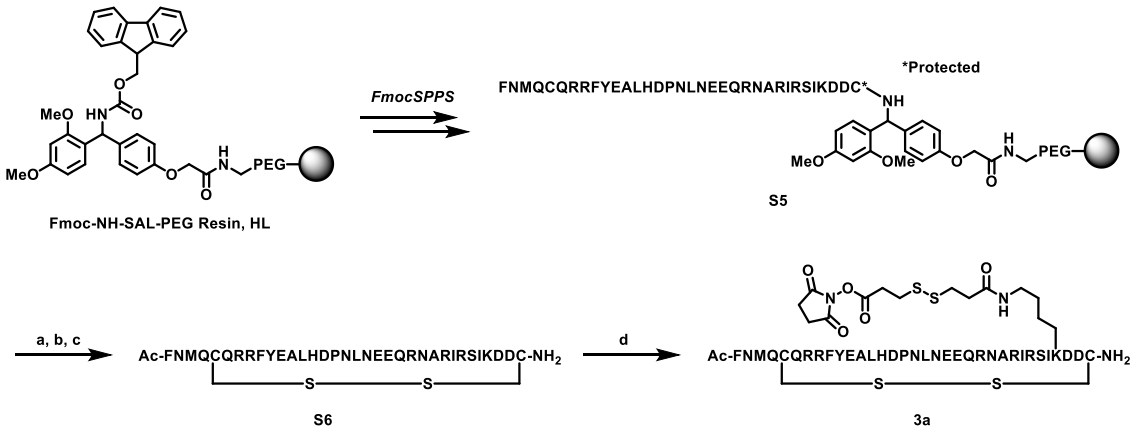

Figure 18. Synthesis of peptide reagent **S3**. Conditions of FmocSPPS Coupling: Fmoc-amino acid (4 eq), HATU (4 eq), HOBt (4 eq), DIPEA (6 eq). Fmoc deprotection: 20% piperidine in DMF. Reagents and conditions: (a) 30% Ac_2O/CH_2Cl_2, room temperature, 30 min. (b) TFA/EDT/TIPS/H_2O=95:2:2:1 solution, room temperature, 3 h. (c) GSSG (10 eq), DMSO, room temperature, 12 h. (d) DSP (dithiobis(succinimidyl propionate)) (20 eq), DMF, room temperature, 12 h.

a.

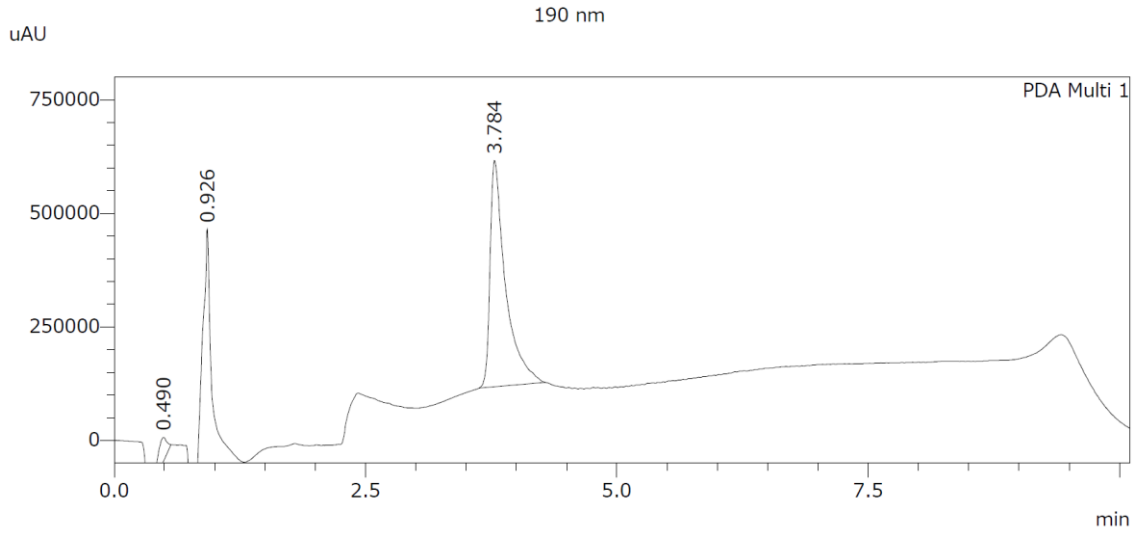

b. ESI-MS at 3.784 min.

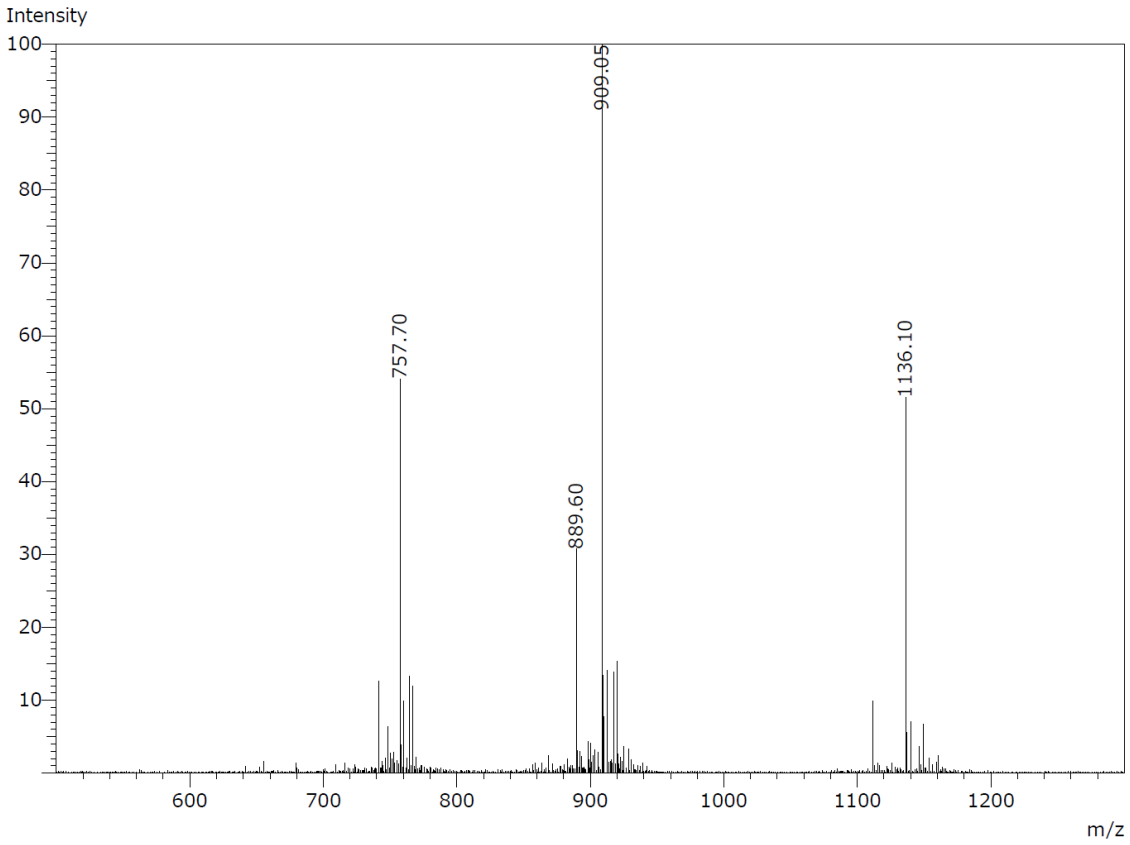

Figure 19. LC-MS results of **3a**. [a]HPLC trace (absorbance 190 nm) and [b]low-resolution ESI-MS spectrum.

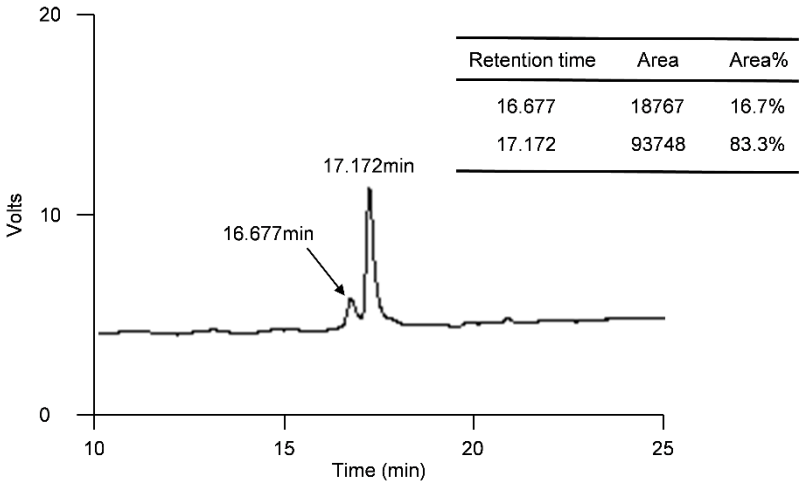

Figure 20. HPLC results of pure product **3a**.

2.3.8.4. Synthesis of and peptide reagent **4a** (Fig. 21)

Synthesis of **S7**

Peptide synthesis was conducted by CEM Liberty Blue HT™ standard method. To remove a Fmoc-protecting group after each coupling, resin (100 µmol) was treated with piperidine (5 mL of 20% in DMF) and washed with DMF. For the coupling Fmoc protected amino acid (4 eq) was mixed with 1-[bis(dimethylamino)methylene]-1H-1,2,3-triazolo[4,5-b]pyridinium 3-oxid hexafluorophosphate (HATU, 4 eq), 1-Hydroxy-1H-benzotriazole, Anhydrous (HOBt, 4 eq) and *N*,*N*-diisopropylethylamine (DIPEA, 6 eq) in DMF.

Synthesis of **S8**

After completion of peptide elongation, the resin was treated with 30% acetic anhydride in CH_2Cl_2 for 30 min and then washed with DMF (2×5 mL) and DCM (3×5 mL). The acetyl-capped resin containing protected peptides was treated with 3 mL of

TFA/EDT/TIPS/H2O=95:2:2:1 solution at room temperature for 3 h. The solution was concentrated by evaporator and the crude peptides were precipitated with cold diethyl ether (5–6 mL) followed by collecting white crystals by filtration. The peptide pellet was dissolved in 0.05% TFA containing water to purify by reverse phase chromatography. After purification the acetonitrile was removed under reduced pressure and water was removed by sublimation to obtain **S7** (42.1 mg, 9.8 µmol) in 9.8% yield as an amorphous colorless solid. To the crude **S7** was added 0.1 M Tris-HCl (pH 8.0) 5 mL, followed by GSSG (60.3 mg, 98.4 µmol) and the reaction mixture was stirred 12 h at room temperature. To this solution was added 2 mL of 0.05%TFA in water and product was purified by reverse phase chromatography. Elution conditions were as follows: mobile phase A = 0.1% TFA water; mobile phase B = 0.1% TFA acetonitrile; gradient over 50 min from A:B = 100:0 to 50:50; flow rate = 1.0 mL min^{-1}, detected by 210 nm absorbance. The fraction containing the desired **S7** product were collected and combined. Acetonitrile and volatile organics were removed under reduced pressure and water was removed by sublimation to obtain target molecule **S8** (29.3 mg, 6.8 µmol) as white solid in 69.4% yield as an amorphous colorless solid.

Synthesis of **4a**

To **S8** (29.3 mg, 6.8 µmol) was added DMF 2 mL and DSP (dithiobis(succinimidyl propionate)) (55.0 mg, 136 µmol, 20 eq) and the reaction mixture was stirred for 12 h. To this solution was added 5 mL of 0.05% TFA in water and the product was purified by preparatory reverse phase chromatography. Elution conditions were as follows: mobile phase A = 0.1% TFA water; mobile phase B = 0.1% TFA acetonitrile; gradient over 50 min from A:B = 100:0 to 50:50; flow rate = 1.0 mL min^{-1}, detected by 210 nm absorbance.

The fractions containing the desired **4a** product were collected and combined. Acetonitrile and volatile organics were removed under reduced pressure and water was removed by sublimation to obtain **4a** (22.8 mg, 5.0 μmol) as an amorphous colorless white solid in 73.5% yield.

MS (ESI) *m/z*: z=4 1142.85 $[M+2H]^{2+}$, z=5 914.45 $[M+2H]^{2+}$, z=6 762.15 $[M+3H]^{3+}$ (calculated: z=1 4567.12, z=4 1141.78, z=5 913.42, z=6 761.19) (Fig. 22)

Purity: 82.9% (17.1% was identified as the hydrolysis decomposition byproduct) (Fig. 23)

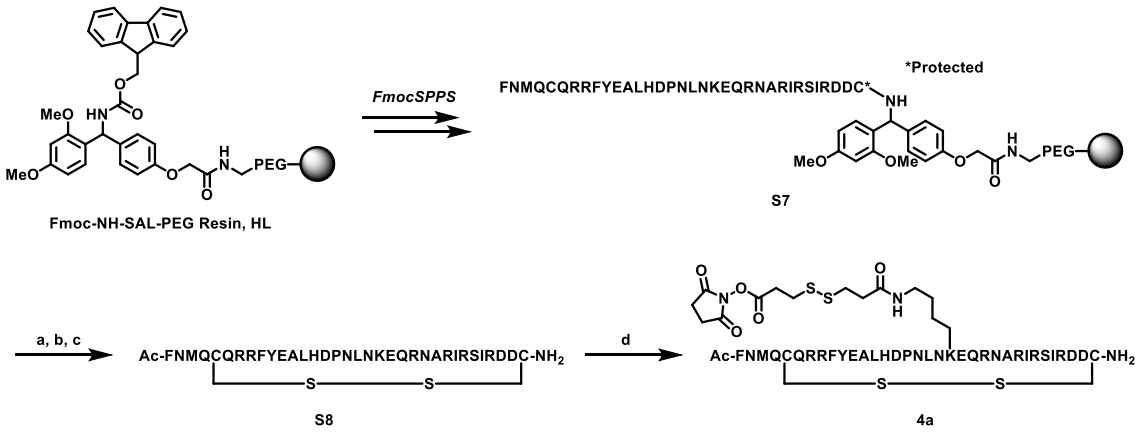

Figure 21. Synthesis of peptide reagent **S3**. Conditions of FmocSPPS Coupling: Fmoc-amino acid (4 eq), HATU (4 eq), HOBt (4 eq), DIPEA (6 eq). Fmoc deprotection: 20% piperidine in DMF. Reagents and conditions: (a) 30% Ac_2O/CH_2Cl_2, room temperature, 30 min. (b) TFA/EDT/TIPS/H_2O=95:2:2:1 solution, room temperature, 3 h. (c) GSSG (10 eq), DMSO, room temperature, 12 h. (d) DSP (dithiobis(succinimidyl propionate)) (20 eq), DMF, room temperature, 12 h.

a.

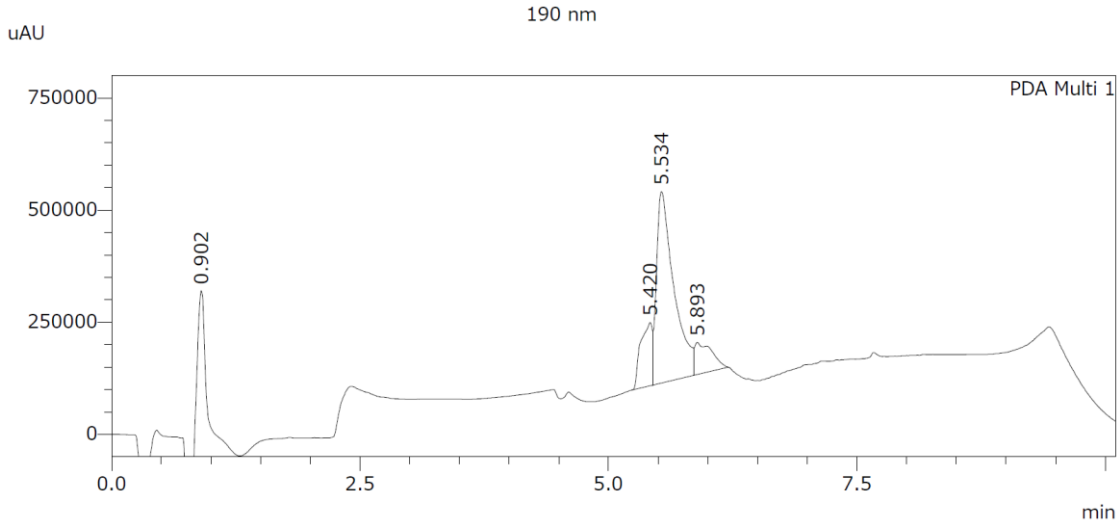

b. ESI-MS at 5.334 min.

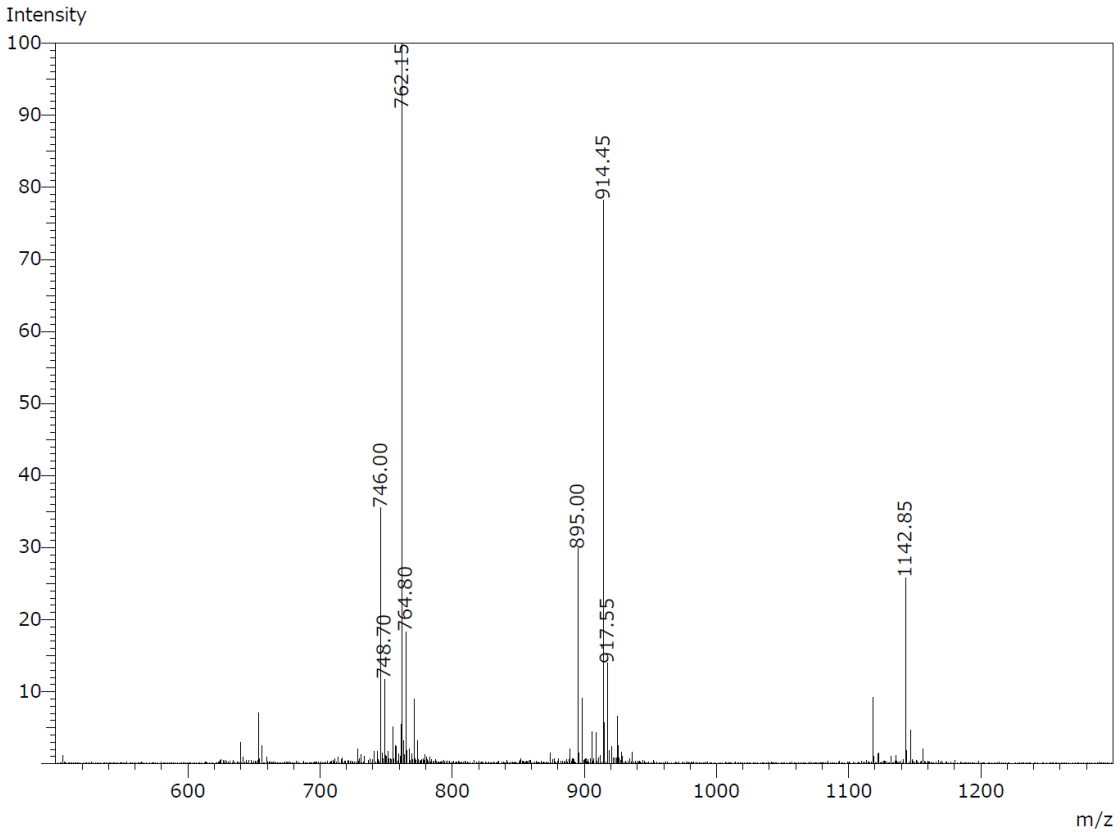

Figure 22. LC-MS results of **4a**. [a]HPLC trace (absorbance 190 nm) and [b]low-resolution ESI-MS spectrum.

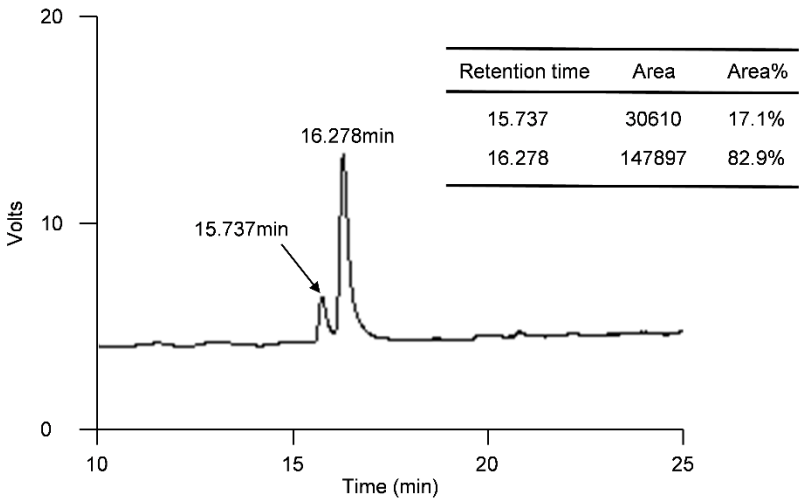

Figure23. HPLC results of pure product **4a**.

2.3.9. Peptide reagent conjugation to mAbs

Before use, each mAb was dialysed in a Spectra/Por Float-A-Lyzer G2 (20 kDa MWCO, 10 mL volume) to exchange the buffer for phosphate-buffered saline (PBS, 50 mM, pH 7.4), and the concentration was measured using a NanoDrop Lite (Thermo Fischer). Before the conjugation study, the mAb was exchanged into the appropriate buffer in an Amicon centrifuge filter (10 kDa MWCO, 0.5 mL volume). 10 equivalent of the peptide reagent (10 mM in DMF) was added to each mAb (2.66 mg mL^{-1}, 60 mM AcONa, pH 5.5), and the mixture was incubated for 1 h at 20 °C. After 1 h, sodium citrate (50 mM, pH 2.5) was added at the same volume as the reaction buffer and centrifuge-filtered once in an Amicon Ultra centrifuge filter (10 kDa MWCO, 0.5 mL volume). Due to peptide reagent binding, this process requires the removal of peptide reagents. The buffer was exchanged for 20 mM PBS buffer (pH 7.0) in an Amicon Ultra centrifuge filter (10 kDa MWCO, 0.5 mL volume) to adjust the concentration to 1 mg mL^{-1} for HIC analysis. For ESI-TOFMS, the buffer was exchanged for 50 mM ammonium acetate by an Amicon Ultra centrifuge filter (10 kDa MWCO, 0.5 mL volume).

2.3.10. Deglycosylation

To a solution of 200 µL of samples (1 mg mL^{-1}, pH 7.4 50 mM PBS buffer), 20 µL of GlycoBuffer and 200 units of PNGase F were added and incubated at 37 °C for 24 h. The buffer exchange by Amicon Ultra 10K-0.5 mL to 50 mM ammonium acetate for ESI-TOFMS analysis.

2.3.11. Peptide mapping results

General procedure of peptide mapping: Each 10 µg of deglycosylated sample was diluted to 1 µg/µL with 50 mM ammonium bicarbonate (ABC) buffer. Antibody reduction was achieved by the addition of 20 mM dithiothreitol (DTT) in 40% trifluoroethanol (TFE) to a final concentration of 10 mM. After incubation at 65 °C for 60 min, alkylation was performed by adding 50 mM iodoacetamide (IAM) to a final concentration of 16.7 mM and incubating at 25 °C for 30 min, in the absence of ambient light. The sample was then diluted up to a total volume of 70 µL with 50 mM ABC buffer. We added 10 µL of 20 ng/µL trypsin (Cat # T6567-5X20UG, Sigma) and incubated at 37 °C to carry out protein digestion. After 18 hours incubation, digestion was quenched by adding 2 µL of 20% trifluoroacetic acid (TFA).

The resulting peptide mixture was analyzed on Orbitrap Fusion Tribrid (Thermo Fischer Scientific) interfaced with Easy-nLC (Thermo Fischer Scientific). We used an Acclaim PepMap® 100 (75 µm x 2 cm, Thermo Fischer Scientific) for the trap column and an ESI-column (75 µm x 12.5 cm, 3 µm, NTCC-360/75-3-125, Nikkyo Technos) for the analysis column. The chromatographic method was consisted of a 0.5 min hold at 2% solvent B (0.1% formic acid in acetonitrile) and 23 min linear gradient from 2 to 30% solvent B. The next wash step was performed as 2 min linear gradient from 30 to 75% solvent B and a 9.5 min hold at 75% solvent B. The solvent A consisted of 0.1% formic acid.

Mass spectrometry analysis was carried out in a data dependent acquisition (DDA) mode with full scans (350–2,000 *m/z*) acquired at a mass resolution of 120,000. A spray voltage and an ion transfer tube temperature were set to 1600 V and 275 °C, respectively. Among detected ions, charge states other than 2-4 were filtered out and run in top speed mode

with 3 s cycles for MS/MS analysis. The tandem mass spectra were produced by collision induced dissociation (CID) method. An AGC target ion number for MS^1 was set to 4e5 and 1e4 for MS^2. A maximum injection time for MS^1 and MS^2 was both set to 50 msec. For the dynamic exclusion, a duration time was set to 15 sec.

The resulted MS/MS data was searched against either trastuzumab sequence (**Fig. 24**) using Proteome Discoverer 1.4 or 2.2 (Thermo Fischer Scientific) and BioPharma Finder 1.1 or 3.0 (Thermo Fischer Scientific). For Proteome Discoverer search, Sequest HT was used as a search engine and a total intensity threshold was set to 0.01% intensity of the base peak chromatogram peak top. Trypsin was selected for digestion. The maximum peptide length was set to 50 amino acids. The mass tolerance of precursor ions and fragment ions were set to 5 ppm and 0.5 Da, respectively. Carbamidomethylation of cysteine (+57.021 Da) was specified as a fixed modification, and oxidation of methionine (+15.995 Da) and 3-(2-amino-2-oxo-ethyl) sulfanylpropionate of lysine (+145.019 Da) were included as variable modifications. Peptides without high peptide confidence were filtered out. For BioPharma Finder search, S/N threshold was set to 100 and ms noise level was defined by ms signal threshold to be 0.01% intensity of the base peak chromatogram peak top. Trypsin was selected for digestion. The maximum peptide length was set to 50 amino acids. The mass tolerance was set to 0.3 Da. Fixed modifications and variable modifications were set similar to Proteome Discoverer search. Peptides with confidence score higher than 80% and with MS^2 spectrum were counted in for the analysis. The resulted data of 3-(2-amino-2-oxo-ethyl)sulfanylpropionate lysine residues and corresponding MS^1 and MS^2 spectrum are shown in **Figs. 25, 27, 29** and **31**, respectively. As shown in **Fig. 24**, the residues in the CH1, CH2 and CH3 domain (heavy chain constant region) are described with EU numbering. On the other hand, residues in the

light chain and VH domain (heavy chain variable region) are labeled with sequence number. Each AAPCs showed site selective modification in both Proteome Discoverer and BioPharma Finder results. Sequence coverage are shown in **Figs. 26, 28, 30** and **32**, respectively.

a. Amino acid sequence of trastuzumab

Light Chain

1	DIQMTQSPSS	LSASVGDRVT	ITCRASQDVN	TAVAWYQQKP	GKAPKLLIYS	50
51	ASFLYSGVPS	RFSGSRSGTD	FTLTISSLQP	EDFATYYCQQ	HYTTPPTFGQ	100
101	GTKVEIKRTV	AAPSVFIFPP	SDEQLKSGTA	SVVCLLNNFY	PREAKVQWKV	150
151	DNALQSGNSQ	ESVTEQDSKD	STYSLSSTLT	LSKADYEKHK	VYACEVTHQG	200
201	LSSPVTKSFN	RGEC				214

Heavy Chain

1	EVQLVESGGG	LVQPGGSLRL	SCAASGFNIK	DTYIHWVRQA	PGKGLEWVAR	50
51	IYPTNGYTRY	ADSVKGRFTI	SADTSKNTAY	LQMNSLRAED	TAVYYCSRWG	100
101	GDGFYAMDYW	GQGTLVTVSS	ASTKGPSVFP	LAPSSKSTSG	GTAALGCLVK	150
151	DYFPEPVTVS	WNSGALTSGV	HTFPAVLQSS	GLYSLSSVVT	VPSSSLGTQT	200
201	YICNVNHKPS	NTKVDKKVEP	KSCDKTHTCP	PCPAPELLGG	PSVFLFPPKP	250
251	KDTLMISRTP	EVTCVVVDVS	HEDPEVKFNW	YVDGVEVHNA	KTKPREEQYN	300
301	STYRVVSVLT	VLHQDWLNGK	EYKCKVSNKA	LPAPIEKTIS	KAKGQPREPQ	350
351	VYTLPPSREE	MTKNQVSLTC	LVKGFYPSDI	AVEWESNGQP	ENNYKTTPPV	400
401	LDSDGSFFLY	SKLTVDKSRW	QQGNVFSCSV	MHEALHNHYT	QKSLSLSPG	449

b. Numbering correspondence table

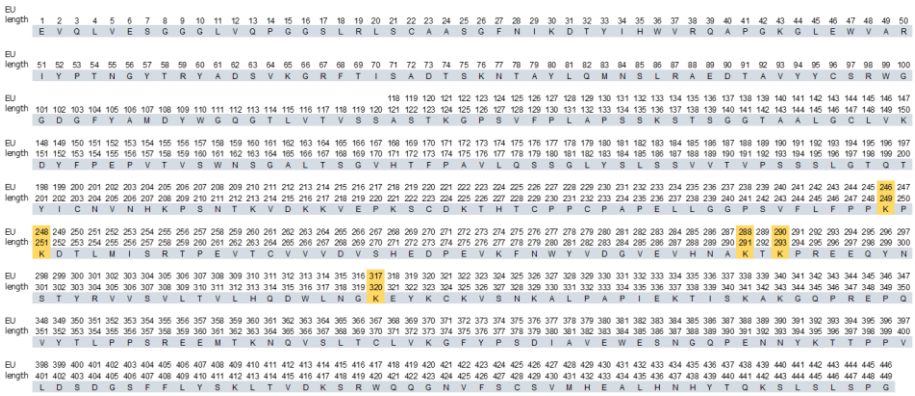

Figure 24. [a]The sequence of trastuzumab used for all peptide mapping analysis of AAPC 1-4. 214 amino acids for the light chain, 449 amino acids for the heavy chain. There are 13 modifiable lysine residues in the light chain and 31 in the heavy chain. [b]The table of trastuzumab heavy chain sequence numbering correspondence. The residues in the CH1, CH2 and CH3 domain (heavy chain constant region) are described with EU numbering. On the other hand, residues in the light chain and VH domain (heavy chain variable region) are labeled with sequence number. The lysine residues identified as modified are marked with yellow.

a. Results of modification search

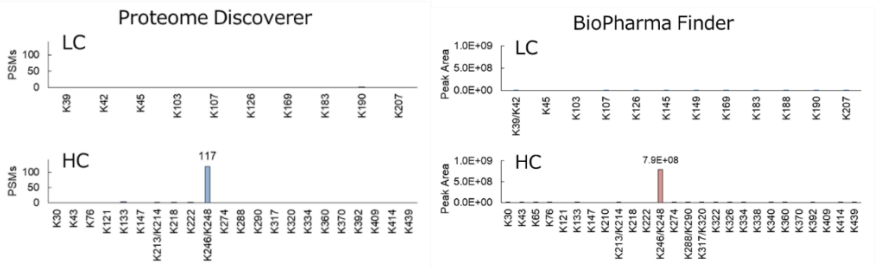

b. Spectrum of modified peptide

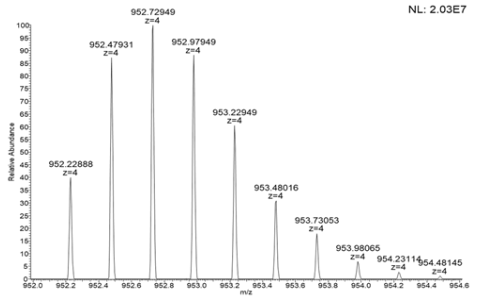

c. MS/MS Spectrum of modified peptide

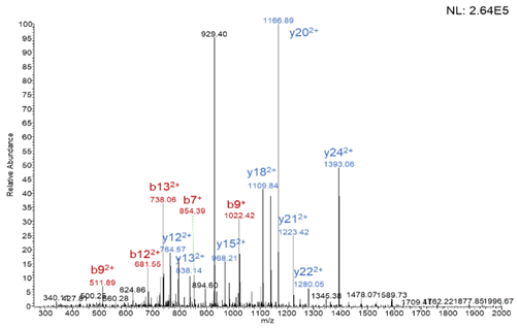

Figure 25. The results of peptide mapping analysis of AAPC **1**. [a]Lysine residues identified as DSP-NHS linker modified are shown. Both in Proteome Discoverer and BioPharma Finder search showed K246/K248 selective modification. [b]The spectrum of 952.22888 representing THTCPPCPAPELLGGPSVFLFPP^{246}KP^{248}KDTLMISR (4+, with double carbamidomethylation and one 3-(2-amino-2-oxo-ethyl) sulfanylpropionation, theoretical *m/z*: 952.22900). [c]MS/MS spectrum of 952.22888 precursor ion.

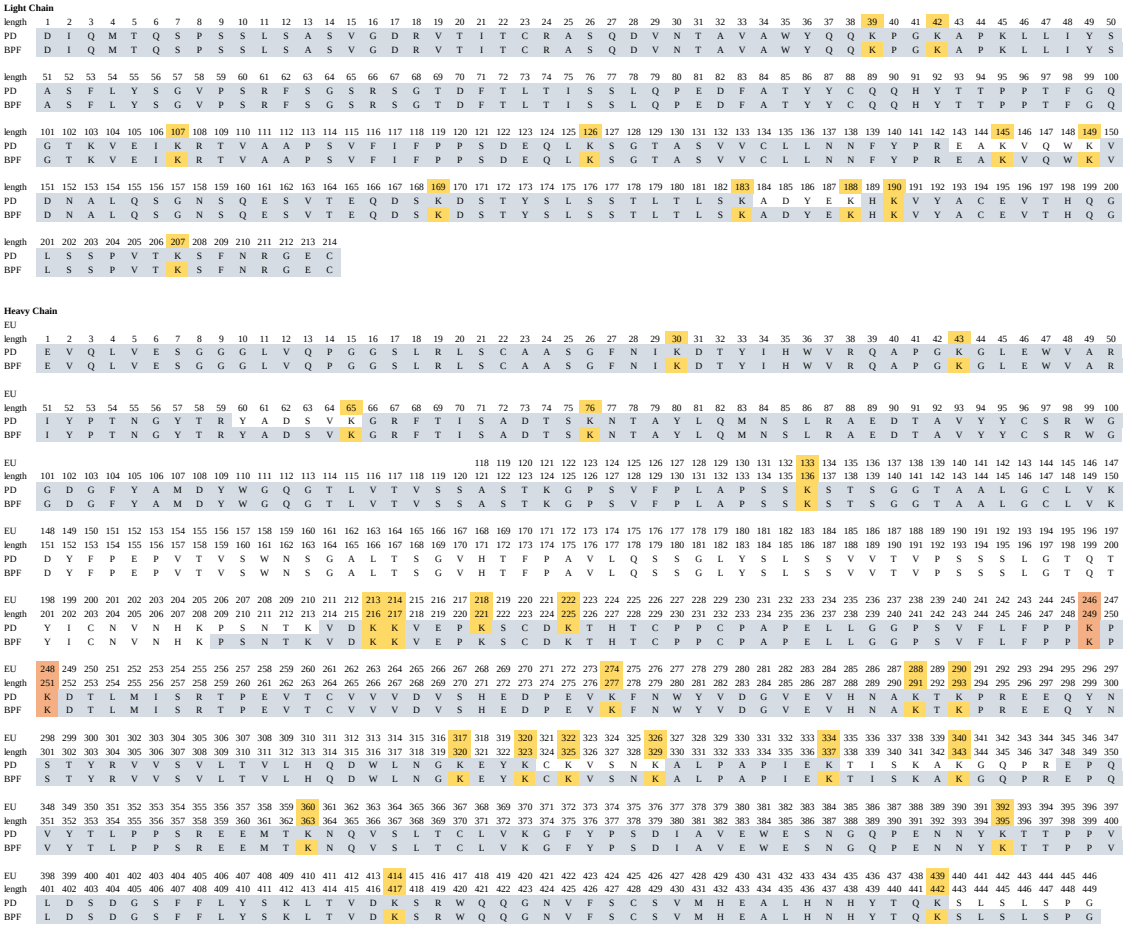

Figure 26. Sequence coverage of acquired peptides. Coverages of light chain were 94.4% and 100%, heavy chain were 79.5% and 87.1% by Proteome Discoverer (PD) and BioPharma Finder (BPF), respectively. Modification observed lysine residues are marked with yellow, and most modified ones are indicated in orange.

a. Results of modification search

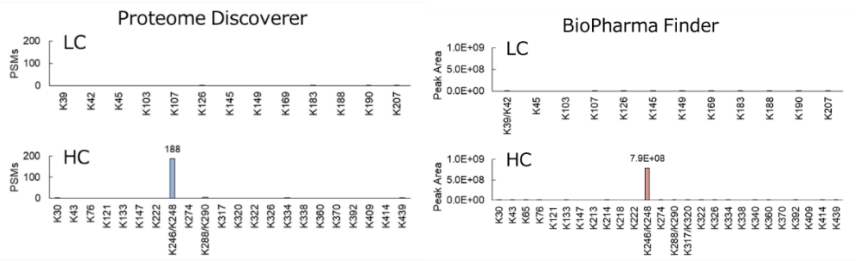

b. Spectrum of modified peptide

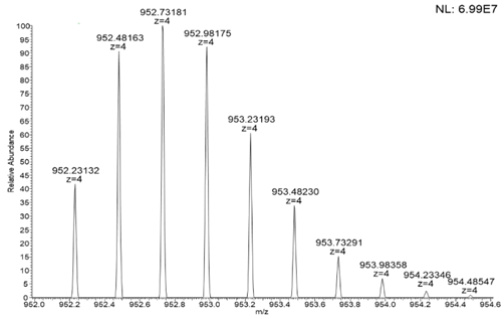

c. MS/MS Spectrum of modified peptide

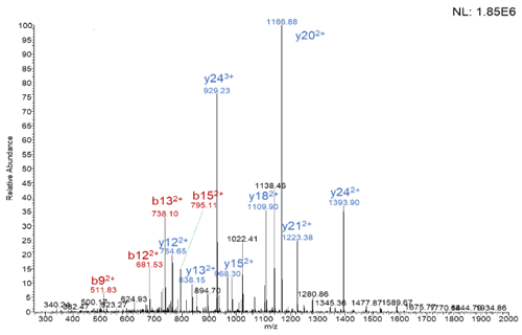

Figure 27. The results of peptide mapping analysis of AAPC **2**. [a]Lysine residues identified as DSP-NHS linker modified are shown. Both in Proteome Discoverer and BioPharma Finder search showed K246/K248 selective modification. [b]The spectrum of 952.23132 representing THTCPPCPAPELLGGPSVFLFPP^{246}KP^{248}KDTLMISR (4+, with double carbamidomethylation and one 3-(2-amino-2-oxo-ethyl)sulfanylpropionation, theoretical *m/z*: 952.22900). [c]MS/MS spectrum of 952.23132 precursor ion.

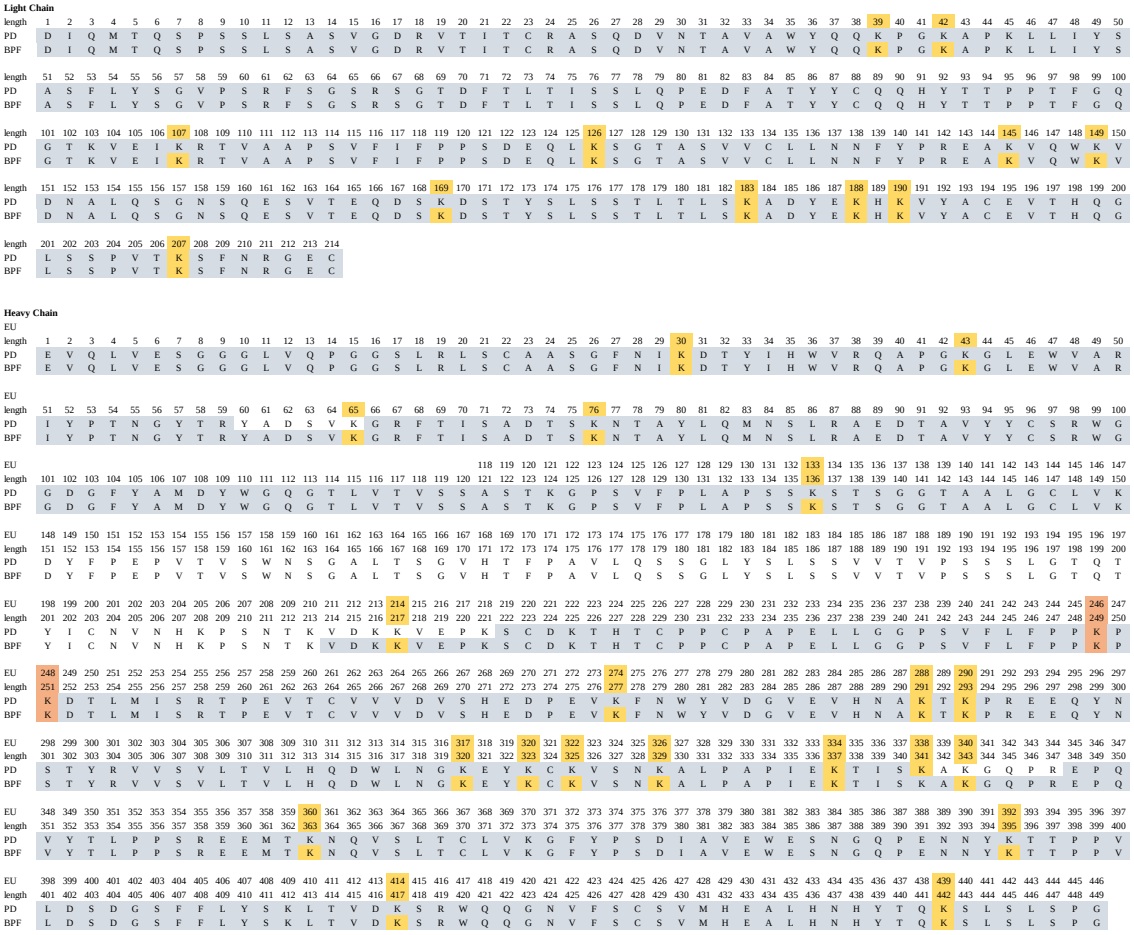

Figure 28. Sequence coverage of acquired peptides. Coverages of light chain were 100% and 100%, heavy chain were 81.5% and 86.0% by Proteome Discoverer (PD) and BioPharma Finder (BPF), respectively. Modification observed lysine residues are marked with yellow, and most modified ones are indicated in orange.

a. Results of modification search

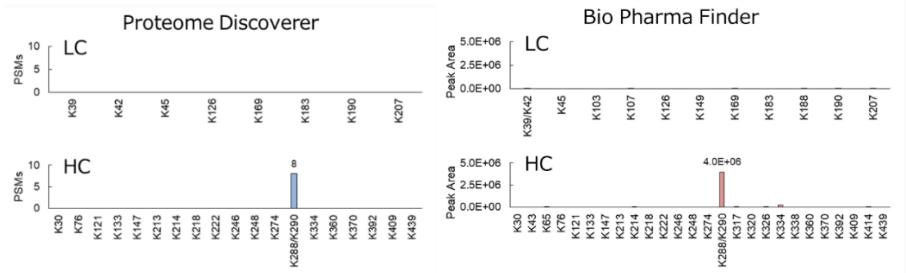

b. Spectrum of modified peptide

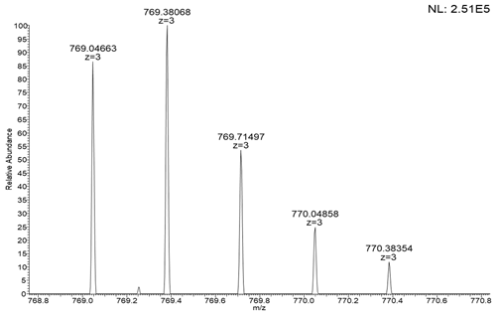

c. MS/MS Spectrum of modified peptide

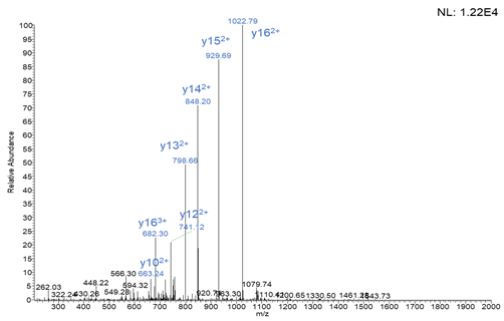

Figure 29. The results of peptide mapping analysis of AAPC **3**. [a]Lysine residues identified as DSP-NHS linker modified are shown. Both in Proteome Discoverer and BioPharma Finder search showed K288/K290 selective modification. [b]The spectrum of 769.04663 representing FNWYVDGVEV-HNA^{288}KT^{290}KPR (3+, with one 3-(2-amino-2-oxo-ethyl)sulfanylpropionation, theoretical *m/z*: 769.04457). [c]MS/MS spectrum of 769.04663 precursor ion.

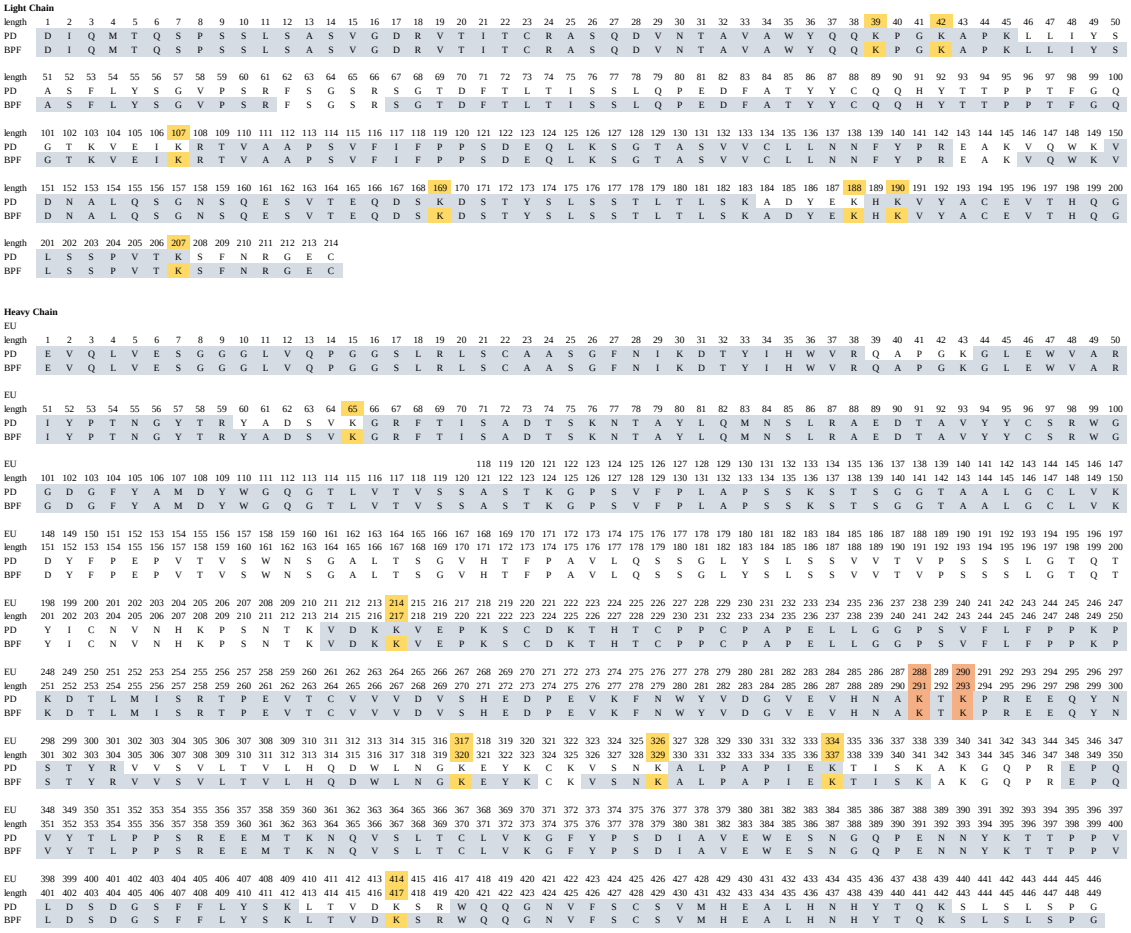

Figure 30. Sequence coverage of acquired peptides. Coverages of light chain were 62.1% and 96.3%, heavy chain were 72.6% and 84.2% by Proteome Discoverer (PD) and BioPharma Finder (BPF), respectively. Modification observed lysine residues are marked with yellow, and most modified ones are indicated in orange.

a. Results of modification search

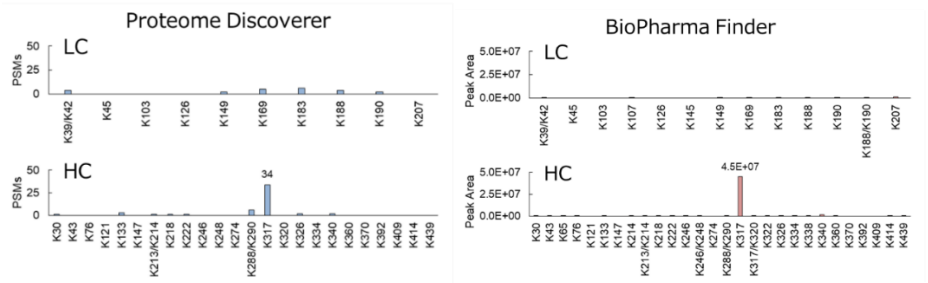

b. Spectrum of modified peptide

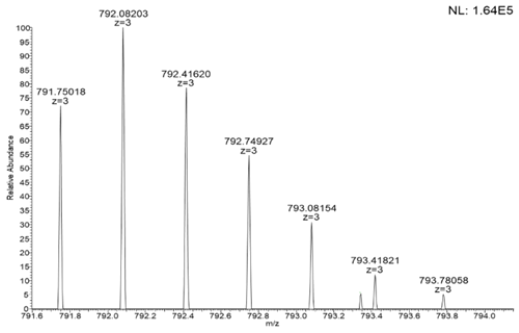

c. MS/MS Spectrum of modified peptide

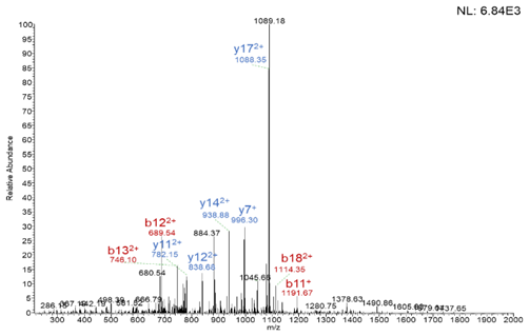

Figure 31. The results of peptide mapping analysis of AAPC **4**. [a]Lysine residues identified as DSP-NHS linker modified are shown. Both in Proteome Discoverer and BioPharma Finder search showed K317 selective modification. [b]The spectrum of 791.75018 representing VVSVLTVLHQDW-LNG^{317}KEYK (3+, with one 3-(2-amino-2-oxo-ethyl)sulfanylpropionation, theoretical *m/z*: 791.74753). [c]MS/MS spectrum of 791.75018 precursor ion.

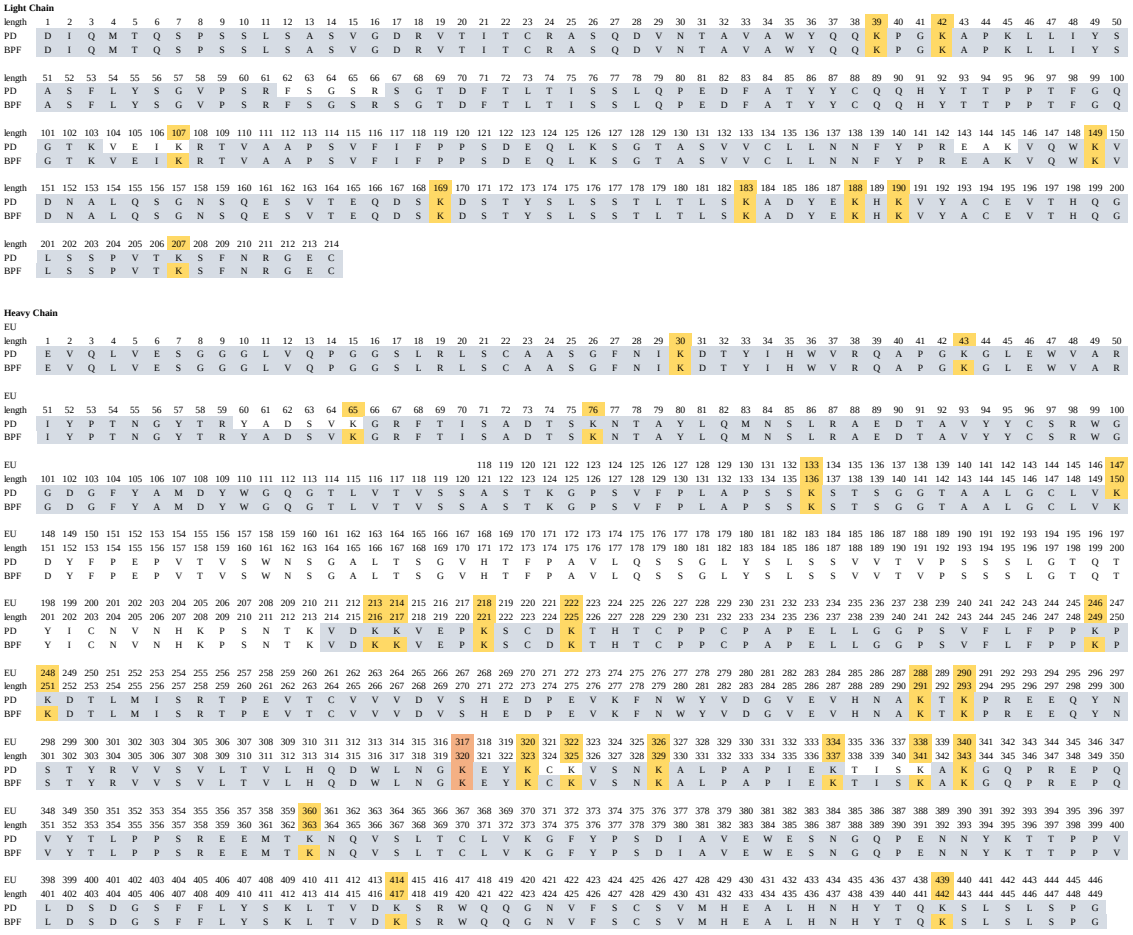

Figure 32. Sequence coverage of acquired peptides. Coverages of light chain were 94.4% and 100%, heavy chain were 83.3% and 86.0% by Proteome Discoverer (PD) and BioPharma Finder (BPF), respectively. Modification observed lysine residues are marked with yellow, and most modified one is indicated in orange.

3. Conjugation to several subtypes of antibodies and reaction mechanism

3.1. Conjugation to several subtypes of antibodies

In the experiments described thus far, we investigated regiodivergent affinity peptide labelling for obtaining AAPCs based on trastuzumab. Next, we examined the possibility of attaching affinity peptides to a range of human IgGs. For use as biopharmaceuticals, FDA has only approved IgG subclasses 1, 2 and 4 [85]. Thus, we chose adalimumab (human anti-TNFα IgG1), denosumab (human anti-RANKL IgG2), and dupilumab (human anti-IL4/13 IgG4) to test our ability to conjugate the Fc-III-derived affinity peptide **1a**, and from the three Z34C peptide derivatives we also selected **2a** for further studies. Gratifyingly, our conjugation was successful with all three mAb isotypes attempted, and the reaction selectivity and PAR were nearly the same as observed for trastuzumab (Table 2 and Figs. 33-38). The selectivity of the peptide conjugations to the mAbs Fc regions was confirmed by the reduction MS spectrum which indicated affinity peptides labelled only in heavy chain of mAbs. Additionally we conducted peptide mapping analysis after conjugation of peptide reagent **1a** to adalimumab. The peptide map-ping analysis indicated similar results as with trastuzumab and we identified residues K246 and K248 (EU numbering) in the Fc fragment as the modified residues (see the 3.3. Experimental Section). Protein A has been reported to bind only to subclasses of human IgG1, 2 and 4, but not human IgG3, and this information is particularly pertinent to understanding the results obtained here[86]. In agreement with a previous report, the Fc-III peptide-binding region is similar to the Z34C binding area, and it there-fore should have an affinity for Fc in human IgG1, IgG2 and IgG4.

Table 2. Results of the conjugation of affinity peptide reagents to adalimumab (human IgG1), denosumab (human IgG2) and dupilumab (human IgG4). PARs were determined by Agilent DAR Calculator.

Type of antibodies	Fc affinity peptide reagents	Peptide/antibody ratio (PAR)			
		0	1	2	3
Adalimumab (Human IgG1)	**1a**	-	7%	93%	-
	2a	-	8%	91%	1%
Denosumab (Human IgG2)	**1a**	-	9%	91%	-
	2a	-	-	100%	-
Dupilumab (Human IgG4)	**1a**	-	8%	92%	-
	2a	-	6%	94%	-

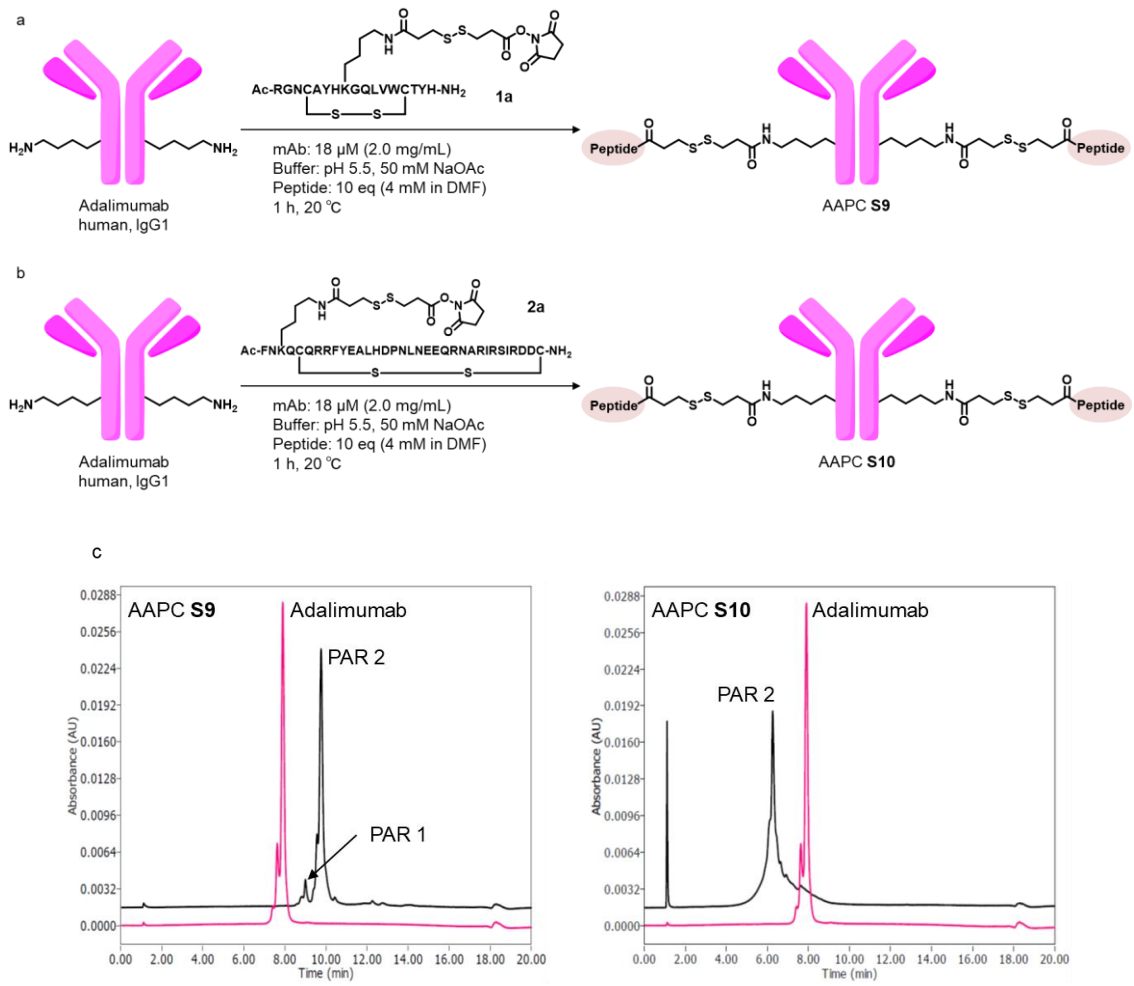

Figure 33. Peptide reagent **1a**, **2a** conjugation to adalimumab. [a]Scheme of conjugation **1a** to adalimumab. [b]Scheme of conjugation **2a** to adalimumab. [c]HIC-HPLC.

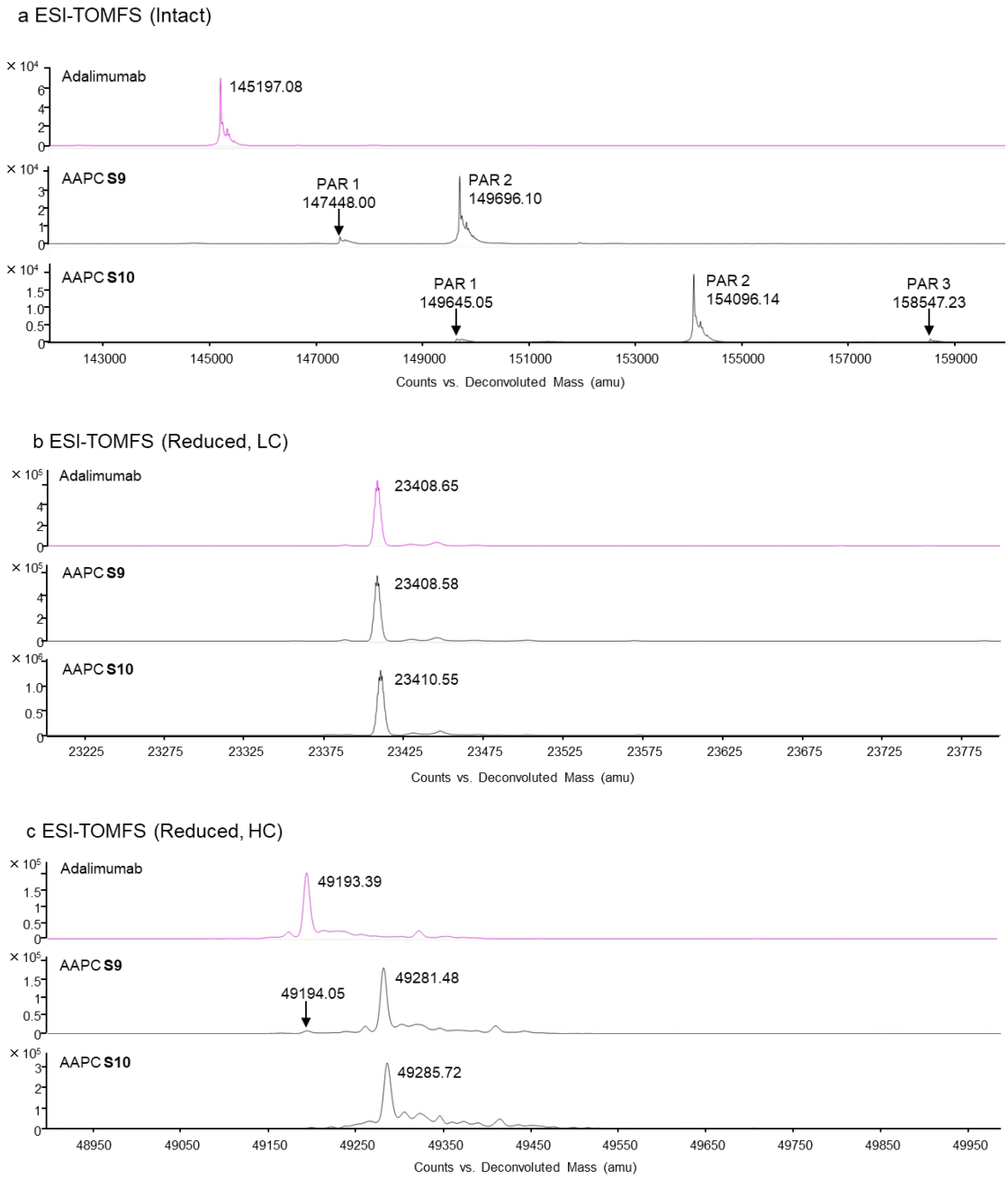

Figure 34. [a]ESI-TOFMS (Intact). [b]ESI-TOFMS (Reduced condition, light chain). [c]ESI-TOFMS (Reduced condition, heavy chain.)

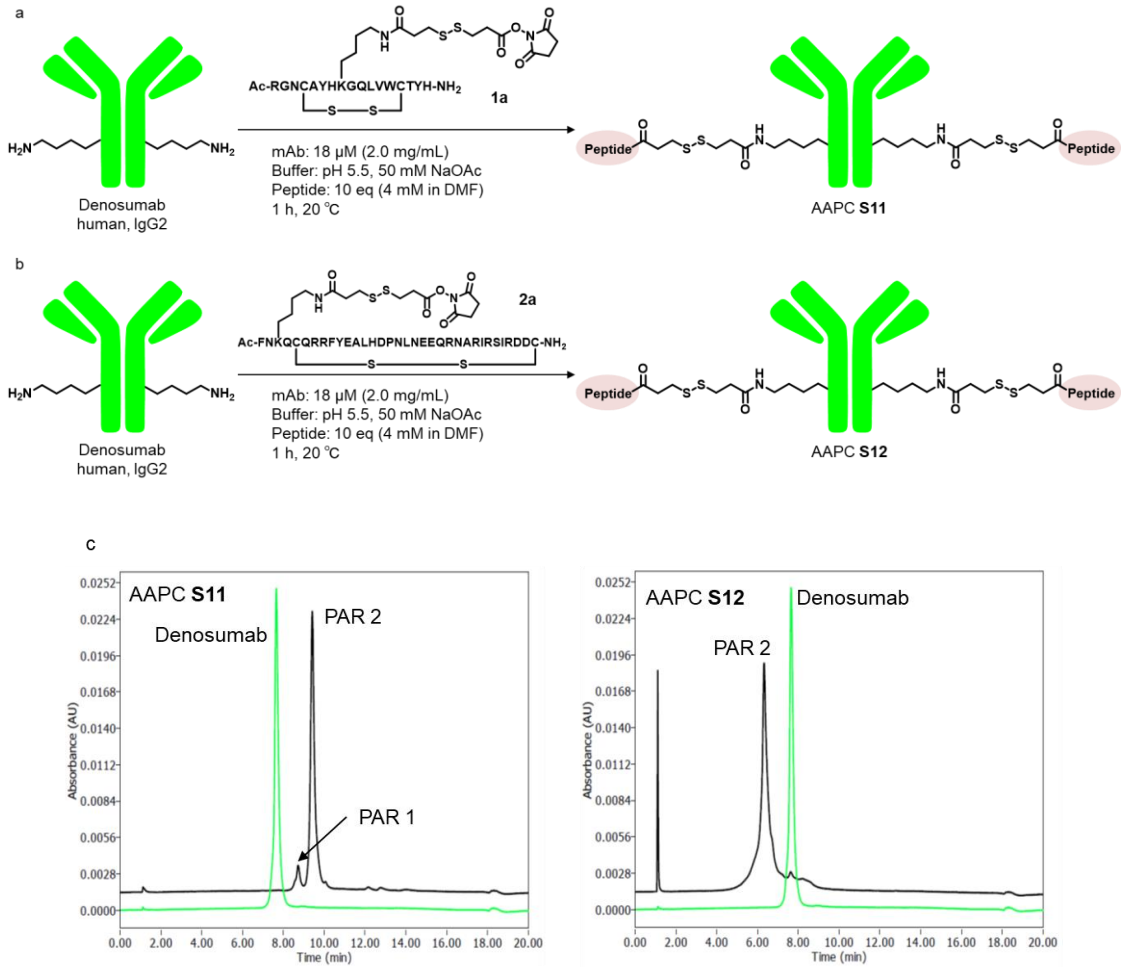

Figure 35. Peptide reagent **1a**, **2a** conjugation to denosumab. [a]Scheme of conjugation **1a** to denosumab. [b]Scheme of conjugation **2a** to denosumab. [c]HIC-HPLC.

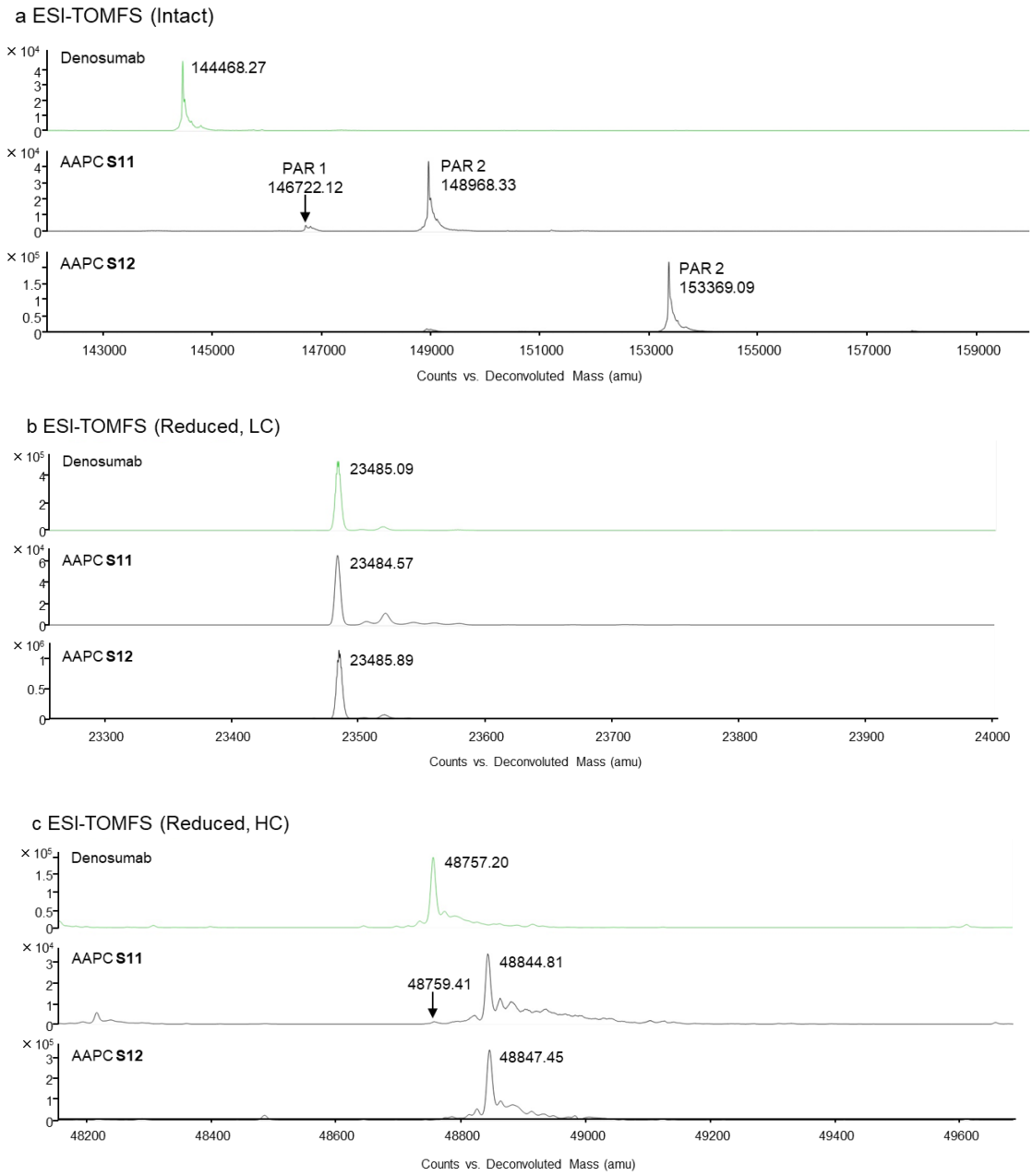

Figure 36. [a]ESI-TOFMS (Intact). [b]ESI-TOFMS (Reduced condition, light chain). [c]ESI-TOFMS (Reduced condition, heavy chain).

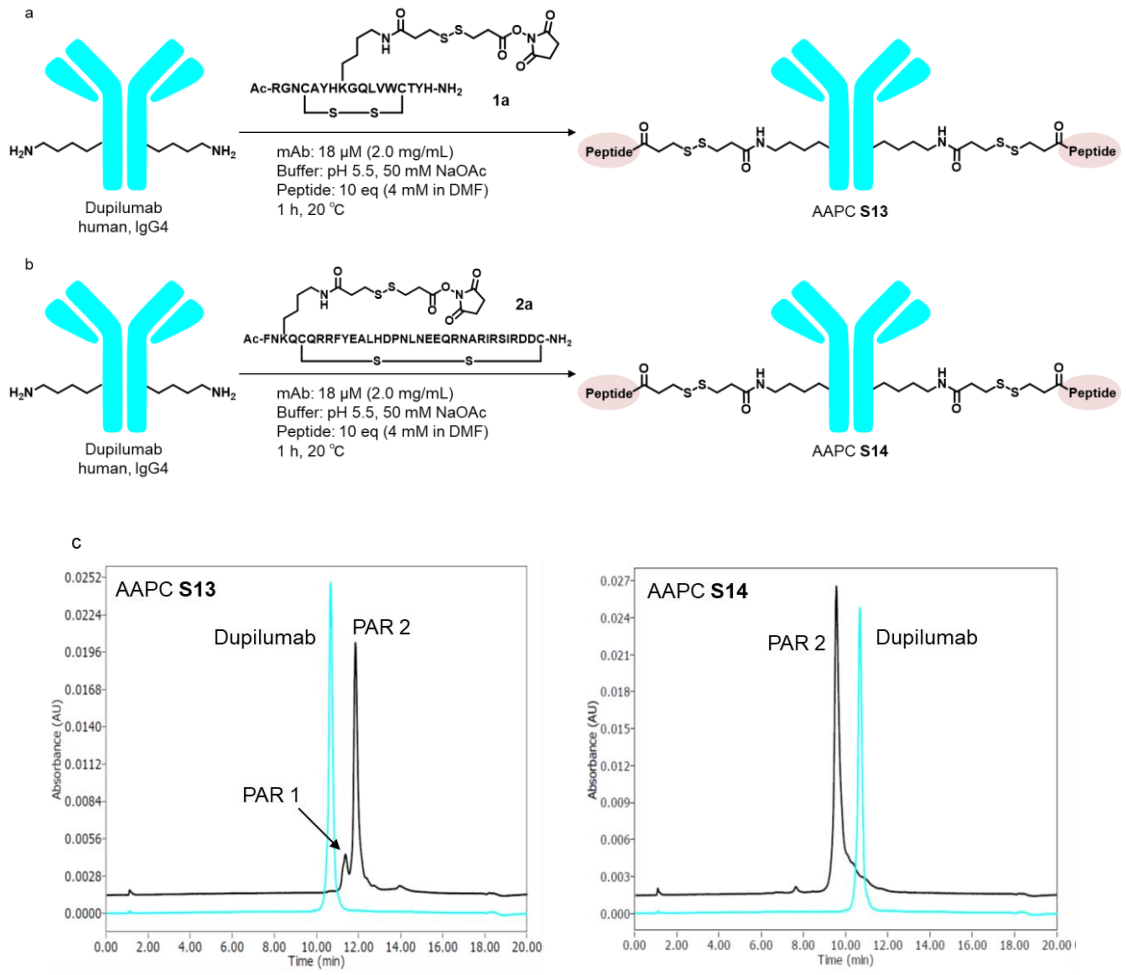

Figure 37. Peptide reagent **1a**, **2a** conjugation to dupilumab. [a]Scheme of conjugation **1a** to dupilumab. [b]Scheme of conjugation **2a** to dupilumab. [c]HIC-HPLC.

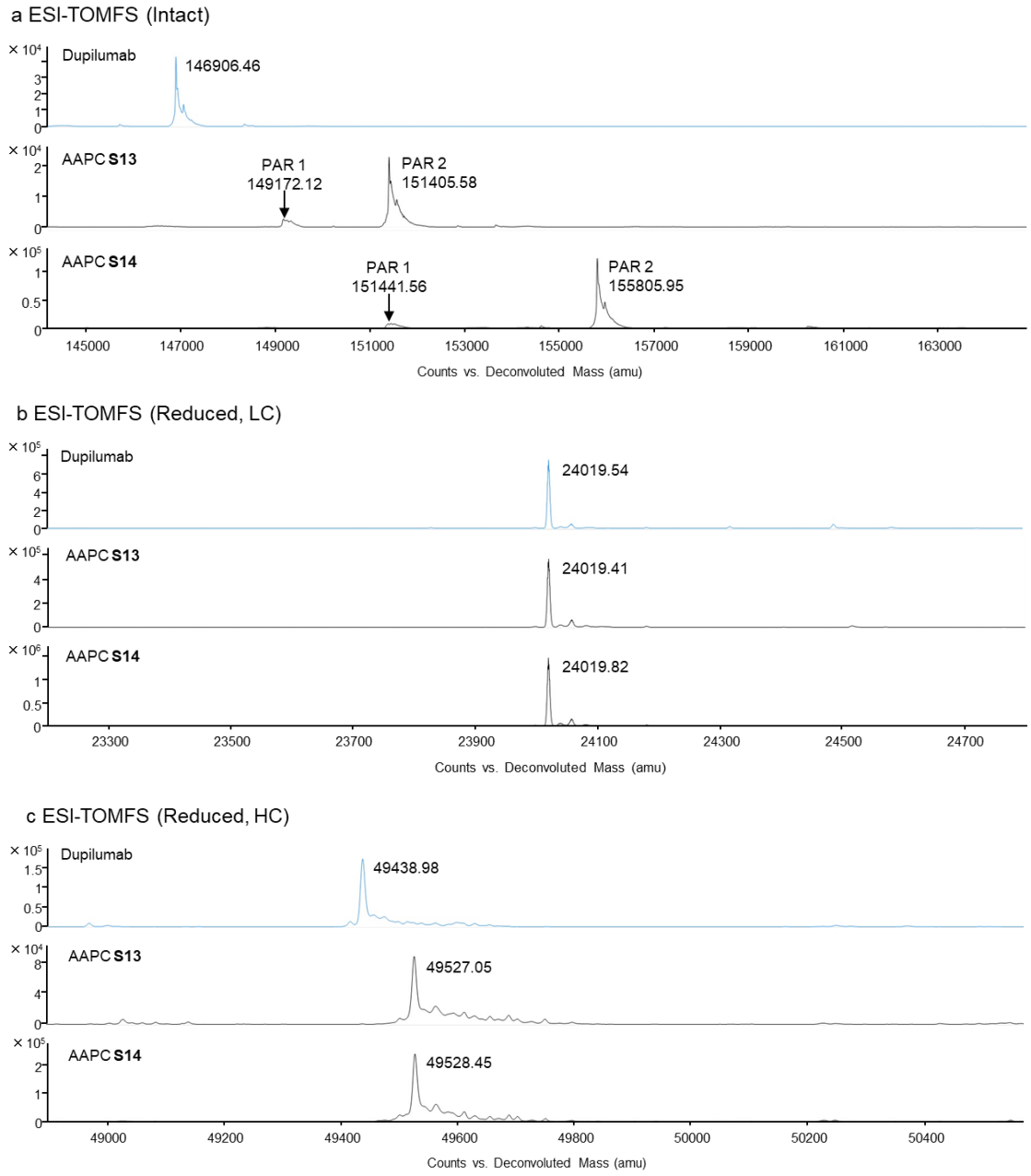

Figure 38. [a]ESI-TOFMS (Intact). [b]ESI-TOFMS (Reduced condition, light chain). [c]ESI-TOFMS (Reduced condition, heavy chain).

3.2. Reaction mechanism

Several mechanistic insights can be inferred from our regiodivergent labelling, and we verified the influence of pH in these reactions. In pH 7.4 HEPES buffer, the conjugation of peptide reagents **1a**–**4a** with trastuzumab was incomplete because the NHS ester immediately decomposed to form the inactivated peptide reagent in situ (see the Supplementary Information). Moreover, after the conjugation reactions of **1a**, **2a** and **4a**, a non-specific mode of modification, LC+3-mercaptopropionate, was observed (Fig. 39). Therefore, acidic conditions in our affinity labelling are essential for completing the reaction in a site-specific manner. Typically, the reaction between primary amines and NHS esters is favoured under neutral to slightly basic conditions. At a lower pH, protonation will render the lysine residues unreactive. However, the protonated and deprotonated forms of lysine exist in dynamic equilibrium in an acidic environment. Lysine condensation with the NHS ester proceeds only if the electrophile exists in the vicinity of the nucleophilic target residue because of the affinity of the peptide for the antibody. Moreover, we propose that lower pH is optimal to prevent non-specific conjugation and allows our unexpected mode of site-specific conjugation to proceed.

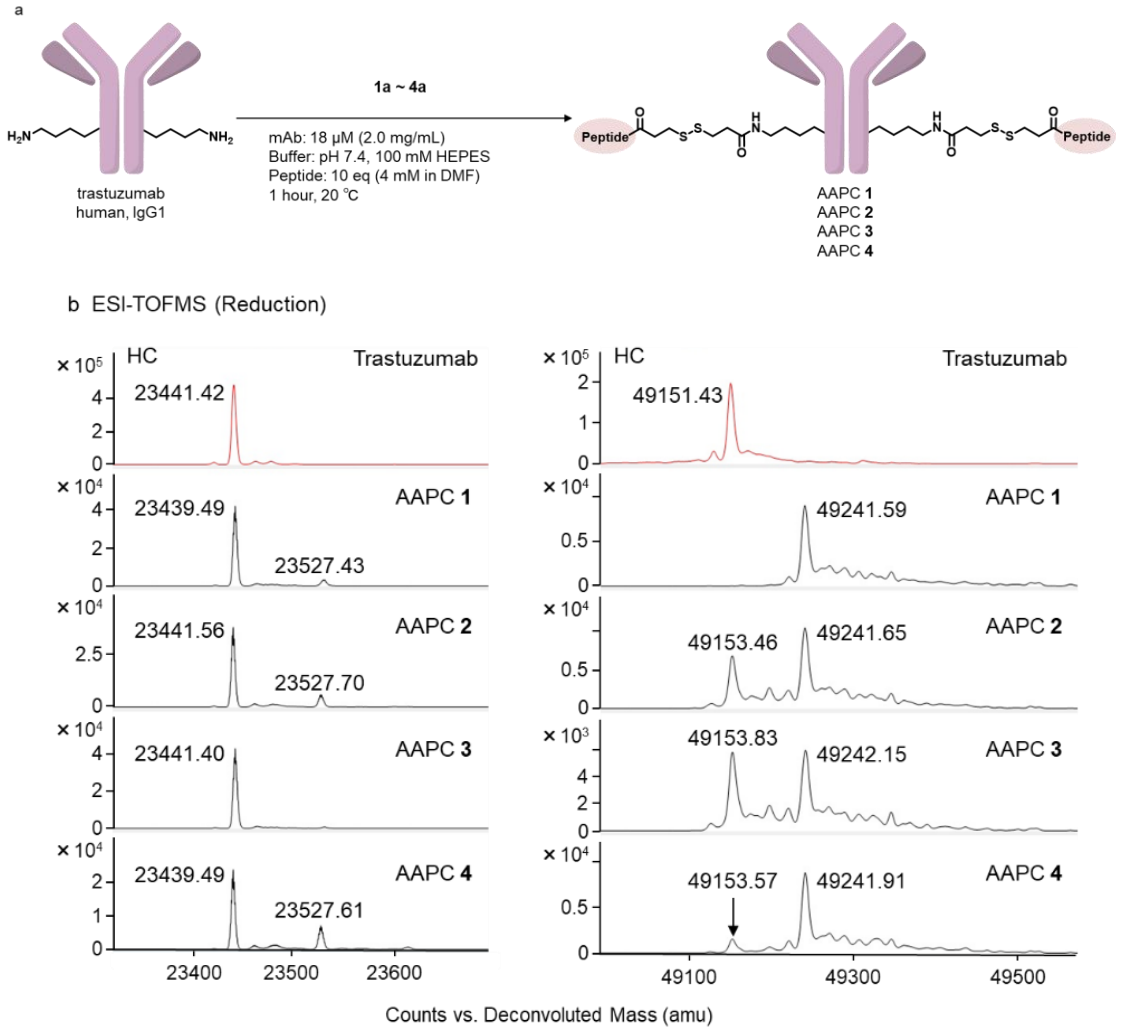

Figure 39. Peptide reagent **1a-4a** conjugation to trastuzumab. [a]Scheme of conjugation **1a-4a** to trastuzumab. [b]ESI-TOFMS (Reduced condition, LC is light chain and HC is heavy chain.)

For emerging site selectivity, the sequence design of peptide reagents is the most important aspect of our methodology. Thus, the lysine in the peptide sequence accurately directs the residue modification in the mAb, and embedded lysines in the peptides must be mutated to arginine. Moreover, these mutated peptides require sufficient affinity to accomplish conjugation. To gain more fundamental insights into the site selectivity, in

this study, the K_d values of hydrolysed peptide reagents were evaluated by using SPR (Table 3 and see the 3.3. Experimental Section Figs. 43-46). Several general conclusions can be drawn at this juncture. First, each peptide retained high affinity for trastuzumab even if we connected a DSP linker and mutated the embedded lysine to arginine. Second, the order of relative affinity to trastuzumab was **1a**>**2a**>**4a**>**3a**, and only **3a** did not completely react. This means that a higher affinity than that of **3a** is required for the reaction in which binding K_d was evaluated as 82.5 ± 0.07 nM.

Table 3. Hydrolysed peptide reagents **1a**-**4a** bind to trastuzumab in the Biacore SPR assay.

Hydrolyzed Peptide reagent	Trastuzumab
	K_D (nM)
1a	12.5 ± 0.01
2a	28.4 ± 0.05
3a	82.5 ± 0.07
4a	36.7 ± 0.06

3.3. Experimental section

3.3.1. Peptide mapping of **S9**

General procedure of peptide mapping: Each 10 µg of deglycosylated sample was diluted to 1 µg/µL with 50 mM ammonium bicarbonate (ABC) buffer. Antibody reduction was achieved by the addition of 20 mM dithiothreitol (DTT) in 40% trifluoroethanol (TFE) to a final concentration of 10 mM. After incubation at 65 °C for 60 min, alkylation was performed by adding 50 mM iodoacetamide (IAM) to a final concentration of 16.7 mM and incubating at 25 °C for 30 min, in the absence of ambient light. The sample was then diluted up to a total volume of 70 µL with 50 mM ABC buffer. We added 10 µL of 20 ng/µL trypsin (Cat # T6567-5X20UG, Sigma) and incubated at 37 °C to carry out protein digestion. After 18 hours incubation, digestion was quenched by adding 2 µL of 20% trifluoroacetic acid (TFA).

The resulting peptide mixture was analyzed on Orbitrap Fusion Tribrid (Thermo Fischer Scientific) interfaced with Easy-nLC (Thermo Fischer Scientific). We used an Acclaim PepMap® 100 (75 µm x 2 cm, Thermo Fischer Scientific) for the trap column and an ESI-column (75 µm x 12.5 cm, 3 µm, NTCC-360/75-3-125, Nikkyo Technos) for the analysis column. The chromatographic method was consisted of a 0.5 min hold at 2% solvent B (0.1% formic acid in acetonitrile) and 23 min linear gradient from 2 to 30% solvent B. The next wash step was performed as 2 min linear gradient from 30 to 75% solvent B and a 9.5 min hold at 75% solvent B. The solvent A consisted of 0.1% formic acid.

Mass spectrometry analysis was carried out in a data dependent acquisition (DDA) mode with full scans (350–2,000 *m/z*) acquired at a mass resolution of 120,000. A spray voltage and an ion transfer tube temperature were set to 1600 V and 275 °C, respectively. Among

detected ions, charge states other than 2-4 were filtered out and run in top speed mode with 3 s cycles for MS/MS analysis. The tandem mass spectra were produced by collision induced dissociation (CID) method. An AGC target ion number for MS^1 was set to 4e5 and 1e4 for MS^2. A maximum injection time for MS^1 and MS^2 was both set to 50 msec. For the dynamic exclusion, a duration time was set to 15 sec.

The resulted MS/MS data was searched against either adalimumab sequence (**Fig. 40**) using Proteome Discoverer 1.4 or 2.2 (Thermo Fischer Scientific) and BioPharma Finder 1.1 or 3.0 (Thermo Fischer Scientific). For Proteome Discoverer search, Sequest HT was used as a search engine and a total intensity threshold was set to 0.01% intensity of the base peak chromatogram peak top. Trypsin was selected for digestion. The maximum peptide length was set to 50 amino acids. The mass tolerance of precursor ions and fragment ions were set to 5 ppm and 0.5 Da, respectively. Carbamidomethylation of cysteine (+57.021 Da) was specified as a fixed modification, and oxidation of methionine (+15.995 Da) and 3-(2-amino-2-oxo-ethyl) sulfanylpropionate of lysine (+145.019 Da) were included as variable modifications. Peptides without high peptide confidence were filtered out. For BioPharma Finder search, S/N threshold was set to 100 and ms noise level was defined by ms signal threshold to be 0.01% intensity of the base peak chromatogram peak top. Trypsin was selected for digestion. The maximum peptide length was set to 50 amino acids. The mass tolerance was set to 0.3 Da. Fixed modifications and variable modifications were set similar to Proteome Discoverer search. Peptides with confidence score higher than 80% and with MS/MS spectrum were counted in for the analysis.

The resulted data of 3-(2-amino-2-oxo-ethyl)sulfanylpropionate lysine residues and corresponding MS and MS/MS spectrum are shown in **Fig. 41**. As shown in **Fig. 42**, the

residues in the CH1, CH2 and CH3 domain (heavy chain constant region) are described with EU numbering. On the other hand, residues in the light chain and VH domain (heavy chain variable region) are labeled with sequence number. AAPC **S9** showed site selective modification in both Proteome Discoverer and BioPharma Finder results. Sequence coverage are shown in **Fig. 42**.

a. Amino acid sequence of adalimumab

Light Chain

1	DIQMTQSPSS	LSASVGDRVT	ITCRASQGIR	NYLAWYQQKP	GKAPKLLIYA	50
51	ASTLQSGVPS	RFSGSGSGTD	FTLTISSLQP	EDVATYYCQR	YNRAPYTFGQ	100
101	GTKVEIKRTV	AAPSVFIFPP	SDEQLKSGTA	SVVCLLNNFY	PREAKVQWKV	150
151	DNALQSGNSQ	ESVTEQDSKD	STYSLSSTLT	LSKADYEKHK	VYACEVTHQG	200
201	LSSPVTKSFN	RGEC				214

Heavy Chain

1	EVQLVESGGG	LVQPGRSLRL	SCAASGFTFD	DYAMHWVRQA	PGKGLEWVSA	50
51	ITWNSGHIDY	ADSVEGRFTI	SRDNAKNSLY	LQMNSLRAED	TAVYYCAKVS	100
101	YLSTASSLDY	WGQGTLVTVS	SASTKGPSVF	PLAPSSKSTS	GGTAALGCLV	150
151	KDYFPEPVTV	SWNSGALTSG	VHTFPAVLQS	SGLYSLSSVV	TVPSSSLGTQ	200
201	TYICNVNHKP	SNTKVDKKVE	PKSCDKTHTC	PPCPAPELLG	GPSVFLFPPK	250
251	PKDTLMISRT	PEVTCVVVDV	SHEDPEVKFN	WYVDGVEVHN	AKTKPREEQY	300
301	NSTYRVVSVL	TVLHQDWLNG	KEYKCKVSNK	ALPAPIEKTI	SKAKGQPREP	350
351	QVYTLPPSRD	ELTKNQVSLT	CLVKGFYPSD	IAVEWESNGQ	PENNYKTTPP	400
401	VLDSDGSFFL	YSKLTVDKSR	WQQGNVFSCS	VMHEALHNHY	TQKSLSLSPG	450

b. Numbering correspondence table

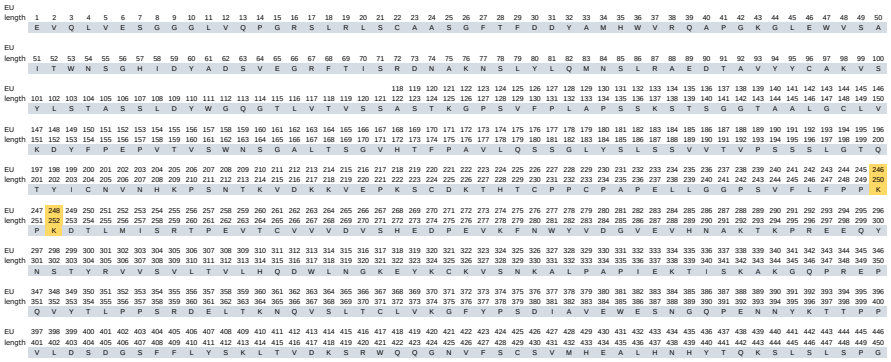

Figure 40. [a]The sequence of adalimumab used for peptide mapping analysis of AAPC S9. 214 amino acids for the light chain, 450 amino acids for the heavy chain. There are 13 modifiable lysine residues in the light chain and 30 in the heavy chain. [b]The table of adalimumab heavy chain sequence numbering correspondence. The residues in the CH1, CH2 and CH3 domain (heavy chain constant region) are described with EU numbering. On the other hand, residues in the light chain and VH domain (heavy chain variable region) are labeled with sequence number. The lysine residues identified as modified are marked with yellow.

a. Results of modification search

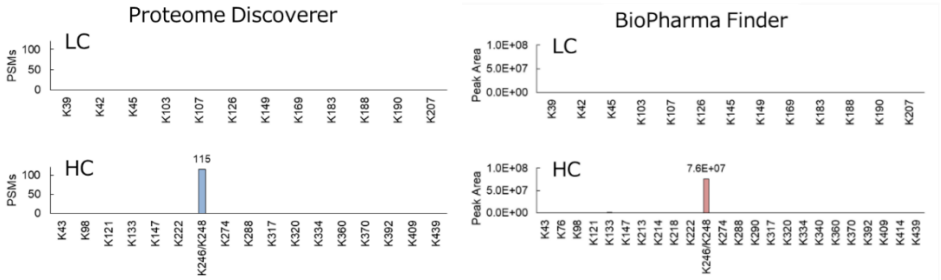

c. Spectrum of modified peptide

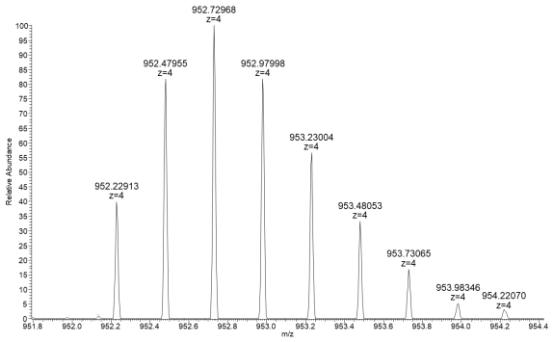

c. MS/MS Spectrum of modified peptide

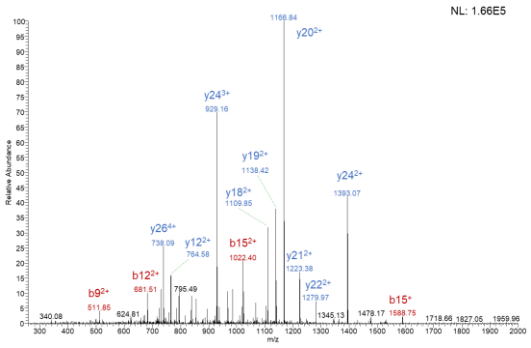

Figure 41. The results of peptide mapping analysis of AAPC **S9**. [a]Lysine residues identified as DSP-NHS linker modified are shown. Both in Proteome Discoverer and BioPharma Finder search showed K246/K248 selective modification. [b]The spectrum of 952.22913 representing THTCPPCPAPELLGGPSVFLFPP^{246}KP^{248}KDTLMISR (4+, with double carbamidomethylation and one 3-(2-amino-2-oxo-ethyl)sulfanylpropionation, theoretical *m/z*: 952.22900). [c]MS/MS spectrum of 952.22913 precursor ion.

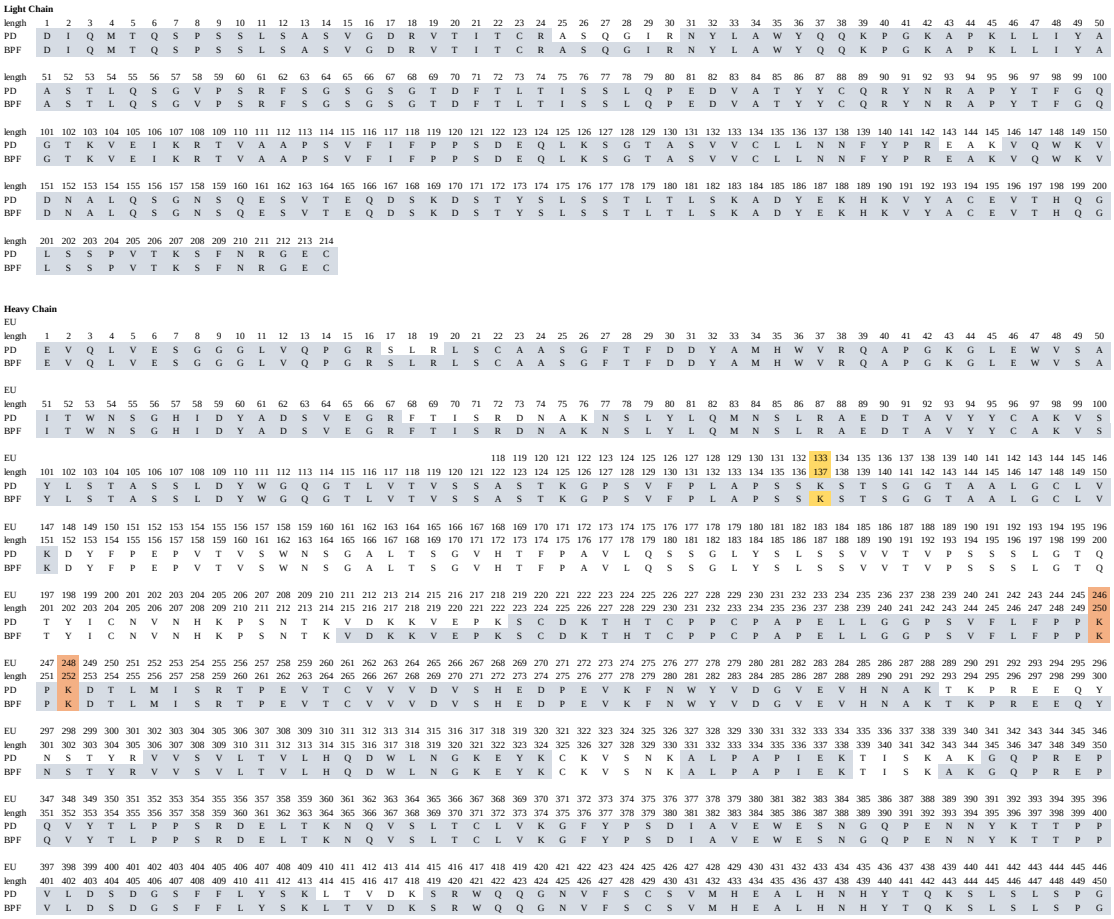

Figure 42. Sequence coverage of acquired peptides. Coverages of light chain were 95.8% and 100%, heavy chain were 74.9% and 83.8% by Proteome Discoverer (PD) and BioPharma Finder (BPF), respectively. Modification observed lysine residues are marked with yellow, and most modified one is indicated in orange.

3.3.2. SPR study

Binding kinetics were determined using a Biacore T-200 system. Trastuzumab was dissolved in sodium acetate buffer (pH 5.5) and immobilized by reaction with premixed *N*-hydroxysuccimimide and 1-[3-(dimethylamino)propyl]-3-ethylcarbodiimide hydrochloride onto a CM5 censor chip. The analytes were adjusted to the desired concentration by serial dilution in a running buffer (HBS-EP; 0.01 M HEPES, 0.15 M NaCl, 3 mM EDTA, 0.005% Tween 20, pH 7.4; to measure peptide binding, we added 1% DMSO). The sensorgrams were obtained with an association time of 180 s, dissociation time of 600 s, and flow rate of 50 μL min^{-1}. For all samples, the sensor chip was washed with glycine hydrochloride buffer (pH 2.0) twice for 5 s for each sample injection because the dissociation of the analyte was not complete within 600 s. To determine the binding kinetics (k_a, k_d, and K_d values), the obtained sensorgrams were analysed by Biacore T200 Evaluation software v.1.0, using a 1:1 binding model.

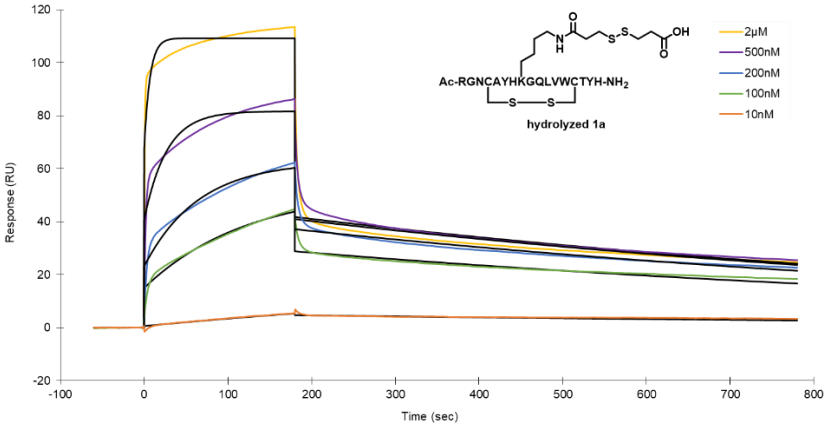

Figure 43. Sensorgrams of the hydrolyzed **1a**. trastuzumab (3500 RU) was immobilized onto a CM5 sensor chip. Curves are corresponding to 10 nM - 2 μM. Black line indicates fitting curve. Binding kinetics of the **1a** against trastuzumab were k_a: 7.32 ± 0.005 (1/ms × 10^4), k_d: 9.16 ± 0.005 (1/s × 10^{-4}), K_D: 12.5 ± 0.01 (nM).

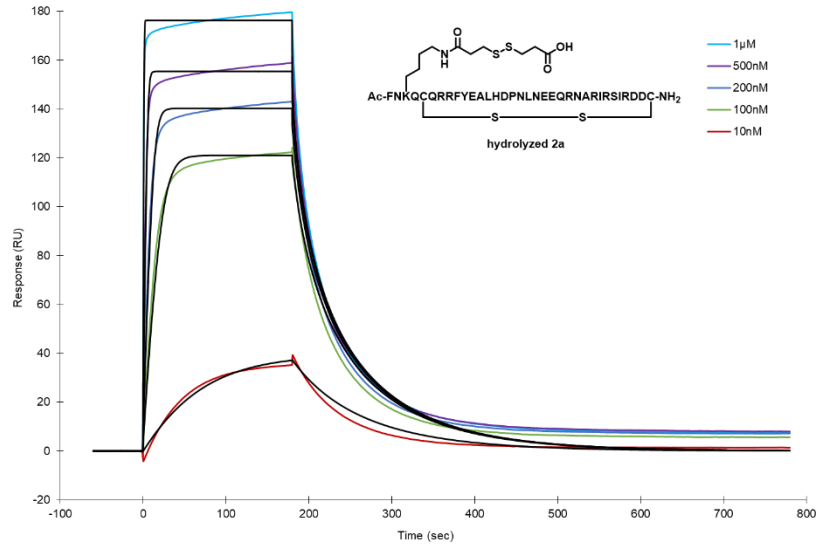

Figure 44. Sensorgrams of the hydrolyzed **2a**. Trastuzumab (3500 RU) was immobilized onto a CM5 sensor chip. Curves are corresponding to 10 nM – 1 μM. Black line indicates fitting curve. Binding kinetics of the **2a** against trastuzumab were k_a: 1.92 ± 0.007 (1/ms × 10^6), k_d: 5.48 ± 0.004 (1/s × 10^{-2}), K_D: 28.4 ± 0.05 (nM).

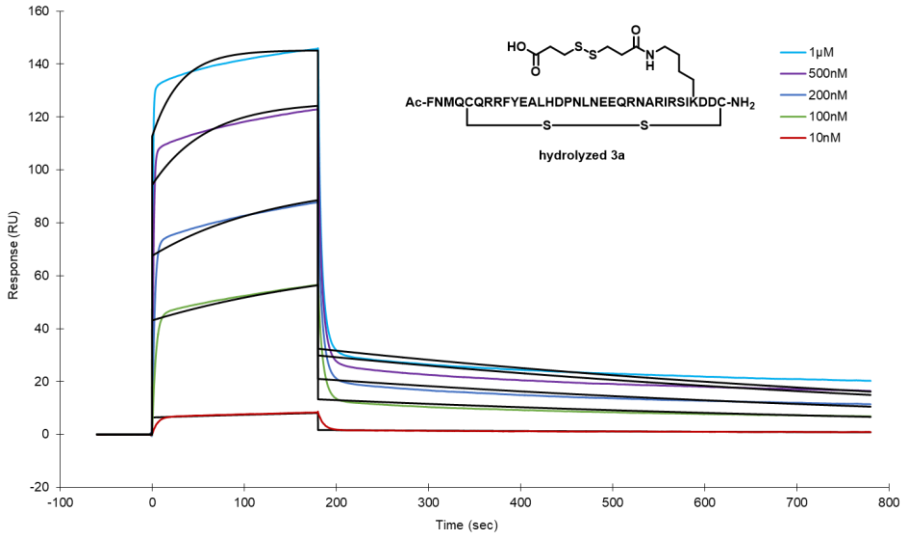

Figure 45. Sensorgrams of the hydrolyzed **3a**. Trastuzumab (3500 RU) was immobilized onto a CM5 sensor chip. Curves are corresponding to 10 nM – 1 μM. Black line indicates fitting curve. Binding kinetics of the **3a** against trastuzumab were k_a: 2.49 ± 0.005 (1/ms × 10^4), k_d: 2.06 ± 0.002 (1/s × 10^{-3}), K_D: 82.5 ± 0.07 (nM).

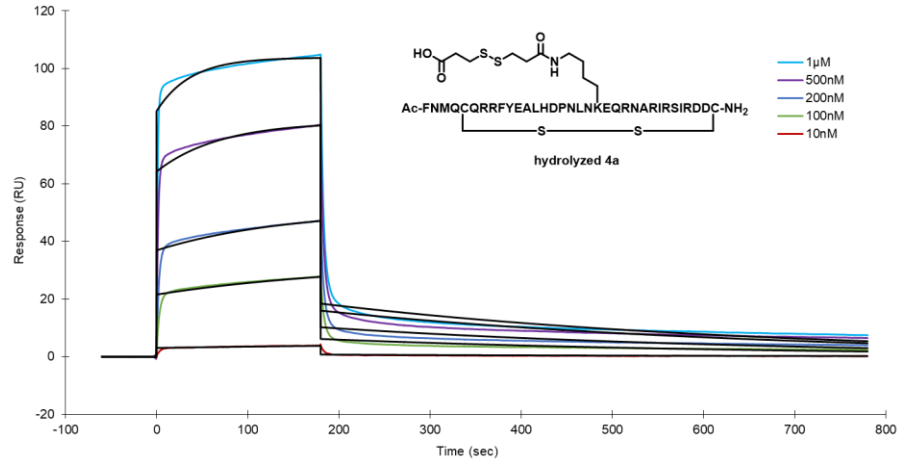

Figure 46. Sensorgrams of the hydrolyzed **4a**. Trastuzumab (3500 RU) was immobilized onto a CM5 sensor chip. Curves are corresponding to 10 nM – 1 μM. Black line indicates fitting curve. Binding kinetics of the **4a** against trastuzumab were k_a: 3.14 ± 0.004 (1/ms × 10^4), k_d: 1.15 ± 0.006 (1/s × 10^{-3}), K_D: 36.7 ± 0.06 (nM).

4. Synthesis of ADC and biological evaluations

4.1. Synthesis of ADC

Having established a reliable conjugation route, we then carefully planned and executed the synthesis of an ADC from an AAPC **1** (Fig. 47). THIOMAB[19] is a well-defined technology that is used in antibody engineering to introduce a reactive cysteine residue in a site-specific manner. To expose reactive cysteine, cleavage inter-chain (and engineered cysteine caps) disulphide bonds with a reducing agent followed by a spontaneous re-oxidation step to re-connect the intermolecular disulfide bond between a heavy chain and a light chain (HC–LC) and/or be-tween the two heavy chains (HC–HC). We hypothesized that these elegant methods could be adapted to the linker cleavage of AAPC **1a**.

To test this hypothesis, we initially began the process with linker cleavage by TCEP. Twenty equivalents of TCEP were added to 1 and the reaction mixture was stirred at 37 °C for 2 h. The reaction proceeded smoothly, and linker-cleaved "HC+3-mercaptopropionate" and non-modified LC products were clearly observed by high-resolution ESI mass spectrometry (Fig. 49). Subsequently, we proceeded to the re-oxidation step after NAP column purification to eliminate excess TCEP. Forty equivalents of dehydroascorbic acid (DHAA) were added to the buffer solution. DHAA acted only as the reconnector of intermolecular disul-fide bonds and did not interact with the thiol moiety, which was newly installed into the Fc. As we had succeeded in obtaining the functionalized non-mutated antibody 1b, we next performed payload conjugation via thiol–maleimide reaction[87] and finally we obtained the desired ADC **1c** with an average DAR of 1.9 (Fig. 48). We measured the free sulfhydryl groups of **1b** using Ellman's assay[88,89] and found the free thiol per antibody ratio to be 1.87 (Table 4).

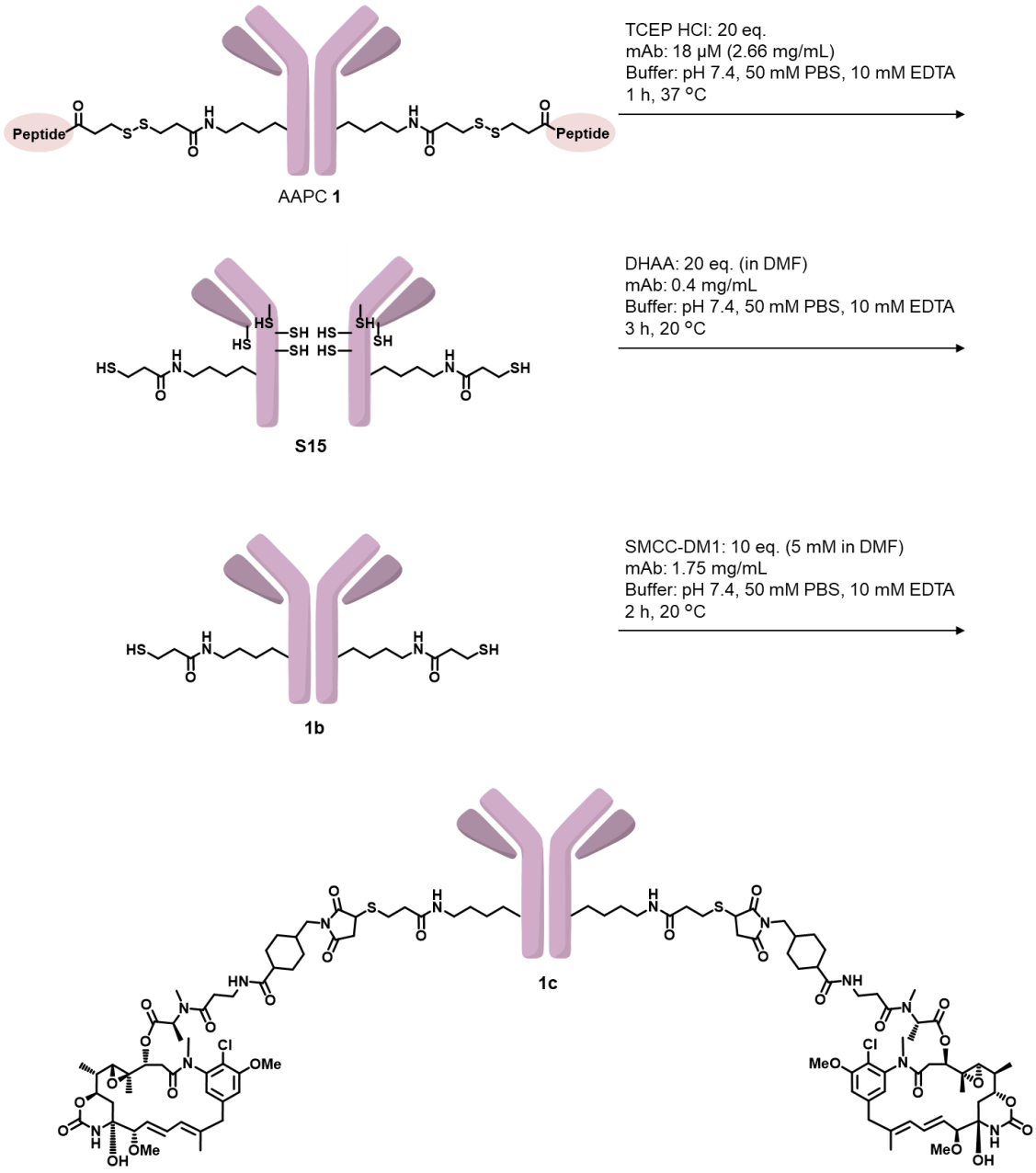

Figure 47. Synthetic route of ADC **1c**.

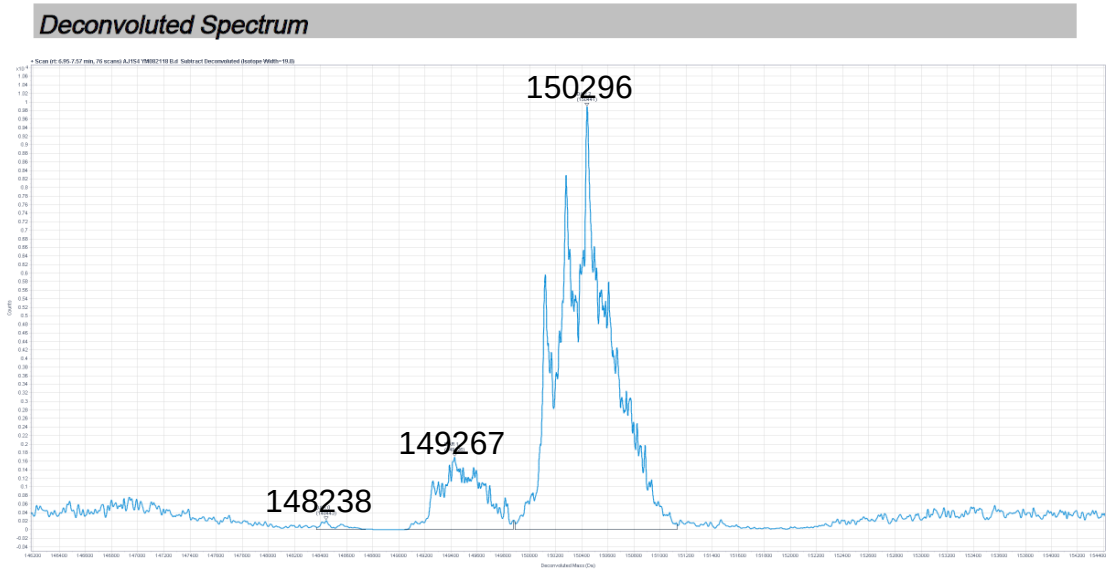

DAR Peak List

DAR Peak	Theoretical Mass (Da)	Observed Mass (Da)	Area	% Area
0	148238	148443	2.93E+004	0.63
1	149267	149426	6.31E+005	13.68
2	150296	150441	3.95E+006	85.69

Figure 48. Result of Agilent DAR Calculator of ADC **1c**. To determine accurate DAR, before deglycosylation MS analysis was used. 0.1363×DAR 1 + 0.8569×DAR 2 = average DAR 1.9.

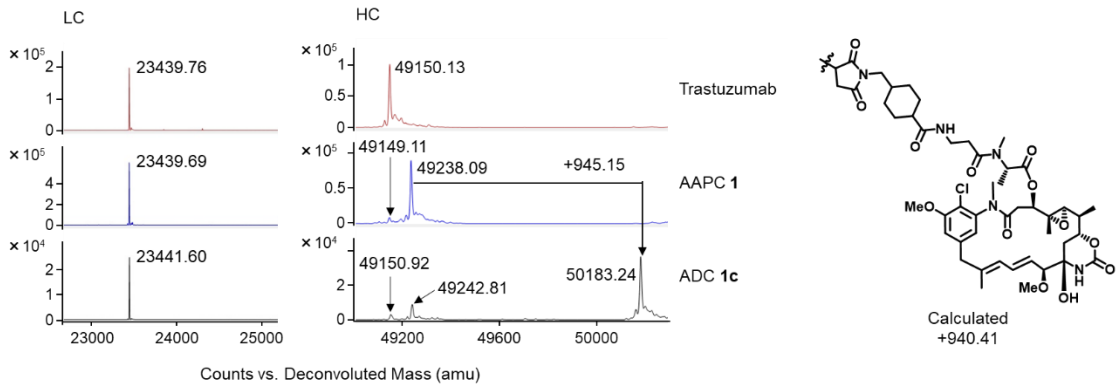

Figure 49. Reduction ESI-TOFMS of ADC **1c** (after deglycosylation).

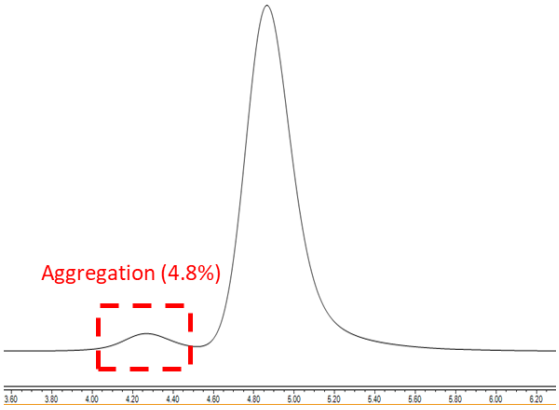

Figure 50. SEC analysis of ADC **1c**.

Table 4. Ellman`s test of **1b**[a].

Sample Name	Condition	Abs (280 nm)	Abs (320 nm)	Abs (412 nm)	Abs (600 nm)	[mAb] M	[SH] M	[SH]/[mAb]
1b+DTNB	Add 2 uL of 10 mM DNTB to 98 µL purified protein	0.35842	0.41296	0.02012	0.00019	No	1.40848E-06	1.871
1b blank	Add 2 uL of buffer to 98 µL purified protein	0.16216	0.00225	0.00084	0.00068	7.52872E-07	-	-

[a] Antibody extinction coefficient (280 nm): 212400 $M^{-1}cm^{-1}$, DTNB extinction coefficient (412nm): 14150 $M^{-1}cm^{-1}$.

4.2. Biological evaluation

To confirm the anticancer potential of our ADC **1c**, we used the Biacore HER2 binding assay and an in vivo xenograft mouse model to observe tumor regression (Figs. 51 and 52). The K_D of **1c** was evaluated as 0.261 pM, which is similar to that of native trastuzumab, K_D was evaluated as 0.232 pM (Fig 51). As expected, our conjugation method-ology to obtain ADC **1c** did not influence antigen binding. In an in vivo study, HER2-positive NCI-N87 cell[90] xenografts were grown to an average volume of 100 mm^3 and then treated twice a week for 2 weeks. Tumor volume and body weight were measured every 3 days during the treatment period. No significant weight loss caused by the administration of either **1c** or trastuzumab (as a positive control) was observed over the course of the study (see the 4.3. Experimental Section Fig. 53). Trastuzumab dosed at 20mg kg^{-1} was able to shrink tumor volumes during the course of treatment, but tumors began to grow slowly a week after treatment was ceased. Notably, a 5 mg kg^{-1} dose of the ADC **1c** shrank the tumor volume to approximately one-half the original size, and the tumors did not regain their original size, even 41 days after the final treatment likely indicating that the remaining mass was devoid of tumor cells (Fig. 52). In short, **1c** showed an efficient mode of ADC action at the in vivo study, causing a greater decrease in tumor volume than did a clinical dose of trastuzumab.

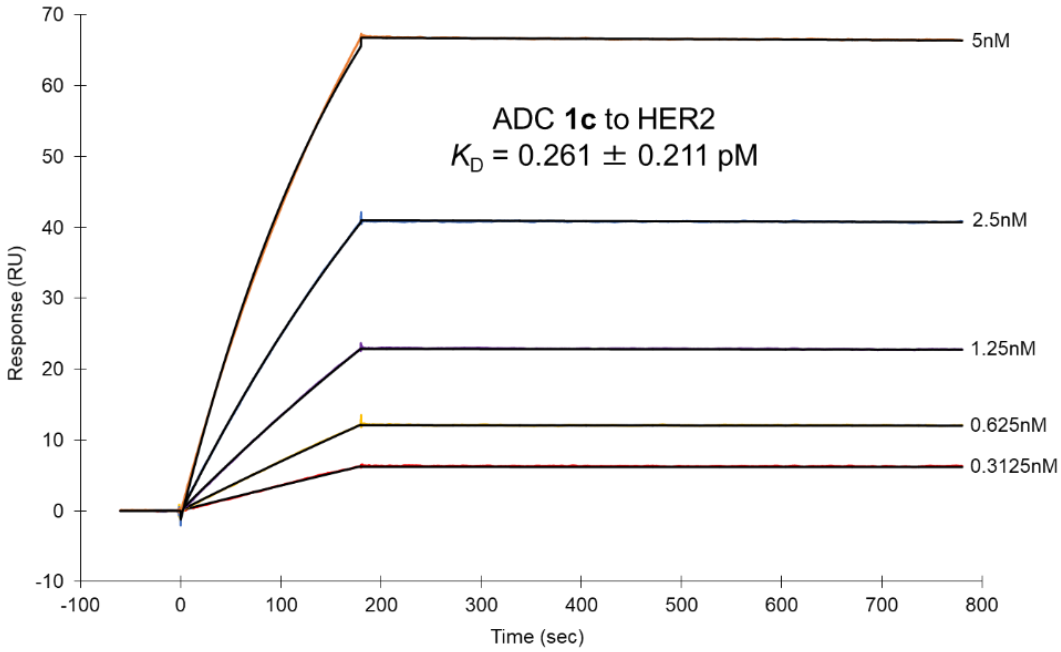

Figure 51. Sensorgrams of the ADC **1c**. HER2-Fc (300 RU) was immobilized onto a CM5 sensor chip. Curves are corresponding to 0.3125 nM – 5 nM. Black line indicates fitting curve. Binding kinetics of the **1c** against HER2-Fc were k_a: 8.77 ± 3.25 (1/ms × 10^6), k_d: 2.29 ± 1.11 (1/s × 10^{-6}), K_D: 0.261 ± 0.211 (pM).

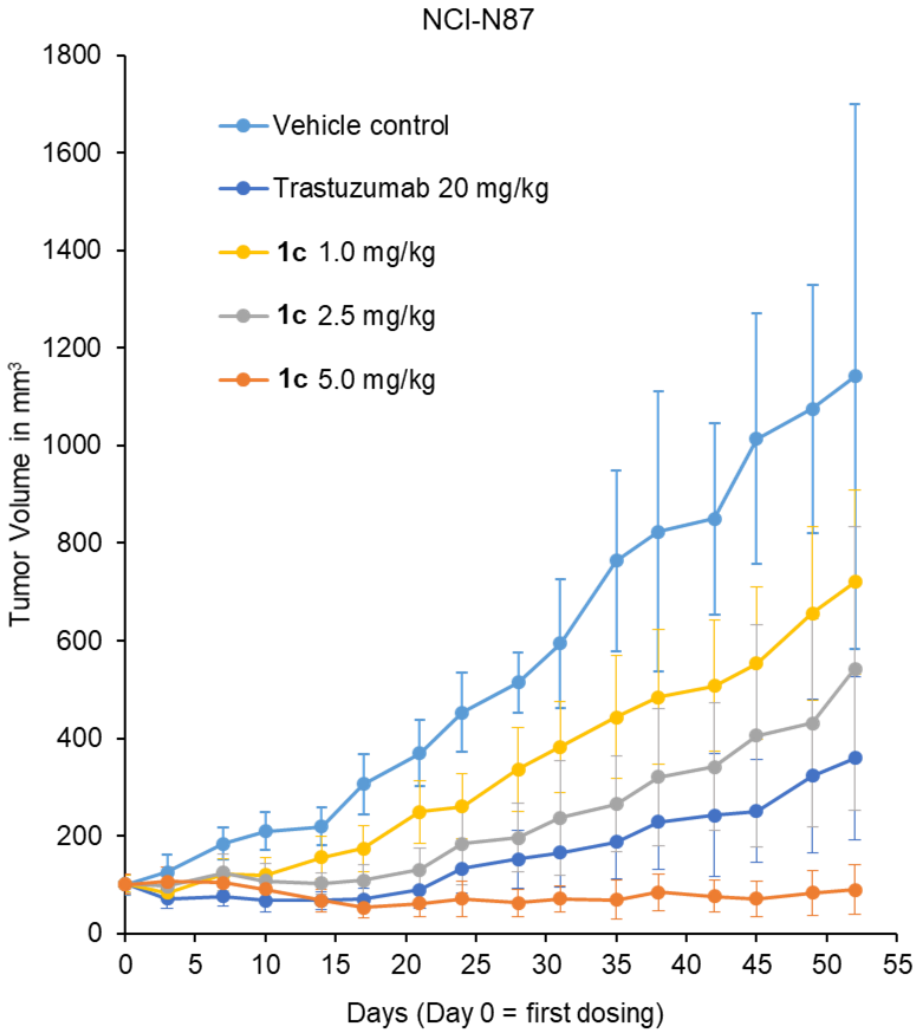

Figure 52. Antitumor activity of anti-HER2 ADC **1c** in the NCI-N87 xenograft tumor models (female NCr nude mice). Trastuzumab (20 mg kg^{-1}, blue), ADC **1c** (1.0 mg kg^{-1}, yellow; 2.5 mg kg^{-1}, grey; 5.0 mg kg^{-1}, orange), or vehicle control (light blue) was administered to mice when the mean tumor volume reached ~100 mm^3. Error bars represent s.e.m.

4.3. Experimental Section

4.3.1. Synthesis of ADC **1c**

4.3.1.1. Linker cleavage and re-oxidation.

Twenty equivalents of TCEP•HCl (4 mM in 50 mM PBS, 10 mM EDTA, pH 7.4) were added to a solution of **1** (2.66 mg mL^{-1} in 50 mM PBS, 10 mM EDTA, pH 7.4) and the reaction mixture was incubated for 1 h at 37 °C. After the reaction was complete, purification was conducted by illustra NAP-10 to remove excess TCEP. After reduction, the material was used immediately while fresh. Subsequently, 20 equivalents of DHAA (4 mM in DMF) were added to a solution of reduced product (0.4 mg mL^{-1} in 50 mM PBS, 10 mM EDTA, pH 7.4), and the reaction mixture was incubated 3 h at 20 °C. The product was purified by illustra NAP-10 to remove excess DHAA to obtain **1b**.

4.3.1.2. Conjugation of SMCC-DM1.

Ten equivalents of SMCC-DM1 (5 mM in DMF) were added to a so-lution of **1b** (11.7 μM, 1.75 mg mL^{-1}, 50 mM PBS, 10 mM EDTA, pH 7.4), and the reaction mixture was incubated for 2 h at 20 °C. After the reaction was complete, 50 equivalents of N-acetylcysteine (50 mM in 50 mM PBS, 10 mM EDTA, pH 7.4) were added and the mixture was incubated at 20 °C for 1 h. Purification was conducted by using an illustra NAP-10 or NAP-25 column to remove excess payload to obtain **1c**.

4.3.2. SPR binding assay

Binding kinetics were determined using a Biacore T-200 system. The ErbB2/HER2 Fc chimaera protein was dissolved in sodium acetate buffer (pH 5.0) and immobilized by

reaction with premixed *N*-hydroxysuccimimide and 1-[3-(dimethylamino)propyl]-3-ethylcarbodiimide hydrochloride onto a CM5 censor chip. The analytes were adjusted to the desired concentration by serial dilution in a running buffer (HBS-EP; 0.01 M HEPES, 0.15 M NaCl, 3 mM EDTA, 0.005% Tween 20, pH 7.4). The sensorgrams were obtained with an association time of 180 s, dissociation time of 600 s, and flow rate of 50 μL min^{-1}. For all samples, the sensor chip was washed with glycine hydrochloride buffer (pH 2.0) twice for 5 s for each sample injection because the dissociation of the analyte was not complete within 600 s. To determine the binding kinetics (k_a, k_d, and K_d values), the obtained sensorgrams were analysed by Biacore T200 Evaluation software v.1.0, using a 1:1 binding model.

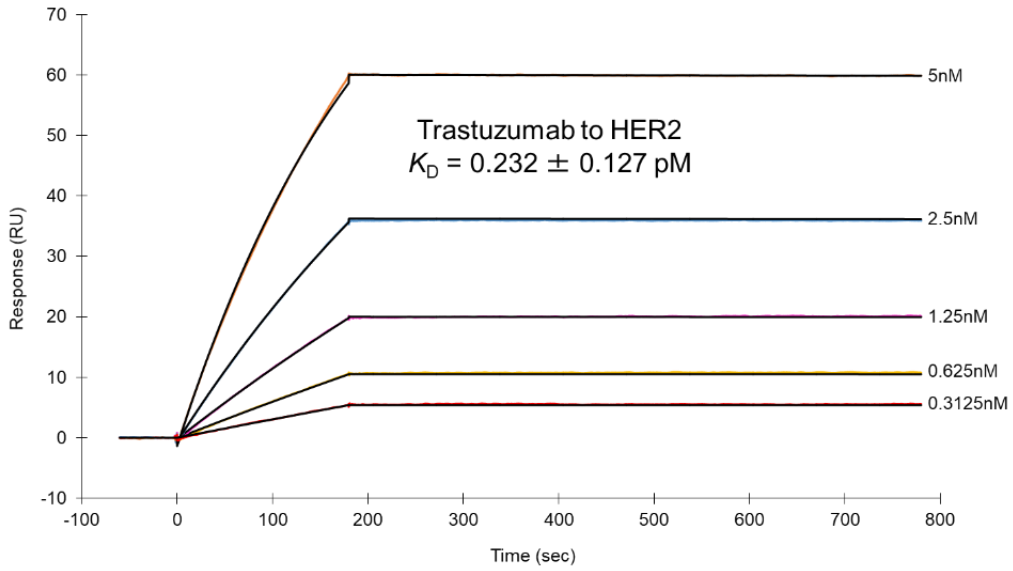

Figure 53. Sensorgrams of the trastuzumab. HER2-Fc (300 RU) was immobilized onto a CM5 sensor chip. Curves are corresponding to 0.3125 nM – 5 nM. Black line indicates fitting curve. Binding kinetics of the trastuzumab against HER2-Fc were k_a: 9.99 ± 1.22 (1/ms × 10^6), k_d: 2.32 ± 0.57 (1/s × 10^{-6}), K_D: 0.232 ± 0.127 (pM).

4.3.3. Xenograft assay

4.3.3.1. Test articles

1) AJ1 (ADC), 5 mL at 2 mg/mL

2) Herceptin, 5 mL at 5 mg/mL

3) Formulation buffer (20 mM Histidine, 5% Trehalose, pH 5.2), 250 mL

4.3.3.2. NCI-N87 cells

NCI-N87 cells ATCC (ATCC CRL-5822) were cultured in RPMI supplemented with 10% FBS and 1%P/S, in a humidified incubator at 37 °C and 5% CO_2.

4.3.3.3. Animal experiments

All procedures were approved by the Institutional Animal Care and were performed according to the NIH guide for the care.

4.3.3.4. Animals

NOD.CB17 Prkdc<Scid>/J homozygous mice were procured through Jackson Laboratory (Strain 001303, Female, DOB +/-3 days). Mice were fed Teklad irradiated (sterilized) mouse diet and bedded with Teklad irradiated (sterilized) corncob bedding from Envigo (Indianapolis, IN). Mice were housed in Optimice carousel sterile quarters with filtered air supply in disposable cages from Animal Care Systems, Inc. (Centennial, CO).

4.3.3.5. NCI-N87 implantation

On the day of implantation, NCI-N87 cells were trypsinized and allowed to detach from flasks. Trypsin was then neutralized with complete media and cells were spun at 400 x g. Media was aspirated and cells were resuspended in 50:50 Cultrex:RPMI at a concentration of 5 x 10^7 cells / mL. A volume of 100 µL was injected into the right hind flank of each animal (a total of 5 x 10^6 cells).

[Cultrex: BME, Type 3, Trevigen Cat. # 3632-005-02, Lot # 40498J17]

4.3.3.6. Study Arms and Treatments

Tumor volumes were monitored, and on when mean tumor volume reached 100 mm^3, mice were stratified and placed into 5 treatment groups of 10 mice as outlined in Table 5. Treatments were administered by tail vein injection (100 µL volumes). Doses were administered two times a week for a total of 4 doses.

Table 5. Study arms (n=10 mice per arm), with all doses as mg/kg.

Group	n	Treatment	mg/kg
1	10	Vehicle	NA
2	10	**1c**	5
3	10	**1c**	2.5
4	10	**1c**	1
5	10	Trastuzumab	20

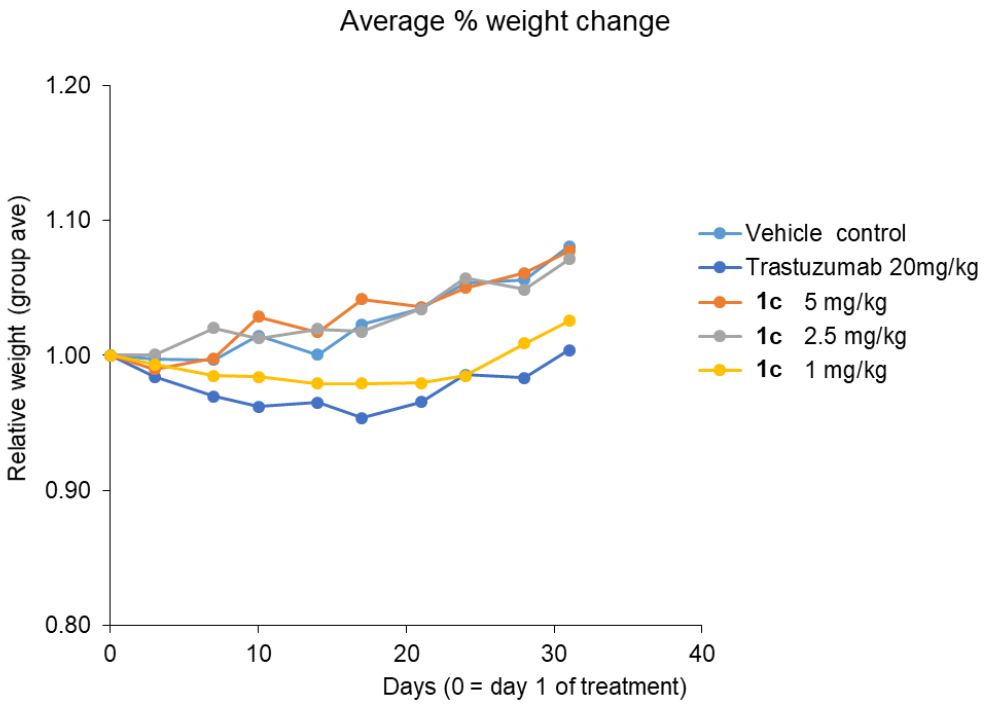

Figure 54. Average animal weight relative to day 0. Overall the group averages did not change dramatically from the first day of treatment through day 31 (the scale of the Y axis is narrow in Figure 1). Interestingly, the average weight dipped slightly for the trastuzumab arm and the lowest dose of **1c**, however, the higher doses of **1c** mimicked that of the vehicle only group. It is unclear why the **1c** low dose mice lost weight, while the 5 mg/kg and 2.5 mg/kg groups did not. All animals except one of the control animals survived the study without outward manifestations of morbidity. Animal #3 in the control group (labeled cage 1A, 2 notches in left ear) had a quickly growing tumor, and then suddenly lost significant weight between days 35-42, and had to be euthanized due to poor health. It did not appear that other animals in the same cage were contributing to the decline in health.

Table 6. Returned p-values using a type 2, 2-sided t-test using tumor volumes at 52 days.

samples	p-value
1c 5 mg/kg	7.07E-08
1c 2.5 mg/kg	3.30E-04
1c 1 mg/kg	1.44E-03
Trastuzumab	6.23E-06

5. Conclusion

In conclusion, we expect the chemistry of the affinity peptide mediated regiodivergent functionalization of IgGs to be valuable for the construction of complex antibody-related biomolecules. Site-specific synthesis of ADCs is a growing area of pharmaceutical research. However, compared to the existing methodologies, our strategy has the following advantages: (1) engineering of mAbs is not required to site-specifically synthesize ADCs from native mAbs regardless of glycosylation status, enabling us to target the early stage of ADC programmes; (2) the reliable reduction and re-oxidation routes are the same as in THIOMAB and are adaptable to our conjugation system; (3) it is possible to modify other lysine sites in mAbs using other affinity peptides or proteins; and (4) the new affinity-peptide-dependent regiodivergent labelling strategy can be extended not only to ADCs but also to other protein conjugates.

References

[1] N. Krall, F. P. da Cruz, O. Boutureira, G. J. L. Bernardes, *Nat. Chem.* **2015**, *8*, 103-113.

[2] I. S. Carrico, *Chem. Soc. Rev.* **2008**, *37*, 1423-1431.

[3] C. D. Spicer, B. G. Davis, *Nat. Commun.* **2014,** *5*, 4740-4745.

[4] O. Boutureira, G. J. L. Bernardes, *Chem. Rev.* **2015**, *115*, 2174-2195.

[5] N. Stephanopoulos, M. B. Francis, *Nat. Chem. Biol.* **2011**, *7*, 876-884.

[6] A. Beck, L. Goetsch, C. Dumontet, N. Corvaïa, *Nat. Rev. Drug Discovery* **2017**, *16*, 315-337.

[7] R. V. J. Chari, M. L. Miller, W. C. Widdison, *Angew. Chem. Int. Ed.* **2014**, *53*, 3796-3827.

[8] L. Ducry, B. Stump, *Bioconjugate Chem.* **2010**, *21*, 5-13.

[9] S. Hashida, M. Imagawa, S. Inoue, K. H. Ruan, E. Ishikawa, *J. Appl. Biochem.* **1984**, *6*, 56-63.

[10] L. Wang, G. Amphlett, W. A. Blättler, J. M. Lambert, W. Zhang, *Protein Sci.* **2005**, *14*, 2436-2446.

[11] M. M. C. Sun, K. S. Beam, C. G. Cerveny, K. J. Hamblett, R. S. Blackmore, M. Y. Torgov, F. G. M. Handley, N. C. Ihle, P. D. Senter, S. C. Alley, *Bioconjugate Chem.* **2005**, *16*, 1282-1290.

[12] S. Verma, D. Miles, L. Gianni, I. E. Krop, M. Welslau, J. Baselga, M. Pegram, D. Y. Oh, V. Diéras, E. Guardino, L. Fang, M. W. Lu, S. Olsen, K. Blackwell, *N. Engl. J. Med.* **2012**, *367*, 1783-1791.

[13] P. M. LoRusso, D. Weiss, E. Guardino, S. Girish, M. X. Sliwkowski, *Cancer Res.* **2011**, *17*, 6437-6447.

[14] A. Younes, L. N. Bartlett, J. P. Leonard, D. A. Kennedy, C. M. Lynch, E. L. Sievers, A. F. Torres, *N. Engl. J. Med.* **2010**, *363*, 1812-1821.

[15] P. D. Senter, E. L. Sievers, *Nat. Biotechnol.* **2012**, *30*, 631-637.

[16] B. Q. Shen, K. Xu, L. Liu, H. Raab, S. Bhakta, M. Kenrick, K. L. P. Reponte, J. Tien, S. F. Yu, E. Mai, D. Li, J. Tibbitts, J. Baudys, O. M. Saad, S. J. Scales, P. J. McDonald, P. E. Hass, C. Eigenbrot, T. Nguyen, W. A. Solis, R. N. Fuji, K. M. Flagella, D. Patel, S. D. Spencer, L. A. Khawli, A. Ebens, W. L. Wong, R. Vandlen, S. Kaur, M. X. Sliwkowski, R. H. Scheller, P. Polakis, J. R. Junutula, *Nat. Biotechnol.* **2012**, *30*, 184-189.

[17] P. Strop, S. H. Liu, M. Dorywalska, K. Delaria, R. G. Dushin, T. T. Tran, W. H. Ho, S. Farias, M. G. Casas, Y. Abdiche, D.Zhou, R. Chandrasekaran, C. Samain, C. Loo, A. Rossi, M. Rickert, S. Krimm, T. Wong, S. M. Chin, J. Yu, J. Dilley, J. C. Riggers, G. F. Filzen, C. J. O'Donnell, F. Wang, J. S. Myers, J. Pons, D. L. Shelton, A. Rajpal, *Chem. Biol*. **2013**, *20*, 161-167.

[18] A. Lucas, L. Price, A. Schorzman, M. Storrie, J. Piscitelli, J. Razo, W. Zamboni, *Antibodies* **2018**, *7*, 10-17.

[19] J. R. Junutula, H. Raab, S. Clark, S. Bhakta, D. D. Leipold, S. Weir, Y. Chen, M. Simpson, S. P. Tsai, M. S. Dennis, Y. Lu, Y. G. Meng, C. Ng, J. Yang, C. C. Lee1, E. Duenas, J. Gorrell, V. Katta, A. Kim, K. McDorman, K. Flagella, R. Venook, S. Ross, S. D. Spencer, W. L. Wong, H. B. Lowman, R. Vandlen, M. X. Sliwkowski, R. H. Scheller, P. Polakis, W. Mallet, *Nat. Biotechnol.* **2008**, *26*, 925-932.

[20] J. Y. Axup, K. M. Bajjuri, M. Ritland, B. M. Hutchins, C. H. Kim, S. A. Kazane, R. Halder, J. S. Forsyth, A. F. Santidrian, K. Stafin, Y. Lu, H. Tran, A. J. Seller, S. L. Biroc, A. Szydlik, J. K. Pinkstaff, F. Tian, S. C. Sinha, B. F. Habermann, V.

V. Smider, P. G. Schultz, *Proc. Natl. Acad. Sci. U. S. A.* **2012**, *109*, 16101-16106.

[21] E. S. Zimmerman, T. H. Heibeck, A. Gill, X. Li, C. J. Murray, M. R. Madlansacay, C. Tran, N. T. Uter, G. Yin, P. J. Rivers, A. Y. Yam, W. D. Wang, A. R. Steiner, S. U. Bajad, K. Penta, W. Yang, T. J. Hallam, C. D. Thanos, A. K. Sato, *Bioconjugate Chem.* **2014**, *25*, 351-361.

[22] D. Rabuka, J. S. Rush, G. W. deHart, P. Wu, C. R. Bertozzi, *Nat. Protoc.* **2012**, *7*, 1052-1067.

[23] B. L. Carlson, E. R. Ballister, E. Skordalakes, D. S. King, M. A. Breidenbach, S. A. Gilmore, J. M. Berger, C. R. Bertozzi, *J. Biol. Chem.* **2008**, *283*, 20117-20125.

[24] P. Agarwal, R. Kudirka, A. E. Albers, R. M. Barfield, G. W. de Hart, P. M. Drake, L. C. Jones,, D. Rabuka, *Bioconjugate Chem.* **2013**, *24*, 846−851.

[25] S. Jeger, K. Zimmermann, A. Blanc, J. Grünberg, M. Honer, P. Hunziker, H. Struthers, R. Schibli, *Angew. Chem., Int. Ed.* **2010**, *49*, 9995-9997.

[26] Z. Qu, R. M. Sharkey, H. J. Hansen, L. B. Shih, S. V. Govindan, J. Shen, D. M. Goldenberg, S. Leung, *J. Immunol. Meth.* **1998**, *213*, 131-144.

[27] E. Boeggeman, B. Ramakrishnan, M. Pasek, M. Manzoni, A. Puri, K. H. Loomis, T. J. Waybright,, P. K. Qasba, *Bioconjugate Chem.* **2009**, *20*, 1228-1236.

[28] Z. Zhu, B. Ramakrishnan, J. Li, Y. Wang, Y. Feng, P. Prabakaran, S. Colantonio, M. A.Dyba, P. K. Qasba, D. S. Dimitrov, *mAbs* **2014**, 6, 1-6.

[29] B. M. Zeglis, C. B. Davis, R. Aggeler, H. –C. Kang, A. Chen, B. Agnew, J. S. Lewis, *Bioconjugate Chem.* 2013, *24*, 1057-1067.

[30] X. Li, T. Fang, G. -J. Boons *Angew. Chem., Int. Ed.* **2014**, *53*, 7179-7182.

[31] R. V. Geel, M. A. Wijdeven, R. Heesbeen, J. M. M. Verkade, A. A. Wasiel, S. S. V. Berkel, F. L. V. Delft, *Bioconjugate Chem.* **2015**, *26*, 2233-2242.

[32] D. Ghaderi, R. E. Taylor, V. P-. Karavani, S. Diaz, A. Varki, *Nat. Biotechnol.* **2010**, *28*, 863-867.

[33] J. Du, M. A. Meledeo, Z. Wang, H. S. Khanna, V. D. P. Paruchuri, K. J. Yarema, *Glycobiology* **2009**, *19*, 1382-1401.

[34] M. J. Matos, B. L. Oliveira, N. Marutínez-Sáez, A. Gunerreiro, P. M. S. D. Cal, J. Bertoldo, M. Maneiro, E. Perkins, J. Howard, M. K. Deery, J. M. Chalker, F. Corzana, G. Jiménez-Osés, G. J. L. Bernardes, *J. Am. Chem. Soc.* **2018**, *140*, 4004-4017.

[35] S. R. Adusumalli, D. G. Rawale, U. Singh, P. Tripathi, R. Paul, N. Kalra, R. K. Mishra, S. Shukla,, V. Rai, *J. Am. Chem. Soc.* **2018**, *140*, 15114-15123.

[36] S. O. Doronina, B. E. Toki, M. Y. Torgov, B. A. Mendelsohn, C. G. Cerveny, D. F. Chace, R. L. DeBlanc, R. P. Gearing, T. D. Bovee, C. B. Siegall, J. A. Francisco, A. F. Wahl, D. L. Meyer, P. D. Senter, *Nature Biotechnol.* **2003**, *21*, 778-784.

[37] K. J. Hamblett, P. D. Senter, D. F. Chace, M. M. C. Sun, J. Lenox, C. G. Cerveny, K. M. Kissler, S. X. Bernhardt, A. K. Kopcha, R. F. Zabinski, D. L. Meyer, J. A. Francisco, *Clin. Cancer Res.* **2004**, *10*, 7063-7070.

[38] N. S.Beckley, K. P. Lazzareschi, H. -W. Chih, V. K. Sharma, H. L. Flores, *Bioconjugate Chem.* **2013**, *24*, 1674-1683.

[39] G. Badescu, P. Bryant, M. Bird, K. Henseleit, J. Swierkosz, V. Parekh, R. Tommasi, E. Pawlisz, K. Jurlewicz, M. Farys, N. Camper, X. Sheng, M. Fisher, R. Grygorash, A. Kyle, A. Abhilash, M. Frigerio, J. Edwards, A. Godwin, *Bioconjugate Chem.* **2014**, *25*, 1124-1136.

[40] F. F. Schumacher, J. P. M. Nunes, A. Maruani, V. Chudasama, M. E. B. Smith,

K. A. Chester, J. R. Baker, S. Caddick, *Org. Biomol. Chem.* **2014**, *12*, 7261-7269.

[41] A. Maruani, M. E. B. Smith, E. Miranda, K. A. Chester, V. Chudasama, S. Caddick, *Nature Commun.* **2015**, *6*, 6645-6652.

[42] J. P. M. Nunes, M. Morais, V. Vassileva, E. Robinson, V. S. Rajkumar, M. E. B. Smith, R. B. Pedley, S. Caddick, J. R. Baker, V. Chudasama, *Chem. Commun.* **2015**, *51*, 10624-10627.

[43] A. Maruani, H. Savoie, F. Bryden, S. Caddick, R. Boyle, V. Chudasama, *Chem. Commun.* **2015**, *51*, 15304-15307.

[44] G. Dorman, G. D. Prestwich, *Trends Biotechnol.* 2000, *18*, 64-77.

[45] A. Kawamura, S. Hindi, D. M. Mihai, L. James, O. Aminova, *Bioorg. Med. Chem.* **2008**, *16*, 8824-8829.

[46] Y. Jung, J. M. Lee, J. Kim, J. Yoon, H. Cho, B. H. Chung, *Anal. Chem.* **2009**, *81*, 936-942.

[47] L. Björck, G. Kronvall, *J. Immunol.* **1984**, *133*, 969-974.

[48] B. Åkerström, L. Björck, *J. Biol. Chem.* **1986**, *261*, 10240-10246.

[49] A. E. Sauer-Eriksson, G. J. Kleywegt, M. Uhlén, T. A. Jones, *Structure* **1995**, *3*, 265–278.

[50] A. Konrad, A. E. Karlström, S. Hober, *Bioconjugate Chem.* **2011**, *22*, 2395-2403.

[51] B. Nilsson, T. Moks, B. Jansson, L. Abrahamsen, A. Elmblad, E. Holmgren, C. Henrichson, T. A. Jones, M. Uhlen, *Protein Eng.* **1987**, *1*, 107-113.

[52] L. Cedergren, R. Andersson, B. Jansson, M. Uhlen, B. Nilsson, *Protein Eng.* **1993**, *6*, 441-448.

[53] J. Deisenhofer, *Biochemistry* **1981**, *20*, 2361-2370.

[54] F. Yu, P. Järver, P. Nygren, *PLoS One* **2013**, *8*, e56597.

[55] J. Z. Hui, A. A. Zaki, Z. Cheng , V. Popik, H. Zhang, E. T. L. Prak, A. Tsourkas, *Small* **2014**, *10*, 3354-3363.

[56] A. Perols, A. E. Karlström, *Bioconjugate Chem.* **2014**, *25*, 481-488.

[57] S. Kanje, S. Hober, *Biotechnol. J.* **2015**, *10*, 564-574.

[58] J. Z. Hui, S. Tamsen, Y. Song, A. Tsourkas, *Bioconjugate Chem.* **2015**, *26*, 1456-1460.

[59] J. Z. Hui, A. Tsourkas, *Bioconjugate Chem.* **2014**, *25*, 1709-1719.

[60] S. Kanje, E. von Witting, S. C. C. Chiang, Y. T. Bryceson, S. Hober, *Bioconjugate Chem.* **2016**, *27*, 2095-2102.

[61] J. Park, Y. Lee, B. J. Ko, T. H. Yoo, *Bioconjugate Chem.* **2018**, *29*, 3240-3244.

[62] N. Vance, N. Zacharias, M. Ultsch, G. Li, A. Fourie, P. Liu, J. L. F. Vanasse, J. A. Ernst, W. Sandoval, K. R. Kozak, G. Phillips, W. Wang, J. Sadowsky, *Bioconjugate Chem.* **2019**, *30*, 148-160.

[63] W. L. DeLano, M. H. Ultsch, A. M. de Vos, J. A. Wells, *Science* **2000**, *287*, 1279-1283.

[64] B. A. Kerwin, R. L. Remmele, *J. Pharm. Sci.* **2007**, *96*, 1468-1479.

[65] C. Yu, J. Tang, A. Loredo, Y. Chen, S. Y. Jung, A. Jain, A. Gordon, H. Xiao, *Bioconjugate Chem.* **2018**, *29*, 3522-3526.

[66] S. Kishimoto, Y. Nakashimada, R. Yokota, T. Hatanaka, M. Adachi, Y. Ito, *Bioconjugate Chem.* **2019**, *30*, 698-702.

[67] J. Ohata, Z. T. Ball, *J. Am. Chem. Soc.* **2017**, *139*, 12617-12622.

[68] B. V. Popp, Z. T. Ball, Chem. Sci. 2011, 2, 690-695.

[69] W. Choe, T. Durgannavar, S. Chung, *Materials* **2016**, *9*, 994-998.

[70] N. Kruljec, T. Bratkovič, *Bioconjugate Chem.* **2017**, *28*, 2009-2017.

[71] M. A. Starovasnik, A. C. Braisted, J. A. Wells, *Proc. Natl. Acad. Sci. U. S. A.* **1997**, *94*, 10080-10085.

[72] A. C. Braisted, J. A. Wells, *Proc. Natl. Acad. Sci. U. S. A.* **1996**, *93*, 5688-5692.

[73] A. J. Lomant, G. Fairbanks, *J. Mol. Biol.* **1976**, *104*, 243-246.

[74] S. Henikoff, J. G. Henikoff, *Proc. Natl. Acad. Sci. U. S. A.* **1992**, *89*, 10915-10921.

[75] D. Bordo, P. Argos, *J. Mol. Biol.* **1991**, *217*, 721-726.

[76] J. Eichler, R. A. Houghten, *Protein Pept. Lett.* **1997**, *4*, 157-162.

[77] I. Annis, B. Hargittai, G. Barany, *Methods Enzymol.* **1997**, *289*, 198-202.

[78] J. V. Staros, *Acc. Chem. Res.* **1988**, *21*, 435-439.

[79] P. Cuatrecasas, I. Parikh, *Biochemistry* **1972**, *11*, 2291-2298.

[80] J. Carlsson, H. Drevin, R. Axén, *Biochem. J.* **1978**, *173*, 723-733.

[81] M. D. Partis, D. G. Griffiths, G. C. Roberts, R. B. Beechey, *J. Protein Chem.* **1983**, *2*, 263-268.

[82] T. Mouchahoir, J. E. Schiel, *Anal. Bioanal. Chem.* **2018**, *410*, 2111-2119.

[83] J. Adachi, C. Kumar, Y. Zhang, J. V. Olsen, M. Mann, *Genome Biol.* **2006**, *7*, R80.

[84] Y. P. Lucy, O. Salas-Solano, J. F. Valliere-Douglass, *MABS* **2017**, *9*, 307-318.

[85] P. J. Carter, *Nat. Rev. Immunol.* **2006**, *6*, 343-352.

[86] G. Kronvall, P. G. Quie, R. C. Williams, Jr., *J. Immunol.* **1970**, *104*, 273-283.

[87] S. B. Gunnoo, A. Madder, *ChemBioChem* **2016**, *17*, 529-538.

[88] G. L. Ellman, *Arch. Biochem. Biophys.* **1959**, *82*, 70-78.

[89] F. F. Schumacher, J. P. M. Nunes, A. Maruani, V. Chudasama, M. E. B. Smith, K. A. Chester, J. R. Baker, S. Caddick, *Org. Biomol. Chem.* **2014**, *12*, 7261-7268.

[90] J. G. Park, et al., *Cancer Res.* **1990**, *50*, 2773-2778.

Acknowledgement

I would like to express my sincere gratitude to my supervisor, Professor Yuji Ito for providing me this precious study opportunity as a Ph.D student in his laboratory.

I especially would like to express my deepest appreciation to my colleagues from Ajinomoto Co., Inc., and Ajinomoto Bio-Pharma Services, Inc., as follows: Michiya Kanzaki, Masahiro Yamanashi and Tatsuya Okuzumi for many helpful comments and suggestions in this study; Kazutaka Shimbo, Natsuki Shikida and Reiko Yuji for many helpful experiments and comments on peptide mapping; and Brian A. Mendelsohn, Michael Molony, Samuel Janssen, Zahra Khedri, Josh Toschi and Yutaka Matsuda for critical opinions on ADC synthesis, analysis and biological evaluation; Zhala Tawfiq for technical assistance for Ellman`s assay. There elaborated guidance, considerable encouragement and invaluable discussion that make my research of great achievement and my study life unforgettable.

I am also very grateful to the Ajinomoto Co., Inc. for making my Ph.D. study possible by the financial support.

Finally, I would like to extend my indebtedness to my family for their understanding, support, encouragement and sacrifice throughout my study.